UNIVERSITY OF CALIFORNIA SAN DIEGO

The structure and biofilm-stabilizing activity of Enterococcal surface protein's N-terminal region

A dissertation submitted in partial satisfaction of the requirements for the degree Doctor of Philosophy

in

Chemistry

by

Lindsey Spiegelman

Committee in charge:

Professor Partho Ghosh, Chair
Professor Neal Devaraj
Professor Gourisankar Ghosh
Professor Victor Nizet
Professor Elizabeth Villa

2022

The Dissertation of Lindsey Spiegelman is approved, and it is acceptable in quality and form for publication on microfilm and electronically.

University of California San Diego

2022

DEDICATION

For my husband, Dr. Christopher Fisher

TABLE OF CONTENTS

LIST OF FIGURES AND TABLES

ACKNOWLEDGEMENTS

First and foremost, I would like to thank my thesis advisor Dr. Partho Ghosh for the privilege of working in his lab and the many, many hours he spent advising me on this work. I would also like to thank all my collaborators for their contributions to this project, and in particular, the co-authors of our upcoming paper: Adrian Bahn, Elizabeth Montaño, Ling Zhang, Greg Hura, Katy Patras, Akif Tezcan, Victor Nizet, and Susan Tsutakawa.

I would like to thank former and present members of the Partho Ghosh lab for their helpfulness and kindness in day-to-day work, including sharing their expertise with experiments, letting me borrow reagents when I was in a hurry, and providing feedback on experiments at group meetings and in private conversations. In particular, I would like to thank Dr. Sumit Handa, who has served as a secondary mentor to me for the duration of my time in the Ghosh lab and has been a bottomless source of wisdom and support.

I would like to thank the current and former members of the Victor Nizet, Gouri Ghosh and Neal Devaraj labs for sharing their equipment and time when I needed to do experiments in their space. The spirit of collaboration is strong at UCSD and I am immensely grateful.

I would like to thank my doctoral committee, Drs. Nizet, G. Ghosh, Devaraj, and Villa, for their support and feedback during my time at UCSD.

I would like to thank Dr. Ken Bradley who was my scientific mentor during my truncated stay at UCLA and taught me some of my earliest lessons as a scientist,

including the adage “you find what you look for,” which taught me to always keep an open mind when interpreting results. I would also like to thank Dr. Heather Tseng, who I had the privilege of teaching under and who mentored me in writing curricula and teaching undergraduates.

I would like to thank the excellent scientific mentors I had at Texas A&M, including Drs. Erin Young, Jennifer Cook, Balaji Ramanathan, Wayne Harshbarger and Nathan Romero. All of these people shared both their joy of science and their perspectives on how best to do it, and I have carried all of those lessons with me along the way.

I would like to thank my parents, Drs. Clifford Spiegelman and Katherine Bretzlaff, for instilling a love of science and critical thinking in me from a young age.

Finally, I need to thank my family and loved ones for providing much-needed balance and stability in my life. In particular, I would like to thank my sister Abby, my best friend John O’Connor, the entire community on my beloved gemstone forum ShinyPreciousGems, and of course, my wonderful husband Chris and our two beautiful and perfect feline children, Marten and Ella.

Work presented in Chapters 2, 3, and 4 are being prepared for submission for publication. Spiegelman, Lindsey; Bahn, Adrian; Montaño, Elizabeth; Zhang, Ling; Hura, Greg; Patras, Katy; Tezcan, Akif; Nizet, Victor; Tsutakawa, Susan; and Partho Ghosh. “A portion of the N-terminal region of Enterococcal surface protein forms two Ig-like domains and stabilizes biofilms in a pH-dependent manner.” Title subject to modification. I am the primary author of this work.

VITA

Education

2022 Ph.D., Chemistry
University of California San Diego

2015 M.S., Biochemistry and Structural Biology
University of California Los Angeles

2013 B.S., Biomedical Science
Texas A&M University

Publications

M Zhu et al. *A Strategy for Dual Inhibition of the Proteasome and Fatty Acid Synthase With Belactosin C-Orlistat Hybrids.* Jan 19, 2017 Bioorg Med Chem

Dixon et al . *Distinct Roles for CdtA and CdtC during Intoxication by Cytolethal Distending Toxins.* Nov 30, 2015 PLoS ONE

ABSTRACT OF THE DISSERTATION

The structure and biofilm-stabilizing activity of Enterococcal surface protein's N-terminal region

by

Lindsey Spiegelman

Doctor of Philosophy in Chemistry

University of California San Diego, 2022

Professor Partho Ghosh, Chair

Enterococcal surface protein (Esp) is a cell wall-attached virulence factor of the leading nosocomial pathogens *Enterococcus faecalis* and *E. faecium* and is found predominantly in disease-causing strains. The presence of *esp* is associated with increased bacterial burden in rodent models of enterococcal endocarditis and urinary

tract infection. The mechanism by which Esp enhances colonization of tissues is unknown. The presence of Esp has also been found to enhance biofilms, as assayed by crystal violet staining, in some but not all strains of *Enterococcus*. The circumstances under and extent to which Esp enhances biofilms are not well understood, and conflicting data exist, leaving its role in biofilms undefined. To address the functional role of Esp, we sought to use X-ray crystallography to determine the structure of the unique N-terminal region of Esp, as structure is often indicative of function. We successfully determined the structure of the first 405 amino acids of Esp (Esp452), which revealed that this region is composed of two Ig-type domains typical of bacterial adhesins. While we did not detect binding to host factors, we did find that Esp452 strengthens enterococcal biofilms against mechanical and enzymatic challenge. Further examination revealed that this activity is correlated with the formation of amyloid-like fibrils in a pH-dependent manner. Interestingly, a larger fragment consisting of the entire N-terminal region of Esp, Esp743, did not demonstrate this activity, despite containing Esp452. We used a structural approach to explore the possibility of auto-inhibition, and found by small-angle X-ray scattering that the additional 291 amino acids contained in Esp743 appear to have close contacts with Esp452, supporting a role in structural stabilization of the protein and prevention of the formation of amyloid fibrils. Finally, we explored mechanisms of activation of the N-terminal region. We found that at pH 4.0, Esp743 was capable of strengthening biofilms, suggesting that extreme pH may be sufficient to generate activity of cell wall-attached protein. Alternatively, we found that a shorter truncation fragment of the N-terminal region,

consistent with cleavage by a human protease, was also capable of stabilizing enterococcal biofilms.

Chapter 1

Introduction

BURDEN OF ENTEROCOCCAL DISEASE

Enterococcus faecalis and *faecium* are leading causes of hospital-acquired infection (HAI), accounting for 14.8% of all recorded HAI in the United States between 2016 and 2017 and over 50,000 infections annually as of 2019 [1, 2]. They cause urinary tract infections (UTI), wound infections, endocarditis, and sepsis, with mortality rates of up to 50% in case of the latter two [3-5]. They are also leading causes of dental disease, which is associated with increased risk of bacteremia and endocarditis [6-11]. *E. faecalis* is the species of bacteria most commonly associated with failed root canals [12]. Disease-causing strains are commonly resistant to multiple antibiotics, including vancomycin which is a last line of defense, making infections difficult to treat and resulting in higher mortality rates [4, 13, 14]. They can also survive a wide range of pH, salt concentrations, and temperatures, making them difficult to eradicate from hospital surfaces and equipment [15, 16]. Enterococci can also donate genetic material to other species of bacteria such as *Staphylococcus aureus*, contributing to virulence and antibiotic-resistance in other pathogens [17, 18]. Vancomycin-resistant enterococci are rated as a serious threat by the CDC.

ENTEROCOCCAL BIOFILMS

Biofilms are microbial communities contained within an extracellular matrix including polysaccharides, extracellular DNA, and proteins. This matrix insulates microbes from physical and chemical disturbances, and facilitates the horizontal transfer of genes between cells, allowing resistance genes to spread more readily than in planktonic bacteria [19, 20]. Enterococci form biofilms both on abiotic and biotic

surfaces, making them more difficult to eradicate in the hospital environment from equipment, such as catheters, and during infection. In the context of infection, bacteria within biofilms exhibit enhanced antibiotic resistance compared to their planktonic counterparts and are more able to evade the immune response, leading to a higher risk of recurrent infection [21, 22]. Recent studies have demonstrated that therapies targeting biofilms render bacteria more susceptible to bacteriostatic and bacteriocidal antibiotics [24-26].

Biofilm development occurs in several stages: initial attachment, microcolony formation, maturation, and dispersal [19]. During the initial attachment phase, planktonic bacteria adhere to a surface. Once several bacteria have adhered to the surface in close enough proximity, they are able to signal to each other through the release of small peptides, which stimulates them to produce biofilm components such as extracellular DNA, polysaccharides, proteins, and lipids.

Enterococcal biofilm production is controlled in large part by the quorum-sensing *fsr* locus, which increases transcription of biofilm genes in response to small molecule peptides released by *Enterococcus* once they reach a high enough cell density [27]. Genes controlled by this mechanism include the proteases *gelE* and *sprE*, which are positively correlated with biofilm production and are thought to process protein components of the biofilm during both the maturation and dispersion phases of biofilm growth [28].

ENTEROCOCCAL SURFACE PROTEIN

Enterococcal surface protein (Esp) is a cell wall-attached virulence factor of *E. faecalis* and *E. faecium*. Esp was first identified on a pathogenicity island containing a cytolysin operon in nosocomial *E. faecalis* strain MMH594, and has since been detected in many strains of *E. faecalis* and *E. faecium* [29, 30].

Esp is associated with strains that cause dental disease, urinary tract infections, wound infections, endocarditis, and sepsis [29, 31-35]. Esp is also reported to be correlated with resistance to vancomycin and ampicillin [36]. Although Esp has a large repeat region in its C-terminal region with strong homology to other gram-positive surface proteins, its N-terminal region has little similarity to proteins of characterized function and its sequence is tightly conserved between different strains of *Enterococcus*. Esp has been found to increase bacterial burden in rodent models of enterococcal endocarditis and urinary tract infection, but the mechanism responsible for this effect is unknown [37-39]. While Esp has been proposed to play a direct role in mediating adherence to host tissues, esp-deficient *E. faecium* exhibited only a modest attenuation in binding to human urinary cells *in vitro* despite log-fold differences in colonization of the murine urinary tract [38]. Esp has also been found to increase biofilm production in some but not all strains of *Enterococcus* [40-43]. Due to its association with antibiotic-resistant and disease-causing strains of *Enterococcus*, a better understanding of the specific role of Esp in infection will likely inform potential treatments of enterococcal infection.

RESEARCH GOALS

The work presented here investigates the biochemical properties of the unique N-terminal region of Enterococcal surface protein, which have largely been unstudied to date. Chapter 2 presents the X-ray crystal structure of the majority of the N-terminal region and discusses its structural homologues and potential functions that could be inferred from the structure. Chapter 3 focuses on host factor binding experiments that I conducted to compare the activity of Esp452 to its structural homologues. Chapter 4 explores the biofilm-strengthening activity of the N-terminal region, its amyloid-like state, the conditions that are required for amyloid formation, and the differential activities of several fragments of the region. These studies lead to a proposal for a potential role for Esp in enterococcal biofilms on either abiotic surfaces or during infection, and suggest directions for future study.

Chapter 2

Structural determination of Esp452 and analysis

INTRODUCTION

The majority of studies to date have utilized genetic approaches to probe Esp's function, and little has been determined about the biochemical characteristics of the protein. Esp consists of a N-terminal region of 743 amino acids (aa), followed by a long repeat region with strong homology to common gram-positive bacterial repeats, and a short C-terminal domain with an LPXTG-motif for attachment to the bacterial cell wall. The final 291 amino acids of the 743-amino acid N-terminal region bear similarity to Streptococcal rib domains and are predicted to adopt a similar fold [44]. The first 452 amino acids are tightly conserved between different strains of *Enterococcus* and have little sequence similarity to any characterized proteins. Prediction of the structure of this 452-amino acid region was not forthcoming from *in silico* methods (i.e., Phyre). To address this, we elected to use X-ray crystallography to determine the structure of the unique N-terminal region of Esp and gain insight into its function.

MATERIALS AND METHODS

PROTEIN EXPRESSION CONSTRUCTS

The coding sequence of Esp452 (aa 1-452) was amplified by PCR from *E. faecalis* MMH594 and inserted through restriction digestion and ligation into a modified pET28a vector (Novagen), with either an N-terminal His_6-tag followed by a PreScission protease cleavage site or a C-terminal PreScission protease cleavage site followed by a His_6-tag. The coding sequence of the Esp N-terminal region (aa 47-743), which was amplified by PCR from *E. faecalis* MMH594, was inserted through restriction digestion

and ligation into the modified pET28a vector described above(Novagen), with C-terminal PreScission protease cleavage site and His_6-tag. The sequence of $Esp_{453-743}$ was amplified from the pET28a vector containing Esp743 and inserted through restriction digestion and ligation into the modified pET28a vector. The integrity of DNA constructs was confirmed by sequencing (Genewiz).

EXPRESSION AND PURIFICATION

Plasmids encoding various Esp regions were transformed into *Escherichia coli* BL21 (DE3) Gold, and transformed bacteria were colony purified. For expression, bacteria were grown at 37 °C in LB broth containing 50 μg/mL kanamycin with shaking overnight, and used the following day to inoculate the same growth medium at a 1:100 dilution. Initially, a construct including the putative signal sequence of Esp (aa 1-452) was tested for expression; the signal sequence was included because the SignalP algorithm [45] predicted only a moderate probability of signal sequence cleavage between amino acids 49 and 50. Mass spectrometric analysis (MALDI) of soluble Esp produced by this construct indicated that some of the N-terminal amino acids had been cleaved, resulting in aa 47 being the N-terminus of the protein. In the case of expression of selenomethionine (SeMet)-labeled Esp452, bacteria were grown and SeMet was incorporated as previously described [46]. Bacteria were shaken at 200 rpm at 37˚ C to an optical density of 0.6-0.8 and then induced for expression with 1 mM isopropyl β-D-1-thiogalactopyranoside (IPTG). Following induction, bacteria were grown further with shaking at 16 ˚C overnight. Bacteria were harvested by centrifugation (1,700 x *g,* 20 min, 4 °C), resuspended, and incubated for 15 min in lysis buffer (300 mM NaCl, 20

mM Tris, pH 8.0) supplemented with 1 mg/mL lysozyme and 1 mM PMSF. In the case of Esp743, the lysis buffer also included 20 units/L DNase (Thermo EN0521), 2.5 mM $MgCl_2$, and 1 mM $CaCl_2$. Resuspended bacteria were lysed by sonication. The lysate was centrifuged (16,000 x *g*, 20 min, 4 ˚C) and the supernatant clarified through a 0.8 μM filter using a syringe. The filtered lysate was applied to a Ni^{2+}-NTA column, which had been equilibrated with lysis buffer. In the case of Esp743, the lysate was incubated on the column for 20 min before carrying out the following steps. The column was washed with five column volumes (CV) of lysis buffer, followed by 5 CV of wash buffer (lysis buffer + 0 mM imidazole for Esp452, and 5 mM imidazole for all other constructs). Finally, samples were eluted with lysis buffer supplemented with 100 mM imidazole. After confirmation of purity by SDS-PAGE, eluted fractions were placed in a dialysis bag with 25 μg/mL His_6-tagged PreScission protease in lysis buffer containing 2 mM DTT, and dialyzed overnight in the same buffer. PreScission protease was removed by reverse-nickel chromatography. Esp constructs were then concentrated by ultrafiltration to 10-40 mg/mL ($\varepsilon_{280calc}$ 54780 [Esp452], 69220 [Esp743], 14440 [$Esp_{453-743}$] M^{-1} cm^{-1}), filtered by syringe through a 0.8 μm filter, and applied to a Superdex 200 column (GE Healthcare) for size exclusion chromatography in 150 mM NaCl, 20 mM Tris, pH 8.0. Fractions from the column were pooled and dialyzed into either 10 mM NaCl, 10 mM Tris, pH 8.0 for crystallization or PBS, pH 7.4 for all other experiments.

CRYSTALLIZATION

Crystals of Esp452 were grown by the sitting drop diffusion method with a precipitant solution containing 16% PEG 3350, 200 mM ammonium acetate, pH 7.0 at

20˚ C for 24-48 h. Drops were composed of 1.0 μL of precipitant solution and 1.0 μL of Esp452 at 7.5 mg/mL. The crystals were stabilized with a hydrogel polymer [47]. Briefly, crystals were soaked in precipitant solution supplemented with 100 mM $CalCl_2$, and then soaked in drops of precipitant solution containing 8.625% (w/v) sodium acrylate, 2.5% (w/v) acrylamide, and 0.2% (w/v) bis-acrylamide for 48 hours. The crystals were transferred to fresh drops of precipitant solution containing 1% ammonium persulfate and 1% TEMED for 10 min and flash frozen in liquid N_2. Additionally, crystals of Esp452, which were not stabilized in the hydrogel polymer described above, and SeMet-labeled Esp452 were grown with a precipitant solution containing 20% PEG 3350, 200 mM ammonium citrate, pH 7.0 at 20˚ C for 24-48 h. In the case of native Esp452, the drops also contained 12.5 mM $CaCl_2$, and in the case of SeMet-labeled Esp452, 3.75% sucrose. Drops were composed of 1.0 μL of precipitant solution and 0.75 μL of native or SeMet-labeled Esp452 (8 mg/mL). Crystals were cryoprotected by soaking in precipitant solution supplemented with 20% 2-methyl-2,4-pentanediol, and flash cooled in liquid N_2.

STRUCTURE DETERMINATION

Diffraction data to 1.4 Å resolution limit (Table 1) were collected from hydrogel polymer-stabilized crystals of Esp452 (ALS Beamline 5.0.2), and scaled using Aimless [89]. Phases were determined by molecular replacement using MOLREP with a model of Esp452 described below [90].

Initial phases for Esp452 were determined by single wavelength anomalous dispersion from crystals of SeMet-labeled Esp452. Anomalous dispersion data were

collected to 2.3 Å resolution limit (ALS 12.3.1), indexed, integrated, and scaled using HKL2000 (Table 2.1) [48]. Phases were determined with Autosol [49], which identified four anomalous scatterers per asymmetric unit. These corresponded to four of the six methionines of Esp452. The initial model was generated by automated building in Autosol and refined with phenix.refine using default parameters [49]. Amino acids and other molecules were modeled into electron density manually in Coot, as guided by inspection of σ_A weighted $2mF_o$-DF_c and mF_o-DF_c maps, The model was then further refined against diffraction data of higher resolution limit, 2.1 Å (Advanced Photon Source beamline 24-ID-E), from crystals of native Esp452 that had been soaked in $CaCl_2$. Data were processed as described above, and phases were determined by molecular replacement using Phenix (MR-Phaser) with the model of Esp452 refined against the 2.3 Å resolution data set. The Esp452 model refined against 2.1 Å resolution data served as the phasing model for the 1.4 Å data set. Model building, refinement, and inspection of maps was carried out as described above.

In the final model, the main chain was continuous, except for 48-58, 408-418, and 449-452. Waters were modeled by Coot and verified by manual inspection of difference maps. The final model contains a Ca^{2+} ions and 433 waters. The reflections that were unique to the 1.4 Å resolution dataset constituted 69.3% of total reflections, and the R_{work} and R_{free} of these were 15.4% and 18.9%, respectively. The structure contains 97.1% Ramachandran favored angles, one Ramachandran outlier, and 0 bonds or unfavored angles, as assessed by MolProbity. The structure is above average for all evaluated statistics when compared to structures of similar resolution in the Protein Data Bank (PDB), ID 6ORI. Pymol was used for generating figures.

Table 2.1. Data collection, phasing, and refinement statistics for Esp452 structures.

	Esp Structure 3 (Final)	Esp Structure 1 (SeMet)	Esp Structure 2 (Native)
Data collection	ALS 5.0.2	ALS 12.3.1	APS 24-ID-E
Space group	P1	P1	P1
Cell dimensions			
a, *b*, *c* (Å)	39.9, 50.0, 51.2	40.0, 49.0, 51.0	39.9, 50.0, 51.2
α, β, γ (°)	107.4, 111.4, 90.4	111.0, 111.4, 91.7	107.3, 111.7, 90.1
Resolution (Å)	47.27-1.40 (1.42-1.40)	26.49-2.29 (2.33-2.29)	45.11-2.14 (2.20-2.14)
R_{meas}	.080 (.146)	.075 (.109)	.127 (.000)
R_{pim}	.044 (.082)	.039 (.058)	.090 (.000)
$I / \sigma I$	11.3 (6.2)	35.2 (17.4)	5.4 (3.0)
Completeness (%)	85.4 (83.9)	98.0 (91.1)	92.8 (45.0)
CC 1/2	.99 (.98)	.99 (.98)	.96 (.48)
Redundancy	3.2 (3.0)	3.7 (3.3)	1.9 (1.0)
Refinement			
Resolution (Å)	1.40 Å		
Unique reflections	58,580		
R_{work} / R_{free}	15.2/17.4		
No. atoms			
Protein	3025		
Ligand/ion	1		
Water	433		
B-factors			
Protein	11.9		
Ligand/ion	8.7		
Water	23.5		
R.m.s. deviations			
Bond lengths (Å)	.009		
Bond angles (°)	1.240		

RESULTS

The N-terminal non-repeat portion of mature Esp (amino acids 48-743) was recombinantly expressed in *E. coli* and purified. While crystals of this construct, Esp743, were obtained, no diffraction was observed and efforts to improve the quality of the crystals were unsuccessful. We did find, however, that a shorter construct also starting at 48 but truncated at 452, and called Esp452, yielded crystals that diffracted sufficiently for data collection. A data set was collected from these crystals at 2.3 Å resolution limit. Another data set was later collected with a 1.4 Å limit through the use of a protein-hydrogel polymer hybrid [47]. Initial phases for Esp452 were determined by single anomalous dispersion (SAD) from selenomethionine-labeled protein.

The structure revealed that Esp452 is composed of two globular domains (Fig. 2.1) connected by a 20-amino acid long loop (237-256). The first domain, Esp1, extends from amino acids 58-236, and the second, Esp2, from 257-449. Several amino acids at the N- and C-termini of Esp452 lacked electron density, as did a loop in Esp2 (407-418). Esp1 and Esp2 both have a DE-variant immunoglobulin-fold (DEv-Ig), in which two additional β-strands (D' and D") occur between the D and E strands. In Esp1 the additional strands are part of the canonical CFG β-sheet, and in Esp2 the D' strand is part of the ABED β-sheet while the D'' is part of the CFG β-sheet (Fig. 2.2).

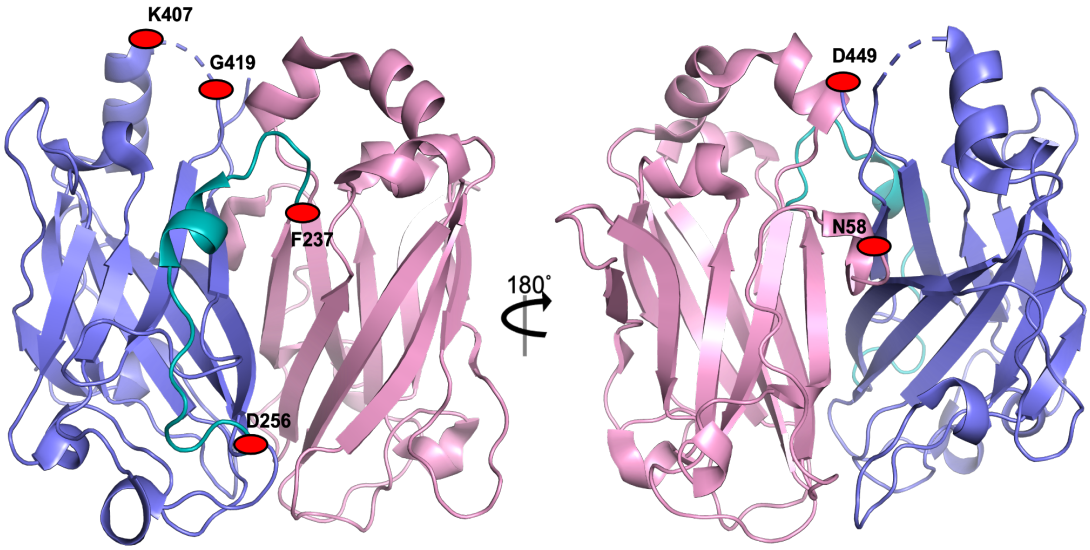

Figure 2.1 Esp452 has two DEv-Ig domains. Esp452 in cartoon format with the Esp1 (N58-Y236) domain in pink and the Esp2 (Q257-D449) domain in purple. The loop connecting the two domains (F237-D256) is in black. The segment between 408-418 lacked electron density and was not modeled, and is shown by a dashed line.

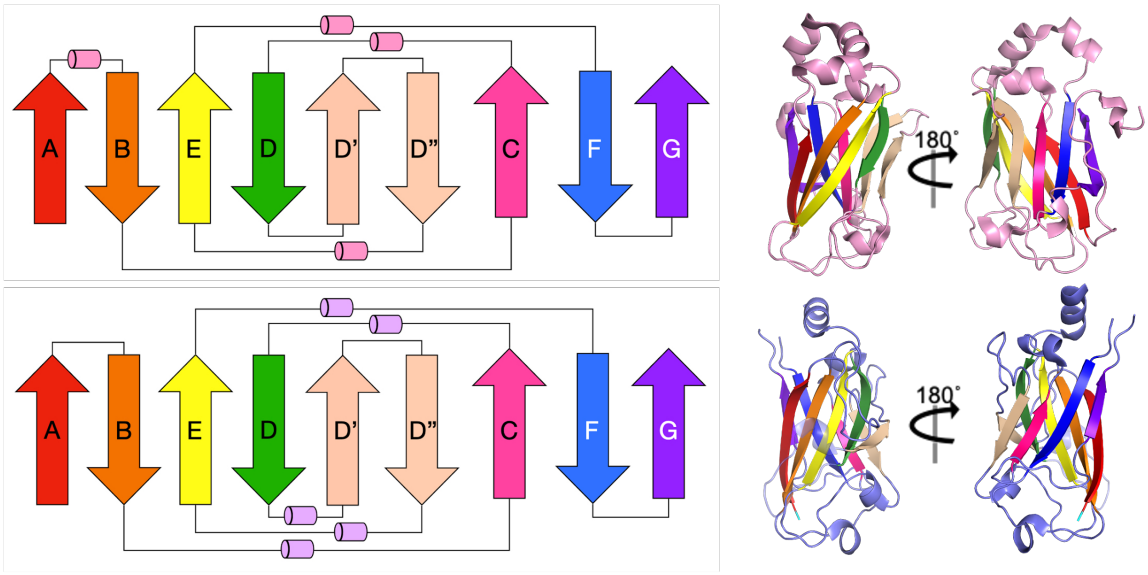

Figure 2.2 Topology map of Esp452. Topology map of Esp1 (top) and Esp2 (bottom) shown in rainbow coloring, with similar coloring of the domains shown in cartoon representation at right.

Some of the loops connecting the β-strands contain short α-helical segments. The two domains are packed closely together, with some side chains within 5 Å of one another, and forming a continuous surface that on one side is predominantly negatively charged and the other positively charged (Fig. 2.3). The loop connecting the two domains appears to be flexible based on its B-factor, which is significantly higher than the overall average of the structure, particularly between amino acids 239-250 which includes a short α-helical segment (Figs. 2.4-2.6). This suggests the capability of the domains to move relative to one another, despite their close orientation in the crystal structure.

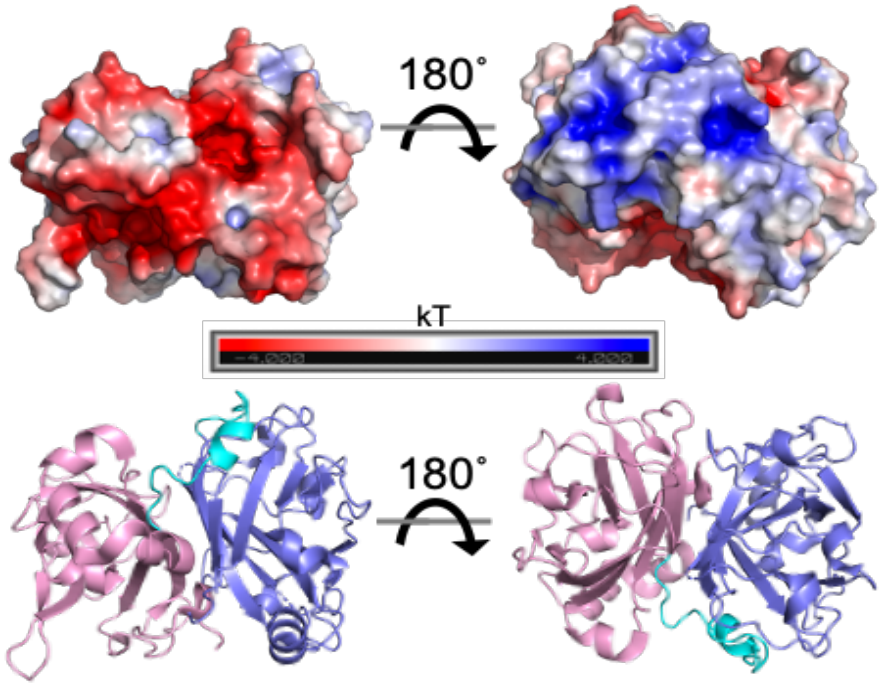

Figure 2.3 Molecular surface of Esp452 viewed perpendicular to the β-sheets. Surfaces with negative character shown in red, neutral in white, and positive in blue, ranging from -4.0 to 4.0 kT. Shown below is the same view in cartoon representation.

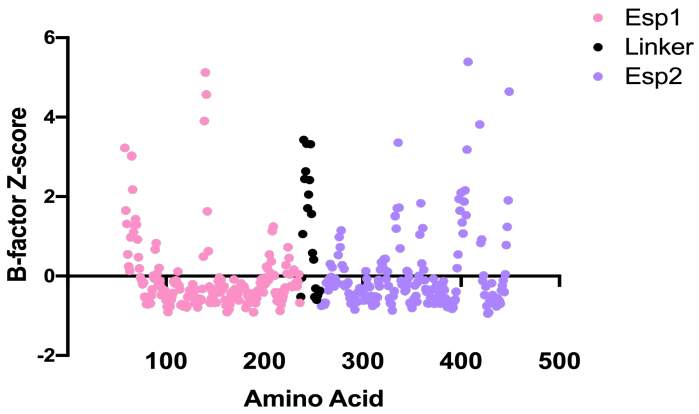

Figure 2.4 Z-score for Cα atom B-factors. Z-scores were calculated with the following formula: $Z=(B_x-B_{avg})/s$, where B_x is the B-factor of a given Cα atom, B_{avg} is the average B-factor of all Cα atoms in the structure, and s is the standard deviation of the Cα B-factors. Esp1 is shown in pink, Esp2 in lavender, and the linker in black. Certain loops and helices connecting β-strands, as well as the N- and C-termini, also have higher than average B-factors.

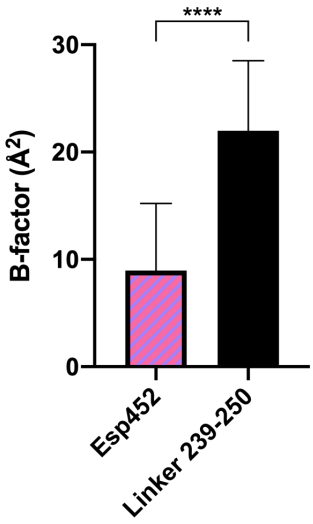

Figure 2.5 B-factors of Esp452. Average Cα atom B-factors for the entire structure (58-449), with standard deviations indicated. Amino acids in the loop (239-250) connecting the two domains have significantly higher B-factors than the average B-factor of Esp452; **** $p < .0001$ as determined by independent t-test with Welch's correction.

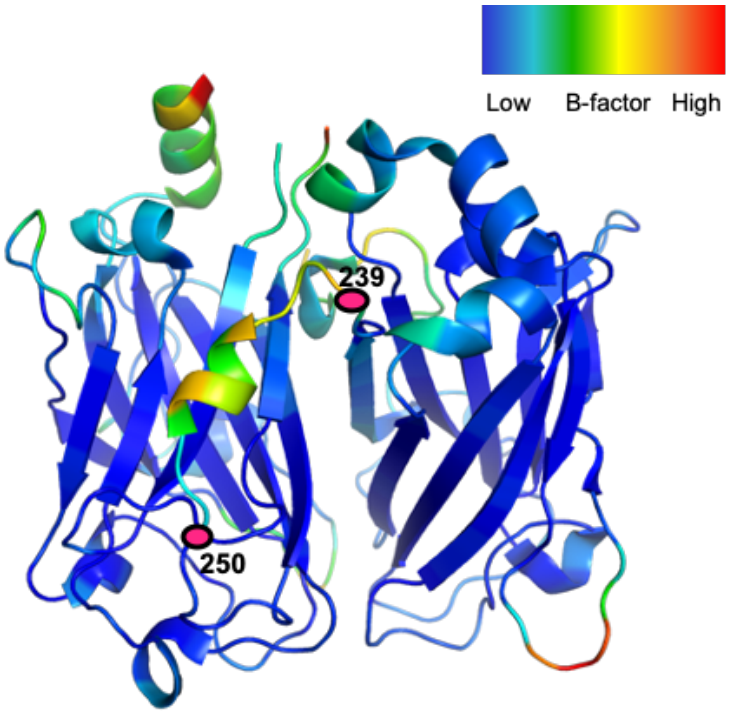

Figure 2.6. B-factors of Esp452. Esp452 shown in cartoon representation colored according to B-factors of Cα atoms, ranging from 3.0 to 42.9 Å^2, with an average of 8.9 Å^2. The central 12 amino acids of the loop connecting the Esp1 and Esp2 domains (239-250) have statistically significantly higher B-factors than the average B-factor of the structure.

A single ion was observed between loops on the negatively-charged surface of the molecule, coordinated between the backbone carbonyl of S209, the side chain of D210, the backbone of G419, L447, and the sidechain of D449 (Figure 2.7). There are five coordinating atoms with an average coordination distance of 2.32 Å, suggestive of a calcium ion. The crystals that yielded the 1.4 Å structure were soaked in 100 mM $CaCl_2$. However, electron density corresponding to the ion was not visible in the 2.3 and 2.1 Å structures, which had not been soaked in $CaCl_2$, and thus it is possible that calcium binding is artifactual.

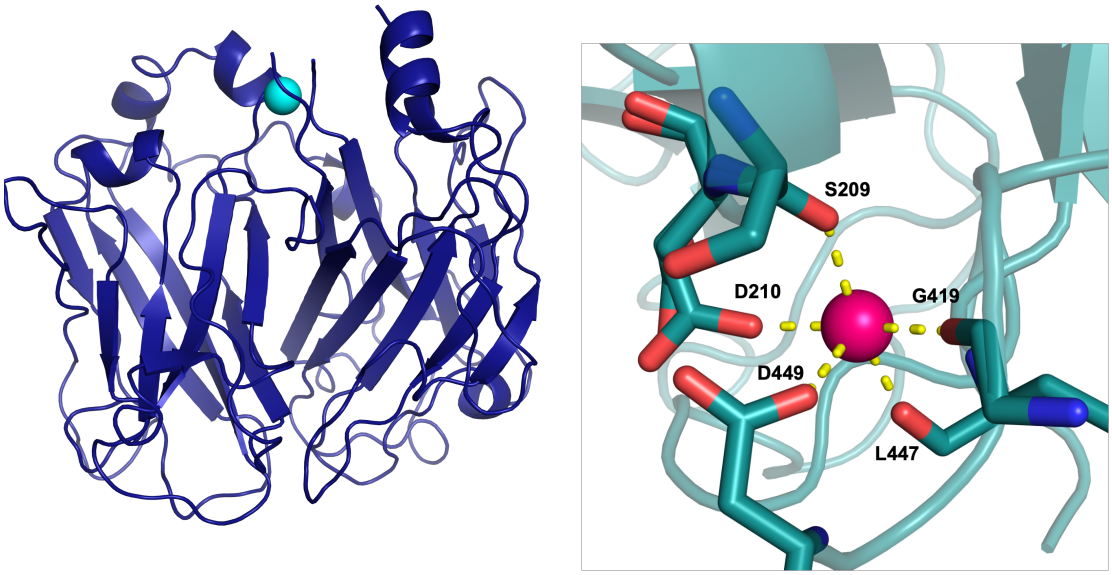

Figure 2.7 Esp452 binds a single calcium ion. The position of the Ca^{2+} ion (cyan) is shown with Esp452 (blue) in ribbon representation (left). The coordination site between five atoms is shown with the calcium in pink (right).

The structure revealed that Esp452 has significant similarity to large families of bacterial adhesins [50], namely the Microbial Surface Components Recognizing Adhesive Matrix Molecules (MSCRAMMs) and the *Streptococcus* Antigen I/II protein families (Table 2).

Table 2.2. Structural homologues of Esp452 identified by the Dali server with a z-score of 6.0 or better. Members of the MSCRAMM family are indicated with an asterisk in the molecule column. Table is continued on next page.

Rcsb code	Z score	rmsd	sequence id%	molecule	species	reported activity
5mkd	8.9	2.7	8	YWEA: putative homologue of BslA	B. subtilis	biofilm
4bhu	8.5	2.7	10	BslA	B. subtilis	biofilm
3opu	8	6.0	8	SPAP	S. mutans	adhesion
2woy	7.9	3.3	11	SspB (Antigen I/II)	S. gordonii	adhesion
3qe5	7.6	5.4	9	Antigen I/II	S. mutans	adhesion
4ofq	7.6	4.2	8	Antigen I/II	S. pyogenes	adhesion
5dza	7.5	6.0	8	BSPA/Antigen I/II	S. agalactiae	adhesion
5jq6	7.1	4.0	8	ClfA*	S. aureus	adhesion
4hsq	7.1	3.7	6	pilin protein SpaD	C. dipthiriae	adhesion
4tsh	7.1	3.5	9	adhesin P1	S. mutans	adhesion
4mbo	6.9	4.1	8	srr1*	S. agalactiae	adhesion
4igb	6.8	5.6	11	Sgo0707	S. gordonii	adhesion
3kpt	6.8	3.9	12	BcpA (pilin)	B. cereus	adhesion
3is1	6.8	4.1	8	Uro-adherence factor A*	S. saprophyticus	adhesion
2wza	6.8	3.4	7	SspB (Antigen I/II)	S. gordonii	adhesion
2ral	6.8	4.0	6	SdrG*	S. epidermis	adhesion
3uxf	6.7	4.6	10	FimP	A. oris	adhesion
4ei0	6.7	3.5	9	uncharacterized protein	P. merdae	unknown

Table 2.2. Structural homologues of Esp452 identified by the Dali server with a z-score of 6.0 or better, continued.

Rcsb code	Z score	rmsd	sequence id%	molecule	species	reported activity
4fx5	6.7	3.7	10	von Willebrand factor A	C. acidiphila	unknown
5fx8	6.5	4.2	6	Zonadhesin	K. pastoris	adhesion
4b60	6.5	4.5	7	rFnBPA*	S. aureus	adhesion
3rpk	6.4	7.1	6	pilin RrgB	S. pneumoniae	adhesion
5z0z	6.4	6.1	5	pilin spaD	L. rhamnosus	adhesion
3zgh	6.3	3.3	4	PsrP	S. pneumoniae	structural
4je0	6.3	5.0	7	sdrD*	S. aureus	adhesion
3qdh	6.3	3.7	7	FimA	Actinomyces	adhesion
4mbr	6.3	4.8	9	Srr2*	S. agalactiae	adhesion
4uzg	6.3	3.5	6	Pilus protein	S. agalactiae	structural
3htl	6.2	3.5	6	pilus protein SpaA	C. dipthiriae	adhesion, structural
4q6k	6.1	3.4	6	putative neurimidase, unconfirmed	B. caccae	hydrolase
5bob	6.1	4.0	10	Fhb	S. suis	immune evasion
5ze8	6.1	5.2	9	Cytochrome C552	T. tepidum	Photo-synthesis
4neh	6.1	3.5	6	integrin alpha-X	H. sapiens	adhesion
4f27	6	4.2	7	ClfB*	S. aureus	adhesion
5wtb	6	4.3	7	SdrE*	S. aureus	adhesion

MSCRAMMS have been identified in *Staphylococcus, Streptococcus*, and *Enterococcus,* and are typically involved in adhesion to host extracellular matrix proteins [51]. Several of these proteins bind their targets through a "dock, lock, and latch" mechanism that requires both DEv-Ig domains. MSCRAMMS all adopt a similar elongated confirmation in crystal structures, in contrast to the compact conformation of Esp452 (Fig. 2.8-2.9).

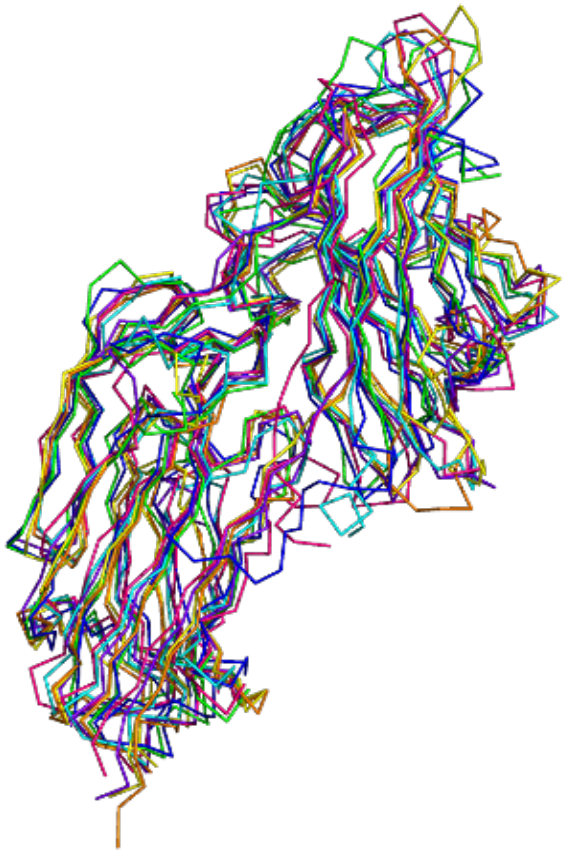

Figure 2.8. The similar conformations of nine MSCRAMMs. SdrD (red), SdrE (orange), SdrG (yellow), Srr1 (green), Srr2 (blue), ClfA (purple), ClfB (pink), UafA (cyan), and FnBPA (black) are represented in ribbon representation, aligned based on Cα atoms of both domains of each structure.

Figure 2.9. Esp452 adopts a different conformation than MSCRAMMs. Esp452 (black) superposed with UafA (cyan). The superposition was based on Esp1 with the N3 domain of UafA. Both are in ribbon representation.

Antigen I/II proteins are streptococcal virulence factors that are primarily found in oral and respiratory colonizers such as *S. mutans and S. pyogenes*, and help mediate attachment of *Streptococcus* to mucins or tissue in a glycan-dependent manner [52]. Esp452 is structurally similar to the C-terminal region of Antigen I/II proteins, which bind glycans attached to fibronectin or salivary agglutinin glycoprotein (SAG) [53]. These proteins typically contain a stabilizing Lys-Asn isopeptide bond and a BAR motif, but Esp452 possesses neither of these features. Esp452 also has structural similarity to *Bacillus subtilis* BslA, a biofilm-coating protein responsible for increasing the hydrophobicity of the biofilm surface [54]. This activity is due to a "cap" of several hydrophobic residues on one surface of BlsA. However, Esp452 does not possess an equivalent hydrophobic cap (Fig. 2.10).

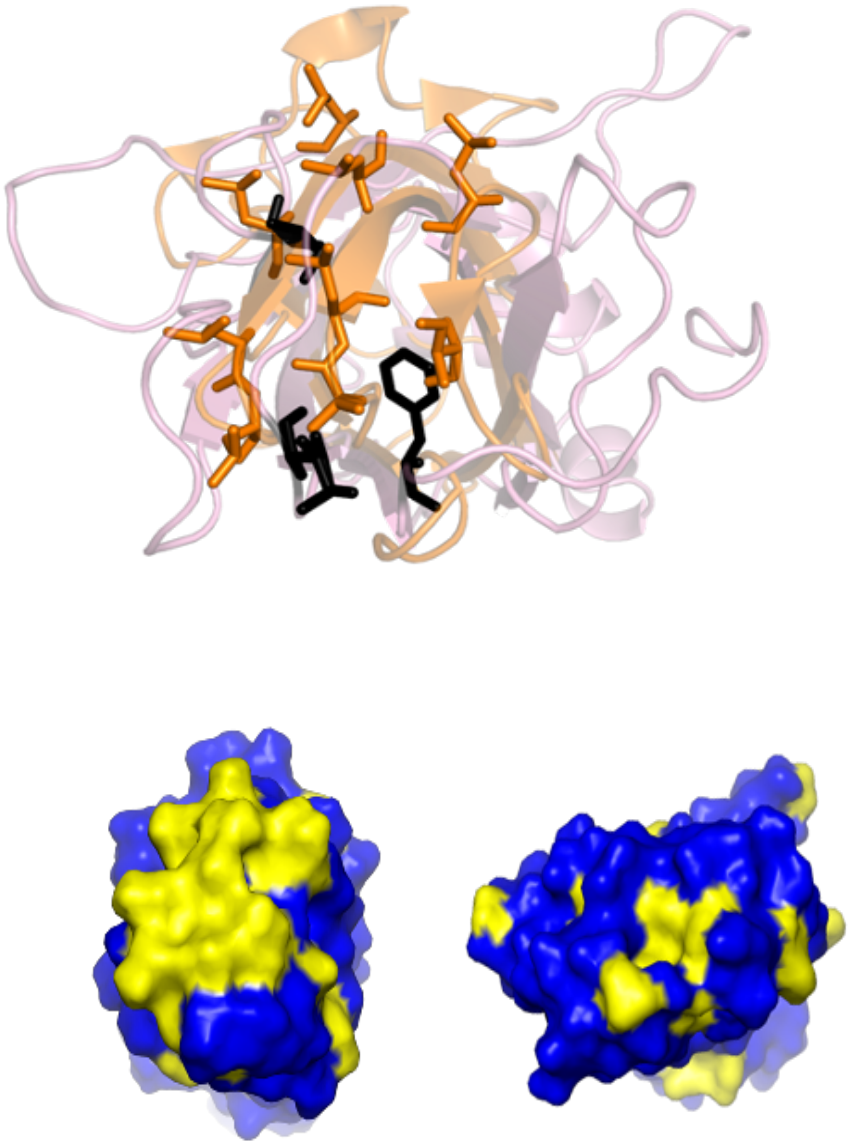

Figure 2.10 Esp does not possess a hydrophobic cap. Esp1 (pink) and BslA (orange) in cartoon representation with hydrophobic amino acids shown as sticks in black and orange, respectively (Top). The surfaces of BslA (left) and Esp1 (right), in the same orientation as panel C, with hydrophobic amino acids in yellow and all others in blue (Bottom).

DISCUSSION

Esp's role in infection remains unclear after over two decades of study. I hoped to gain clues to its function by examining the protein's structure and comparing it to that of other characterized proteins. The sequence of the first 452 amino acids of the N-terminal region (excluding the signal sequence) of Esp had low sequence similarity with proteins of known structure, making prediction of its fold challenging. I crystallized and determined the structure of this region, and the work revealed that Esp452 forms two DEv-Ig domains. Notable features of the structure include that it is β-rich, has a long, flexible loop between the two domains which may allow the two domains to rotate independently from one another, and distinct negatively and positively charged surfaces on opposite faces of the protein.

Ig-like folds, including the DEv-Ig fold, are common in gram-positive adhesins. Esp has been proposed as a potential mediator of attachment to host tissue during infection, and so I focused particularly on adhesins in comparisons. The binding targets of Esp's homologues included glycoproteins and extracellular matrix components, but I was unable to identify a conserved binding site in Esp452. This is not necessarily surprising as the binding sites of these proteins vary widely in terms of their targets, the location within the Ig-fold, and amino acid composition, and I cannot discount that Esp may bind an unidentified target in a unique mode. Additionally, Esp452 had strong similarity to an active region of biofilm protein BslA, but lacked an essential structural element, the hydrophobic cap.

Ultimately, my attempts to determine a clear functional role from the crystal structure were unsuccessful, but due to its unique amino acid sequence, the

determination of this structure was used by those working to improve structure prediction algorithms. Esp452 was used as a prediction target for the 2018 Critical Assessment of protein Structure Prediction (CASP) competition, with most teams able to predict at least some of the structure, but no one able to predict the entire fold [55].

Ling Zhang crystallized Esp452 for the third and final Esp452 structure, collected the data and determined the initial model. Refinements were done in collaboration with me and final preparation for deposition in the PDB was done by me. All other work presented in this chapter was performed by me.

Work presented in Chapter 2 is being prepared for submission for publication. Spiegelman, Lindsey; Bahn, Adrian; Montaño, Elizabeth; Zhang, Ling; Hura, Greg; Patras, Katy; Tezcan, Akif; Nizet, Victor; Tsutakawa, Susan; and Partho Ghosh. “A portion of the N-terminal region of Enterococcal surface protein forms two Ig-like domains and stabilizes biofilms in a pH-dependent manner.” Title subject to modification. I am the primary author of this work.

Chapter 3

Probing for Esp binding to mammalian cells and host factors

INTRODUCTION

Several studies have found that deleting *esp* from *esp*$^+$ strains attenuates the ability of *Enterococcus* to colonize host tissues in rodent models of infection, and the explanation has been posited by many researchers that *esp* plays a role in adhesion to host tissues. I compared the crystal structure of Esp452 to other protein structures and found that the majority of structural homologues are bacterial adhesins, including members of the Antigen I/II and MSCRAMM families. I was unable to identify a site in Esp452 that resembled a characterized binding site in one of its structural homologues, but due to the global structural similarity of Esp452 to gram-positive adhesins, I probed a variety of cell types and host factors for binding by Esp452 and Esp743.

MATERIALS AND METHODS

BACTERIAL STRAINS

MMH594 and the isogenic strain MM594b lacking *esp* were a kind gift of Dr. Michael Gilmore [37, 56].

PROTEINS (CLONING, EXPRESSION AND PURIFICATION)

Esp-His constructs were prepared as described in chapter 2. M1-His was prepared as described previously [57].

The coding sequence for Esp743 was amplified from the previously cloned Esp-His construct with primers that added a sequence encoding a C-terminal Avitag, and the resulting PCR product was inserted through restriction digestion and ligation into a

modified pET28 vector encoding an N-terminal His tag. Addition of the 45-nucleotide sequence encoding the C-terminal Avitag sequence required two sequential rounds of PCR, indicated in Table 3.1 as step one and step two. The pET vector containing His-Esp743-Avitag was co-transformed into *E. coli* BL21-Gold cells along with pBirACm (Avidity). These cells were grown and induced identically to other Esp-expressing strains, except that at the time of induction, biotin was added to a final concentration of 50 μM. His-Esp743-Avitag was purified exactly as Esp743-His as described in chapter two using Ni-NTA resin, and the His-tag was cleaved as described in Chapter 2, generating the final Esp-Avitag protein.

Table 3.1 Primers used to add the Avitag to Esp743

Primer	Primer sequence
His-Esp743-Avitag, 5' end	GGGCCCGGATCCAATGCACAAATGGGTGAAGGAAGATTAGCAAATTATTCTGC
His-Esp743-Avitag, 3' end step one	CGCTTCAAAAATATCGTTCAGGCCATTTTTACTTACAGTTACTGCTAAATCGGTCG
His-Esp743-Avitag, 3' end step two	GTGGTGCTCGAGTTATTCATGCCATTCAATTTTCTGCGCTTCAAAAATATCGTTCAGGCC

GLYCAN SCREEN

Binding of Esp452-His to human glycans was assessed by the National Center for Functional Glycomics at Harvard University (https://ncfg.hms.harvard.edu/). These data are listed in the Appendix.

FIBRINOGEN BINDING ASSAY (ELISA)

Human fibrinogen (Millipore Sigma) was resuspended in PBS at a concentration of 1 ng/µL, and 100 µL was used to coat wells of a 96-well plate (Corning). The plate was incubated overnight at 4˚ C. Wells were washed with 0.1% TBST (Tris Buffered Saline + Tween, 20 mM Tris pH 8.0, 150 mM NaCl) 3X, then blocked with TBST + 0.1% BSA for 1 h at RT. The wells were washed 3X with 0.1% TBST. Esp452-His (3 µg), M1-His (1 µg), or PBS was added to the plate, and the plate was nutated for 1.5 h at RT. The wells were then washed 3X with TBST. Anti-His HRP-conjugated monoclonal antibody was added at 1:500 dilution for 1 hr at RT. The wells were washed 3X with TBST, and then TMB substrate was added, as recommended by the manufacturer (BD Biosciences). The OD_{450} was measured by plate reader (TECAN).

FIBRONECTIN BINDING ASSAY

Esp452-His (5 µg) was incubated with human fibronectin (Sigma, 10 µg) in 100 µL PBS buffer (pH 7.4) for 60 min at 37 ˚C. Ni-NTA resin was equilibrated with PBS and 40 µL of 1:1 resin: PBS was then added to the mixture and nutated for 30 min at 37 ˚C. The resin was then washed 3X with 200 µL PBS supplemented with 10 mM imidazole. Finally, the bound fractions were eluted with 20 µL of PBS supplemented with 200 mM imidazole. Samples were resolved and visualized through Coomassie-stained SDS-PAGE.

Flow Cytometry (Esp expression)

MMH594 and MMH594b were grown with shaking overnight in Brain Heart Infusion (BHI). Cultures were diluted 1:10 in BHI and grown for two additional hours. Cultures were diluted to an OD_{600} of 1.0, and 1 mL of *Enterococcus* was used for each condition. Bacteria were blocked with PBS supplemented with 1% BSA (PBS+BSA) on ice for 30 min. Rabbit anti-Esp antibody was added at a 1:500 dilution and incubated for 1 h on ice. Bacteria were spun at 4,500 x *g* for 5 min, and then washed 3X with PBS. Bacteria were resuspended in PBS+BSA with 1:1000 goat anti-rabbit IgG conjugated to AlexaFluor 647 (Invitrogen) and incubated 1 hr on ice. Bacteria were washed 3X with PBS and resuspended in PBS+BSA. Bacteria were then diluted 1:10 in PBS for analysis by flow cytometry (BD Accuri).

Flow Cytometry (Esp Binding to Mammalian Cells)

Human platelets (2×10^7) and THP-1 cells ($2x10^5$) were blocked in PBS + 1% BSA for 1 h on ice. Esp-His was added to the samples, and the samples were rocked for 1 h at 37 ˚C. Samples were spun down, washed once in PBS, and resuspended in PBS + 3% BSA + mouse anti-His antibody. Samples were incubated for 1 h on ice, then washed twice with PBS. Esp-His samples were resuspended in PBS + 1% BSA + mouse Anti-His FITC-conjugated monoclonal IgG antibody (Thermo Fisher) at a dilution of 1:200 and incubated for 30 min on ice. Cells were washed 2X in PBS and resuspended in PBS + 3% BSA for analysis by flow cytometry (BD Facscalibur).

Samples with Esp743-Avitag constructs were treated identically, except that Streptavidin-Cy5 was substituted for the anti-His antibody.

WESTERN BLOT

Mammalian cells were grown according to ATCC recommendations in a 24-well plate to approximately 80% confluence. The culture supernatant was removed and replaced with 200 µL DMEM supplemented with 10 µM Esp743-Avitag. The plate was incubated at 37 ˚C for 1 h, and then the wells were washed 2X with 500 µL PBS. SDS-PAGE loading buffer (50 µL) was added directly to the wells and the plate was rocked at 25 ˚C for 10 min. Samples were analyzed by western blot for the presence of Esp743-Avitag, as detected with Streptavidin-Cy5 and a fluorescent blot imager (Bio-Rad).

UTI MODEL OF INFECTION

Ten week-old C57bl6 mice (Jackson Laboratory) were used for this experiment. *E. faecalis* MMH594 and MMH594b were grown overnight in BHI media to approximately 2.8 x 10^9 CFU. Urine was voided from the mice and 50 µL of bacteria was injected through the urethra. At 1 day after inoculation, urine from each mouse was collected, diluted, and plated on BHI agar containing 20 µg/mL erythromycin. Five mice were sacrificed, and their kidneys and bladders homogenized and plated. This procedure was repeated on days 3 and 5.

RESULTS

Esp452 is structurally similar to members of the Antigen I/II family, as previously mentioned in Chapter 2. Antigen I/II family members are glycan-binding streptococcal adhesins which contain multiple Ig-like domains. The glycan-binding sites of Antigen I/II proteins are variable, but are typically characterized by a Lys-Asn isopeptide bond that covalently connects the two β-sheets of each Ig-like domain, and a BAR motif, a short α-helical segment of variable sequence [91-93]. While Esp452 possesses neither of these structural features, it remained possible that Esp452 targeted glycans. We therefore tested glycan-binding of Esp452 using a human glycan microarray screen. Esp452 did not bind any glycans in the screen to a significant level (Appendix), including sialic acid, lactose, and GalNAc, which have been shown to bind Antigen I/II proteins [58].

Eight of the MSCRAMMs identified to have structural similarity to Esp452 bind fibrinogen (Fg) or fibronectin (Fn), with the binding mode and target sites on fibrinogen and fibronectin varying among MSCRAMMs [59][94]. To ascertain whether Esp452 also bound Fg, I carried out an ELISA with intact Fg and Esp452. To assess whether Esp452 bound Fn, I conducted a co-precipitation assay with His-tagged Esp452 and Ni-NTA resin. While I observed binding between Fg and *Streptococcus pyogenes* M1 protein, which served as a positive control, I detected no binding between Fg and Esp452 (Fig. 3.1). No binding of Fn by Esp452 was observed by co-precipitation (Fig. 3.2).

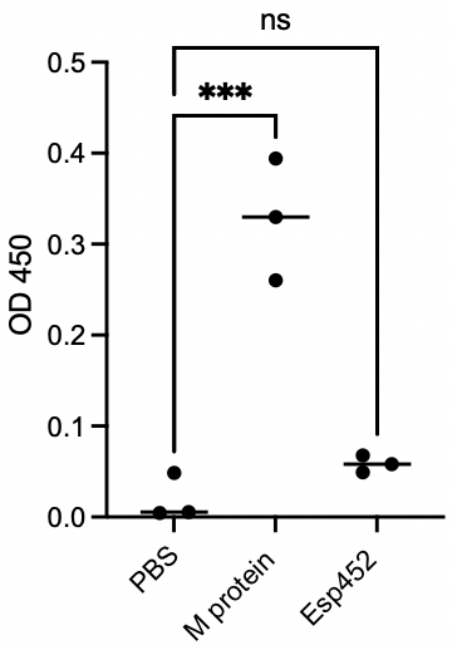

Figure 3.1. Fibrinogen binding of Esp452 compared to M1 protein. Wells of a plate were coated with fibrinogen and then incubated with either PBS or an equimolar amount of His-tagged Esp452 or M1 protein and assayed for binding by ELISA. Samples were compared by 1-Way ANOVA. *** $p < 0.001$

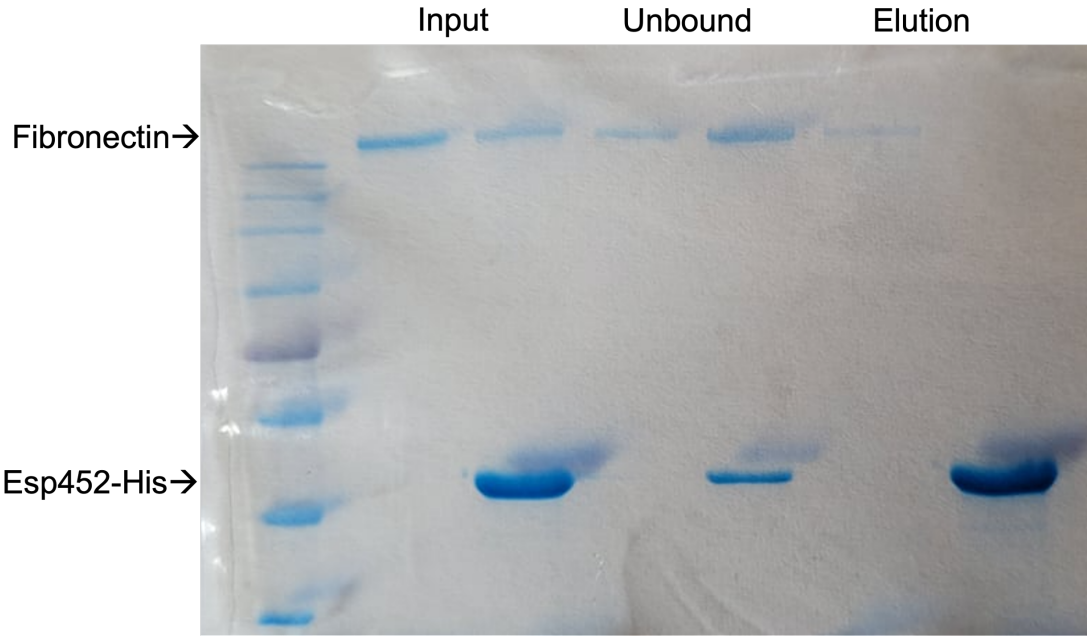

Figure 3.2. Fibronectin binding by Esp452. Ni^{2+}-NTA resin was incubated with Esp452-His or a PBS control and human fibronectin. The resin was then washed and protein eluted with imidazole. No fibronectin was observed to bind Esp452.

I next asked if Esp binds mammalian cells. I first assessed Esp452 for binding to human platelets and monocytes by flow cytometry. Cells were incubated with Esp452-His, washed to remove unbound Esp452-His, and then incubated with an antibody recognizing the His-tag and conjugated to FITC. I observed a slight shift in fluorescence signal for platelets and THP-1 incubated with Esp452-His; however, the difference in fluorescence between the Esp-bound samples and the samples exposed only to the anti-His-FITC antibody was roughly the same as the shift generated by the antibody compared to the platelet-only control, which suggested to me that the binding of Esp might be due to general protein-cell interactions rather than a specific binding event to a particular binding partner. (Fig 3.3-3.4).

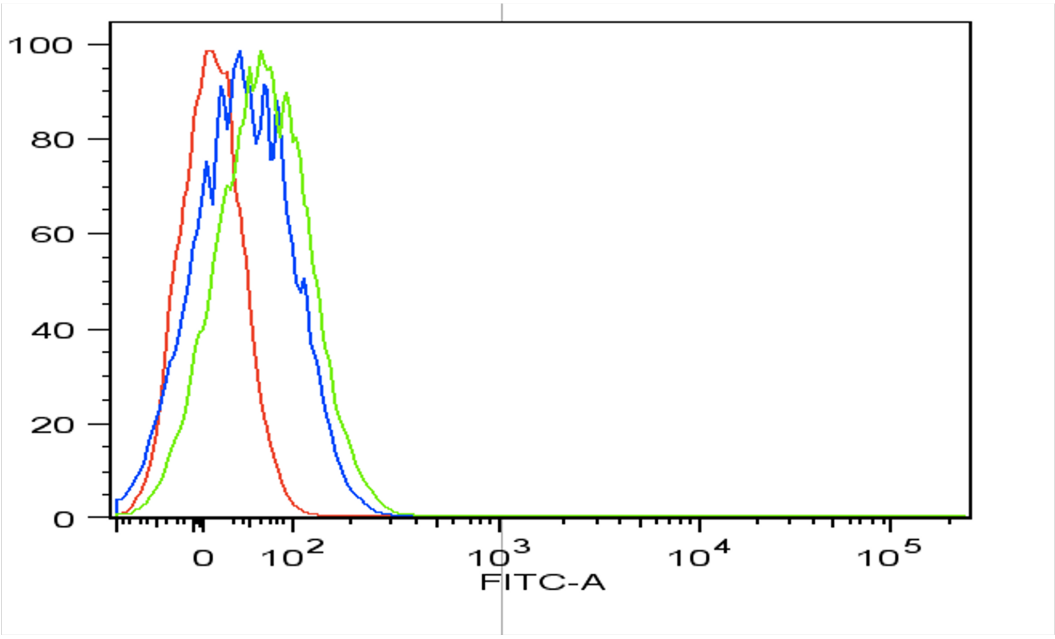

Figure 3.3. Esp452 binding to platelets. Human platelets were isolated from blood, incubated with Esp452-His and then probed with an anti-His antibody conjugated to FITC (green). Platelets (red) and platelets incubated with anti-His-FITC (blue) were measured to assess background binding and fluorescence.

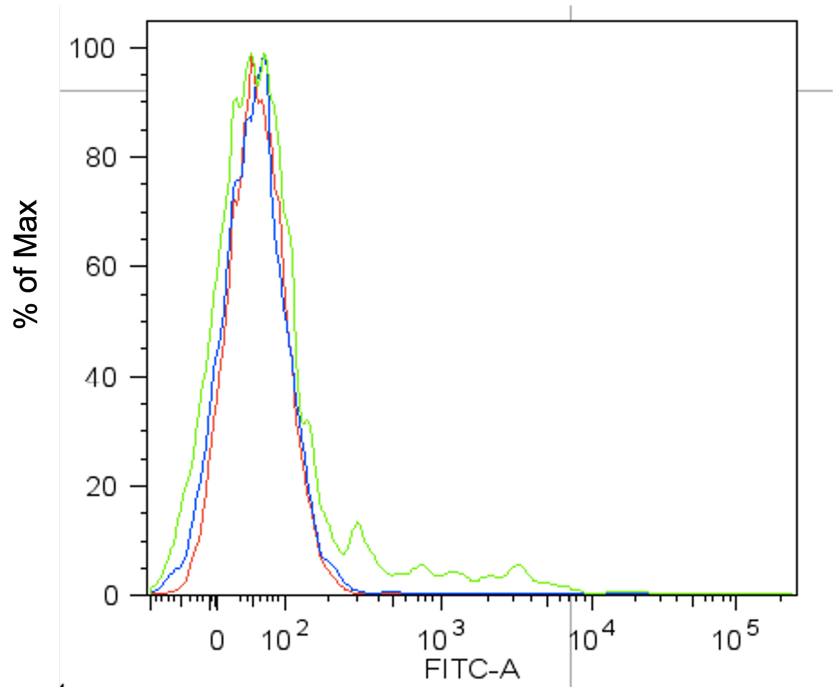

Figure 3.4. Esp452 binding to monocytes. THP-1 cells were incubated with Esp452-His and then probed with an anti-His antibody conjugated to FITC(green). Platelets (red) and platelets incubated with anti-His-FITC (blue) were measured to assess background binding and fluorescence.

After these initial experiments, I decided to use Esp743 for further experiments to ensure that I was not overlooking an effect of the remaining amino acids of the N-terminal region. To reduce the possibility of background signal from nonspecific binding of the anti-His antibodies, I cloned, expressed, and purified a construct of Esp743 with a C-terminal Avitag, which is biotinylated when co-expressed with BirA [95, 96]. I initially found that Esp743-Avitag seemed to exhibit a dose-dependent binding of both platelets and monocytes (Fig 3.5-3.6).

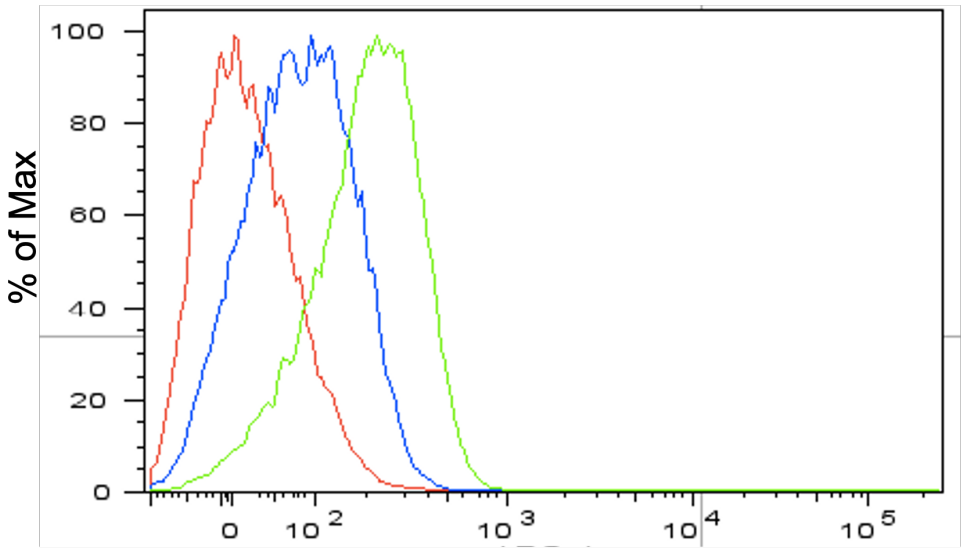

Figure 3.5. Esp743 binding to platelets Human platelets were isolated from blood, incubated with biotinylated Esp743-Avitag at either 5.0 µM (blue) or 15.0 µM (green) and then probed with Streptavidin conjugated to Cy5. Platelets with streptavidin-Cy5 only are shown in red. Fluorescence units are indicated on the x-axis.

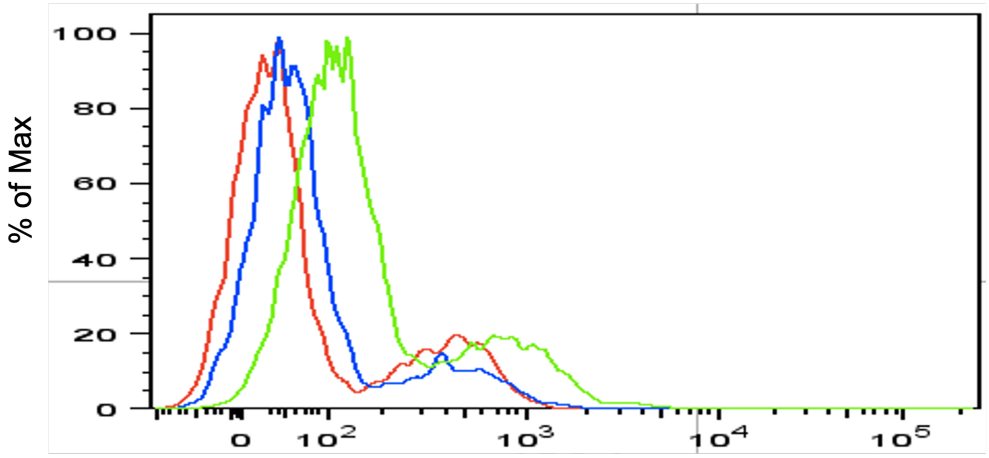

Figure 3.6. Esp743 binding to monocytes. THP-1 cells incubated with biotinylated Esp743-Avitag at either 5.0 µM (blue) or 15.0 µM (green) and then probed with Streptavidin conjugated to Cy5. Platelets with streptavidin-Cy5 only are shown in red. Fluorescence units are indicated on the x-axis.

While it seemed that Esp743 bound blood cells, it was unclear to me if I was observing a specific binding effect or general stickiness of the protein. At this point, I sought to establish if Esp exhibited preferential binding to any particular cell type, which would suggest binding to a specific target rather than weak non-specific binding to a variety of cell types. I incubated Esp743-Avitag with HEK293, 3T3, HeLa, CHO, and human platelets, washed the cells, and then added loading buffer directly to the cells and probed for the presence of Esp743-Avitag by western blot with Streptavidin-Cy5. This experiment was conducted twice and run together for analysis by western blot (Fig 3.5). No preferential binding by Esp743-Avitag was observed for any particular cell type, suggesting that Esp does not exhibit specific binding to any of the cell types tested.

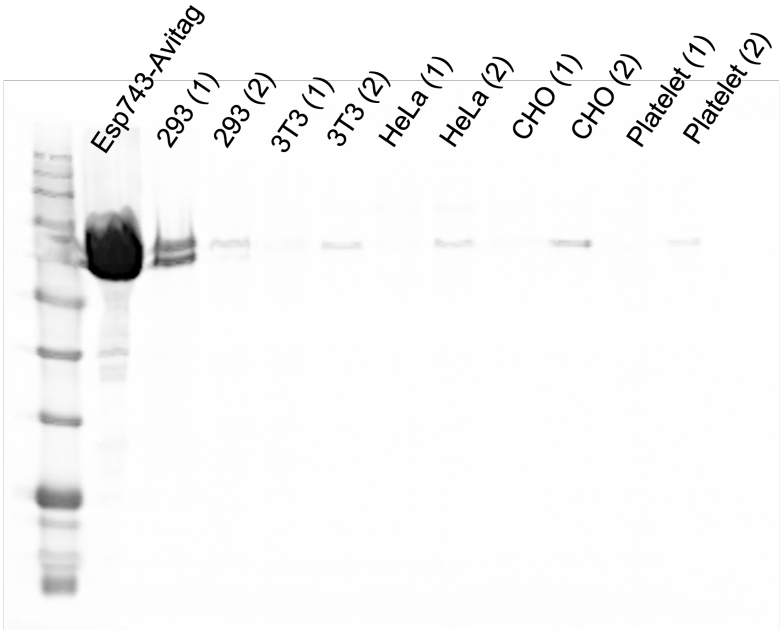

Figure 3.7. Esp743 binding to mammalian cells. Esp743-Avitag was incubated with the indicated cell lines. Cells were washed and then lysed in SDS-PAGE buffer and run on an SDS-PAGE gel. Strepavidin-Cy5 was used to detect Esp743-Avitag. The experiment was conducted twice, with replicate number in parenthesis.

It has been previously published that Esp enhances colonization of *Enterococcus* in rodent models of UTI [37, 38]. One possible explanation for this is that Esp directly mediates attachment to host tissue. We first sought to replicate these published results, in which it was reported that MMH594 was recovered at higher numbers from urinary tissue than the isogenic *esp* deletion mutant MMH594b. However, we found no difference in bacterial burden in mouse tissue or urine in a model of UTI (Fig 3.8-3.9). Due to the lack of expected enhancement of colonization, we performed flow cytometry to confirm expression of Esp on MMH594 bacteria and found that it was indeed expressed (3.10).

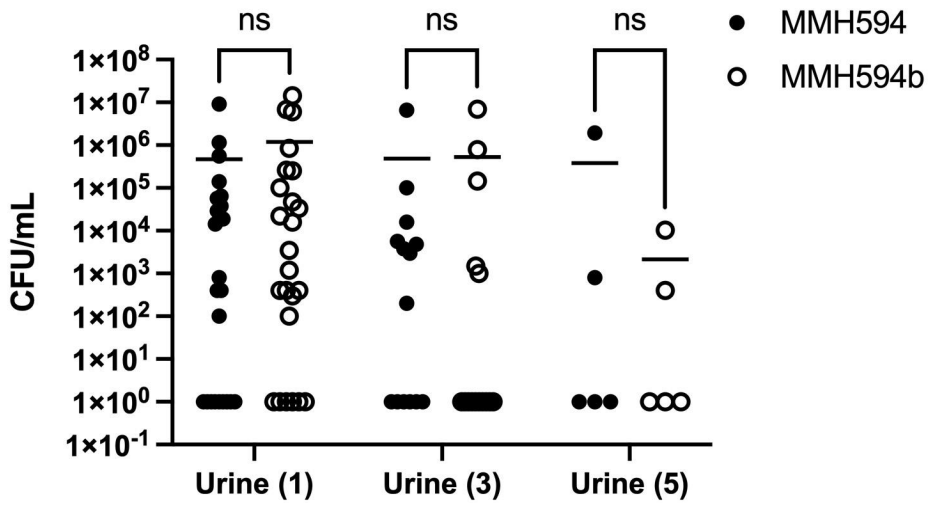

Figure 3.8 Esp has no effect on bacterial burden of urine in a mouse model of UTI. Mice were inoculated through the urethra with either MMH594 or MMH594b. Urine was collected, diluted, and plated on 1-, 3-, and 5-days post-inoculation, and data is shown as CFU/mL of urine. The experiment was performed with five mice per sample day and the experiment was performed twice for 1 and 3 days and once for 5 days. Means are indicated with horizontal lines. Samples were compared by 2-Way ANOVA with Šídák's multiple comparison test.

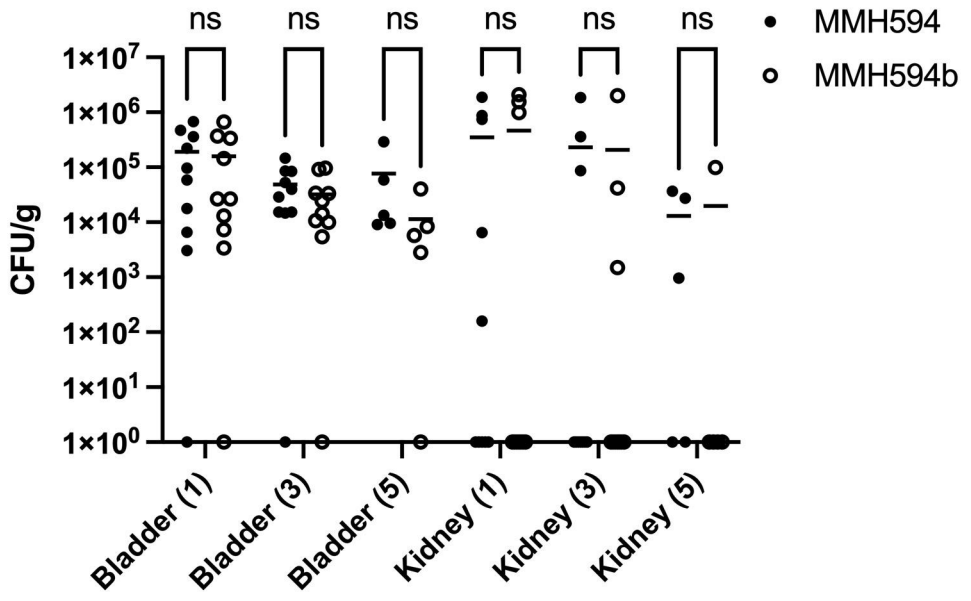

Figure 3.9. Esp has no effect on bacterial burden of urinary tissues in a mouse model of UTI. Mice were inoculated through the urethra with either MMH594 or MMH594b. At 1, 3 or 5 days after inoculation, mice were sacrificed and tissues were homogenized in PBS buffer and plated. Data is shown as CFU/g of tissue. The experiment was performed with five mice per sacrifice day and independent experiments were performed twice for 1 and 3 days and once for 5 days. Samples were compared by 2-Way ANOVA with Šídák's multiple comparison test.

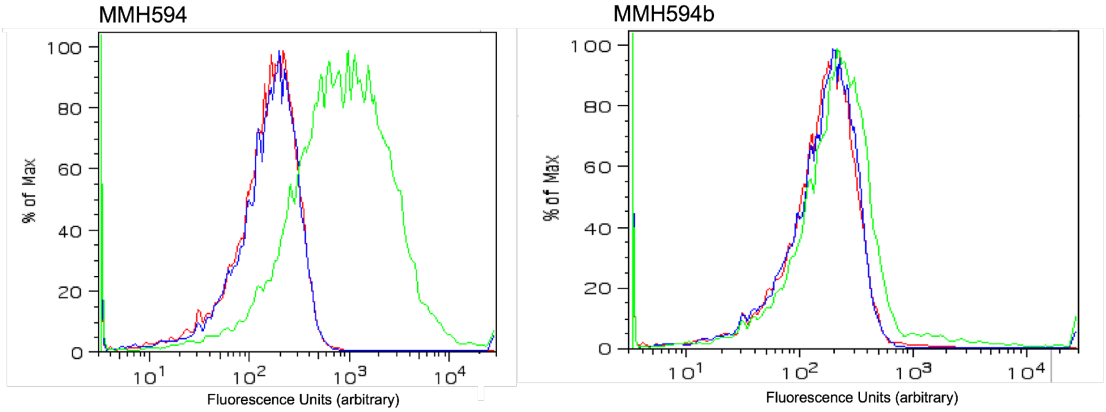

Figure 3.10. MMH594 expresses Esp. MMH594 (left) and MMH594b (right) were incubated with rabbit anti-Esp452 antibodies followed by secondary antibodies conjugated to Alexa Fluor 647 (green). Bacteria with no antibodies (red) and with secondary antibody only (blue) were measured to assess background fluorescence. Data were graphed with FloJo.

DISCUSSION

It is still unclear whether Esp plays a role in direct binding to host tissues during infection. Several studies have identified an increased bacterial burden of esp$^+$ *Enterococcus* in animal models compared to isogenic strains lacking *esp*, but the cause for this is unknown. Esp has been observed to enhance binding of *Enterococcus* to abiotic surfaces and cultured human cells, but the degree of this effect is often modest [38]. Many of the adhesins that we identified as structurally similar to Esp452 in Chapter 2 have known binding partners, and so I wanted to assess whether the N-terminal region of Esp exhibited specific binding for a particular host factor or cell type. My exploratory data indicates that Esp has some degree of binding to a variety of cell types but does not seem to exhibit preferential binding to any particular cell type. To be conclusive regarding this point, positive control experiments would need to be done for each cell type. It is possible that Esp possesses non-specific weak binding to a variety of cell types, strengthened by avidity on the bacterial surface, which aids in initial attachment of the bacteria to host tissues without a specific binding partner.

We were unable to replicate previous findings that Esp enhances colonization of the murine urinary tract. While we are unsure of the reason for this, we did confirm that MMH594 expresses Esp. The strains of *E. faecalis* and mice used in our experiments were a different combination than either of the previous studies; one used C57BL/6 mice and *E. faecium* strain E1162, and the other used CBA/J mice and *E. faecalis* strain MMH594, while our study used C57BL/6 mice and MMH594. It is possible that there are specific host factors or microenvironments required for this effect and variation between strains of *Enterococcus* or mice is the reason for the difference. Regardless, it

represents one more example of the inconsistency of results attained when assessing Esp's activity.

Katy Patras performed all mouse experiments and normalized the data. Statistical analyses were performed by me. Esp expression experiments were performed by me.

Work presented in Chapter 3 is being prepared for submission for publication. Spiegelman, Lindsey; Bahn, Adrian; Montaño, Elizabeth; Zhang, Ling; Hura, Greg; Patras, Katy; Tezcan, Akif; Nizet, Victor; Tsutakawa, Susan; and Partho Ghosh. "A portion of the N-terminal region of Enterococcal surface protein forms two Ig-like domains and stabilizes biofilms in a pH-dependent manner." Title subject to modification. I am the primary author of this work.

Chapter 4

Esp452 stabilizes enterococcal biofilms in a pH-dependent manner

INTRODUCTION

The extent of the involvement of Esp in enterococcal biofilms remains a subject of debate. Its role in biofilms was first proposed due to its 33% sequence similarity to the Biofilm Associated Protein of *S. aureus* [60]. Harboring the *esp* gene is positively associated with the ability to form biofilms by *Enterococcus* but is not required. In *E. faecalis* strains 11279 and 11262 and *E. faecium* strain 1162, biofilm production was reduced when Esp was knocked out, as measured by crystal violet staining; however, there was no effect when *esp* was knocked out in *E. faecalis* strain 54, which is a strong biofilm former [42, 60]. When transformed into *E. faecalis* strains OG1RF, FA2-2, and 23, *esp* enhanced the ability of the strains to form biofilms, as measured by crystal violet staining [40, 60]; however, there was no effect on biofilm production of *E. faecium* strain 617 when the bacteria was transformed with *esp* [61]. Enterococcal biofilm mass increases when more glucose is supplied to the bacteria, and the enhancing effect of Esp on biofilms has primarily been observed *in vitro* when glucose is supplemented in the media to 0.5% or higher [40, 62]. One report found that while the existence of *esp* was not required for biofilm formation in either clinical or environmental strains, the presence of the *esp* and the ability to form biofilms correlated only in clinical isolates of *E. faecium* and not in environmental strains [63]. Taken together, previous data suggests that *esp* sometimes enhances enterococcal biofilms, but the circumstances in and extent to which it plays a role are unclear.

MATERIALS AND METHODS

BACTERIAL STRAINS AND MEDIA

MMH594 and MMH594b were a kind gift of Mike Gilmore, as noted in chapter 3. FA2-2 was a kind gift of Gary Dunny.

CLONING AND DNA MANIPULATION

Esp1 (aa 1-241), and Esp_{DDDK} (aa 1-226) were cloned by inverse PCR from the Esp452 construct described in chapter 2 with the Agilent Quikchange II kit, resulting in the deletion of aa 242-452 and 227-452, respectively. Esp2 (aa 251-452) was cloned by inverse PCR from the Esp452 construct in the same manner, resulting in the deletion of aa 1-250. The integrity of DNA constructs was confirmed by sequencing (Genewiz).

Competent *E. faecalis* strain FA2-2 was prepared as described elsewhere [64] and electroporated with pEsp, which was a kind gift of Nathan Shankar [40].

PROTEIN EXPRESSION AND PURIFICATION

Esp constructs were expressed and purified as described in Chapter 2. Mass spectrometric analysis (ESI) of soluble Esp1 and Esp_{DDDK} produced by these constructs indicated that some of the N-terminal amino acids had been cleaved, resulting in aa 49 being the N-termini of the proteins. Fluorescent constructs for microscopy were by adding Alexa Fluor™ 647 NHS Ester (Invitrogen) to recombinant protein, according to manufacturer's recommendations.

BIOFILM ASSAY

E. faecalis MMH594 was grown on plates containing Brain Heart Infusion (BHI) agar supplemented with 20 μg/mL erythromycin (Erm), as were *E. faecalis* MMH594 (*Δesp*) (also called MMH594b) except with an additional 20 μg/mL chloramphenicol (Cm). *E. faecalis* FA2-2 were grown on plates containing BHI agar supplemented with 15 μg/mL rifampicin (Rif). Single colonies were picked from plates and grown in 5 mL shaking cultures of BHI containing either 20 μg/mL Erm or 15 μg/mL Rif overnight, and diluted to an OD_{600} of 2.7. This culture was inoculated 1:100 into 1.0 mL of Tryptic Soy Broth (TSB) containing 0.5% w/v glucose (TSBG) in a 12-well plate and grown overnight at 37 ˚C, with varying concentrations and constructs of Esp or an equivalent volume of PBS for 19-20 h. The planktonic fraction of the culture was removed by pipette. The biofilms were washed twice with 500 μL TSB, and then resuspended in 500 μL 1.5 M NaCl. The resuspensions were centrifuged (4500 x *g*, 5 min, 4 ˚C) and the supernatants discarded. Bacterial pellets were resuspended in 1.0 mL TSB, and 100 μL of each sample added to a black, clear-bottom well of a 96-well plate. Reconstituted CellTiter-Glo reagent was added to each well and samples were measured for luminescence according to manufacturer's recommendations with a TECAN well-plate reader. For DNase experiments, biofilms were grown as described above. At 19 h after inoculation, DNase II (Sigma) to a final concentration of 750 µg/mL or an equivalent volume of water (10 μL) was added to the cultures. Biofilms were incubated for an additional 3 h at 37 ˚C and then washed and harvested as described above.

For crystal violet staining experiments, bacteria were grown as described above but in 96-well plates. Biofilms were washed twice with PBS and dried inverted for 1 h

at RT. They were then stained with 0.2% crystal violet for 20 min and washed three times with water. The stain was extracted with 100 µL of 80% acetone, 20% ethanol and the OD_{595} was measured by plate reader (TECAN) or nanodrop spectrophotometer (Fisher).

THIOFLAVIN T ASSAY

For *in vitro* experiments, Esp constructs were serially diluted in a 96-well plate in either PBS, pH 7.4 or 100 mM sodium citrate, pH 4.5 containing 20 μM Thioflavin T. The plate was shaken for 60 seconds in a well-plate reader and fluorescence at 454 nm was measured, which was considered the background, then incubated for 24 h at 37 ˚C and measured again, which was considered the signal. Background was subtracted from the signal.

For biofilm experiments, Esp was serially diluted in TSBG in a 96-well plate. A culture of *E. faecalis* grown overnight was diluted to an OD_{600} of 2.7 and inoculated 1:100 into the wells. At 19-20 h after inoculation, the culture supernatant was aspirated and biofilms were washed twice with 50 μL TSB. Thioflavin T was added to each well in sodium citrate, pH 4.5 and incubated for 10 min without shaking. Fluorescence was detected by a TECAN well plate reader.

CONFOCAL MICROSCOPY

Biofilms were grown at 37 ˚C for 19-20 h in stationary culture in an 8 well chamber slide (NuncR Lab-TekTM II, Thermo Scientific) containing 250 µL tryptic soy

broth (TSB) with 0.5% glucose, 2.5 µL of *E. faecalis* MMH594b overnight culture (OD_{600} 0.027), and Esp-AF647 constructs. The biofilms were washed with 500 µL TSB, incubated with 250 µL Syto 13 (1 µM) at 37 ˚C for 15 min, and washed twice with PBS. Slides were prepared by removing the chambers, followed by the addition of 1 drop of ProlongGold antifade mounting solution, and a coverslip. Slides were cured for 2 h at RT in the dark.

Biofilms were imaged using a Leica TCS-SPE confocal system with coded DMI4000B-CS inverted microscope (Leica, Wetzlar, Germany) using a 10x/0.30 NA HC PL Fluotar dry objective. Confocal images were obtained from each sample with an average of 35 Z slices scanned with a 1.2 µm step size at a resolution of 512 x 512 pixels. Simultaneous dual-channel imaging was used to display Syto13 (green) and Alexa Fluor 647 (far red) fluorescence (nucleic acids and Esp surface protein, respectively). Emission wavelengths for green fluorescence ranged between 495-553 nm and for red fluorescence between 650-670 nm. The excitation wavelength and laser power were 488 nm and 55% for the FITC (green) emission filter and 635 nm and 30% for the Cy5 (red) emission filter. The pinhole aperture was 488 nm-128.6 µM, 1.36 AU (frame average 1) and 635 nm-94.3 uM 0.99 AU (frame average 4). The PMT detector gains and offsets used were 670 and -5 for the 488 nm laser line and 600 and -5 for the 635 laser line. Z stack images were taken for each sample; the upper and lower stacks were set by cycling through the axial range, in both directions, until no fluorescence was observed (or the image was out of focus). The stack at which no fluorescence was observed was set as the start and end of the stack. LAS AF software was used for image

acquisition and to export the data into individual image files (JPEG/TIFF). Mander's overlap coefficients were calculated with Image J.

MULTI-ANGLE LIGHT SCATTERING AND SMALL ANGLE X-RAY SCATTERING COUPLED TO SIZE-EXCLUSION CHROMATOGRAPHY

Size exclusion chromatography coupled MALS and SAXS (SEC-SAXS-MALS) were carried out at the SIBYLS beamline 12.3.1 at the Advanced Light Source [65]. Esp proteins were loaded onto a Shodex KW803 SEC column, equilibrated in 100 mM NaCl, 100 mM Tris, pH 7.2 with a flow rate of 0.5 ml/min at 20 °C. SEC eluent was split 3:1 between a SAXS flow cell and MALS cell. Three second SAXS exposures were collected continuously at wavelength of 1.127 Å, and with a sample-to-detector distance set of 2.1 m. Scattering from buffer fractions following the protein peak were averaged and used for subtraction of background. Based on SEC UV and total intensity of the SAXS curve, the proteins composed one major peak. SAXS frames with consistent Rg were merged for further analysis. MALS was measured on an 18-angle DAWN HELEOS II light scattering detector connected in tandem to an Optilab refractive index concentration detector (Wyatt Technology). The MALS was calibrated with BSA (45 µl, 10 mg/ml) in the same run, and data processed with ASTRA Version 6.1.6.5 (Wyatt Technology) with d*n*/d*c* set at 0.19. SEC-SAXS data was analyzed on SCÅTTER (https://bl1231.als.lbl.gov/scatter/); GNOM (ATSAS package) [66], and FOXS/ FOXSDOCK [67].

Precipitation Assay

Sodium citrate buffer (100 mM) was prepared over a range of pH, and 50 μg of Esp construct was incubated in 100 μL of buffer in a well of a 96-well plate for 1.5 h at 37 ˚C. The wells were washed two times with water before photographing or staining. For staining experiments, the wells were dried upside down for 1 h at RT and then stained with crystal violet as described above for biofilm experiments.

RESULTS

ESP452 STABILIZES *E. FAECALIS* BIOFILMS AGAINST WASHING.

Whether Esp affects biofilm production in the MMH594 strain had not been reported. Therefore, we examined this using a standard crystal violet staining assay, and found no difference in biofilm production between wild-type MMH594 and an isogenic strain lacking Esp, MMH594b (Fig. 4.1). Biofilm production by Esp in *Enterococcus* strain OG1RF had been reported to be promoted by glucose [40], and indeed we observed increased biofilm production in the presence of glucose, but no difference between wild-type MMH594 and the isogenic Esp deletion (Fig. 4.2).

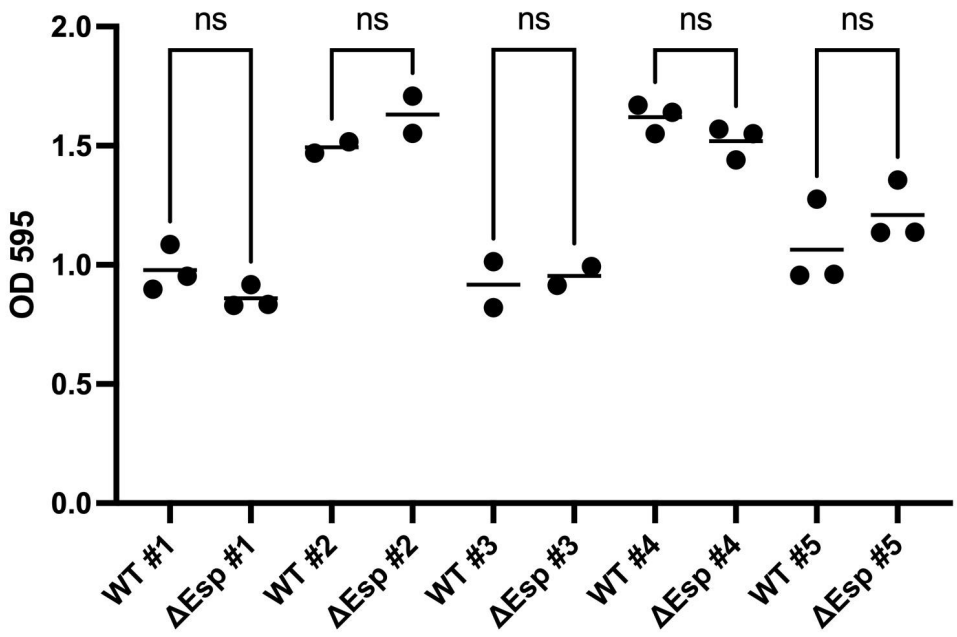

Figure 4.1 Biofilm production of MMH594 and MMH594b. Absorbance at 595 nm of crystal violet-stained biofilms generated by *E. faecalis* strain MMH594 or the isogenic Esp mutant in TSB + 0.5% glucose. Results from five independent experiments are shown. Samples were compared by student's t-test for each experiment.

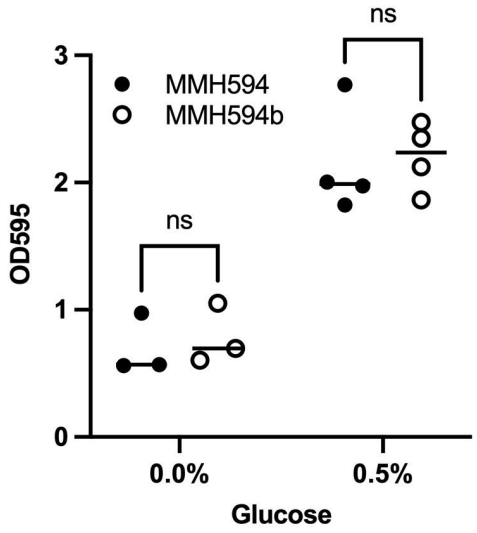

Figure 4.2. The effect of glucose on MMH594 and MMH594b biofilms. The absorbance at 595 nm of crystal violet-stained biofilms grown with or without 0.5% glucose in TSB. Samples were compared by student's t-test.

It was also reported that Esp enhances attachment of *E. faecalis* to polystyrene, and that the N-terminal region of Esp is necessary and sufficient for Esp-dependent biofilm formation *in vitro* [42, 61]. I therefore wondered if N-terminal fragments of Esp might competitively inhibit the ability of MMH594 to attach to polystyrene wells, and to test this, added recombinant Esp452 to biofilm cultures at the start of inoculation. After 19 hours of incubation at 37 °C, the culture was observed to form a biofilm. I found, surprisingly, that crystal violet staining increased 4-fold when cultures were supplemented with Esp452 (Fig. 4.3).

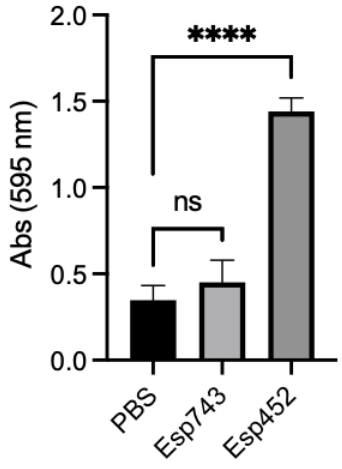

Figure 4.3. Crystal violet staining of biofilms grown with recombinant Esp. Absorbance at 595 nm of crystal-violet stained biofilms supplemented with PBS, Esp743, or Esp452. Samples were compared by 1-Way ANOVA and Tukey's multiple comparison test. ****, $p < .0001$

We realized that this additional staining might be a direct result of the addition of protein, necessitating a different type of measurement to explore a potential functional role of Esp in biofilms, and decided instead to assay the amount of bacteria remaining on the plate after washing.

To determine whether Esp had an effect on biofilms aside from increased staining, fragments of the Esp N-terminal domain were added to stationary cultures of *E. faecalis* which had been placed in polystyrene wells to form biofilms. To eliminate any confounding effect of native Esp, only the *Δesp* strain was used for the remaining experiments. To some wells, Esp452 was added and to others $Esp_{453\text{-}743}$, which encompasses the remaining portion of the N-terminal domain of Esp; as a control, PBS was added to other wells. To determine the bacterial content of biofilms, culture supernatants containing planktonic bacteria were removed from biofilms, and biofilms were washed twice. Biofilms were then solubilized with 1.5 M NaCl [68] and collected. Bacteria in each fraction were enumerated based on ATP content, which was quantified by luminescence generated by an ATP-dependent reaction catalyzed by firefly luciferase. The relationship between bacterial optical density (OD_{600}) and ATP-dependent luminescence was verified to be linear (Fig. 4.4).

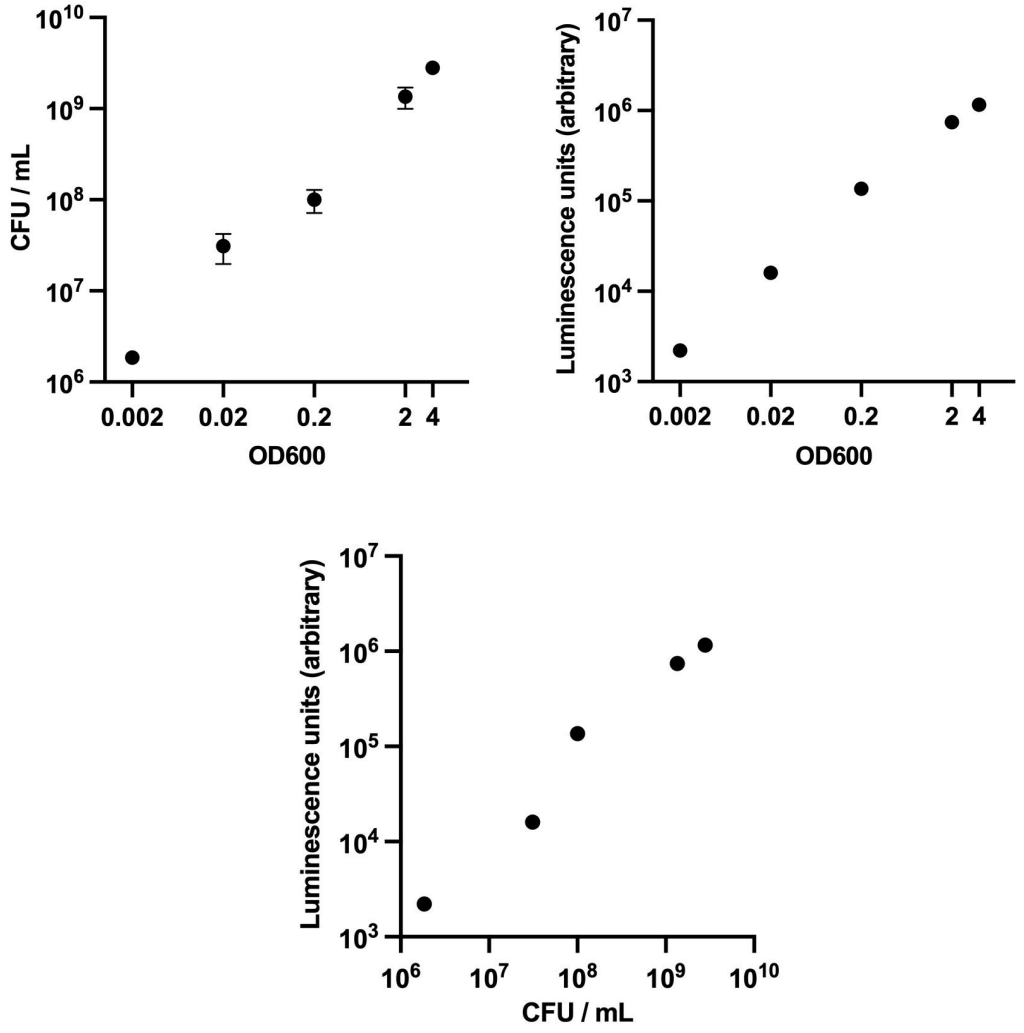

Figure 4.4. The relationship between OD600, CFU, and luminescence.
The OD_{600}, luminescence, and CFU/mL of serial dilutions of *E. faecalis*. The OD_{600} and CFU/mL (top left), OD_{600} and luminescence signal (top right), CFU / mL and luminescence signal (bottom) are shown as dot plots. The Pearson correlation coefficient was 0.99 and $p < 0.01$ for all three graphs.

T

There was no difference in total luminescence for biofilms grown with the addition of PBS, Esp452, or $Esp_{453\text{-}743}$ (Fig. 4.5), indicating that these treatments had no effect on bacterial number. Total luminescence values varied randomly between experiments. Numerous factors contributed to raw luminescence values, such as the age of the reagent, the temperature of the reagent at the time of data collection, and the length of time between thawing the reagent stock and measurement.

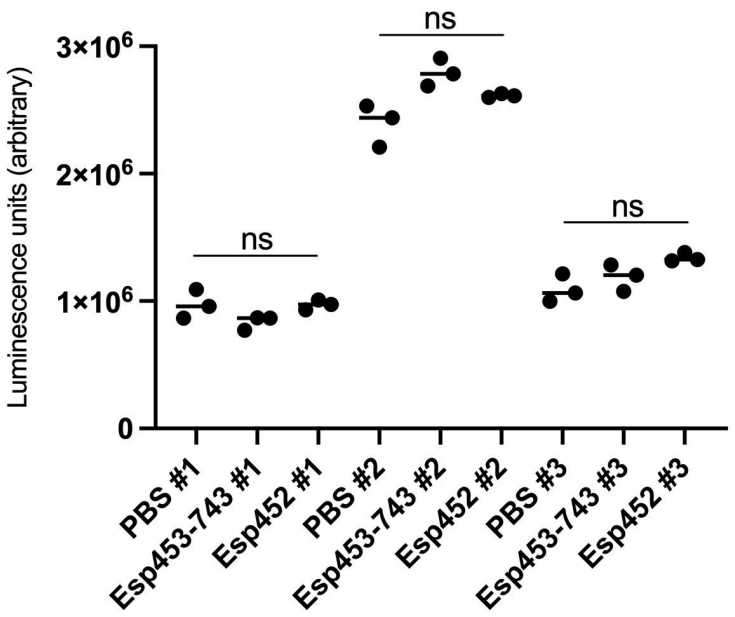

Figure 4.5. Total luminescence of biofilm cultures supplemented with PBS, $Esp_{453\text{-}743}$, or Esp452. The total luminescence values of each well in three independent experiments are shown. Samples in each experiment were compared by Welch's ANOVA with Dunnett T3 post hoc test.

Likewise, no difference in luminescence for planktonic fractions was observed for these three treatments. However, a statistically significant difference was observed for the two wash fractions, in which fewer bacteria were washed away from the biofilm supplemented with Esp452 as compared to the biofilms supplemented with $Esp_{453\text{-}743}$ or PBS (Fig. 3.5). Consistent with this result, significantly more bacteria were recovered from the biofilm supplemented with Esp452 as compared to those supplemented with $Esp_{453\text{-}743}$ or PBS (Fig. 4.6). These results indicate that Esp452 stabilizes biofilms against mechanical disruption (i.e., washing).

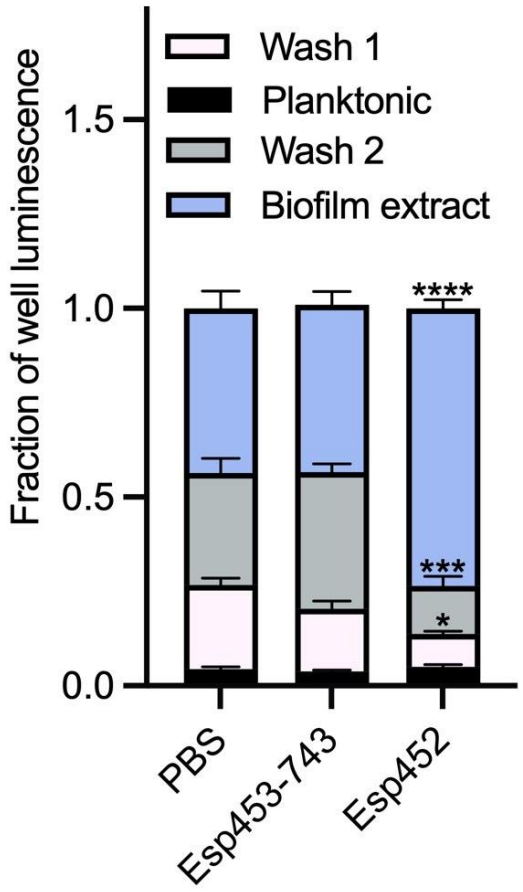

Figure 4.6. **Luminescence of enterococcal biofilms supplemented with Esp452**
Proportion of total luminescence generated by the planktonic fraction, wash fractions, or biofilm fraction of *E. faecalis* biofilms supplemented with PBS, $Esp_{453\text{-}743}$ or Esp452 and grown overnight. Bacteria in each fraction were lysed and ATP was quantified with luciferase. Samples were collected in triplicate for each of three independent experiments. Each luminescence measurement was divided by the total luminescence of the corresponding well. The standard error of the mean (SEM) is indicated with error bars. Esp453-743 and Esp452 fractions were compared to the corresponding PBS fraction by Welch's ANOVA and D3 Dunnett's post hoc test. All significant results are indicated on the graph. * $p < 0.01$, *** $p < 0.0001$, **** $p < 0.00001$

This effect of Esp452 on biofilm resistance to washing was dose-dependent. The results described above were carried out at 4.0 μM Esp452 or $Esp_{453-743}$. We found that 4.0 μM Esp452 was saturating and that the EC_{50} was approximately 740 nM (Fig. 4.7). In comparison, the addition of Esp453-743 at the higher concentration of 8 μM continued to have no effect on biofilms as compared to the addition of PBS.

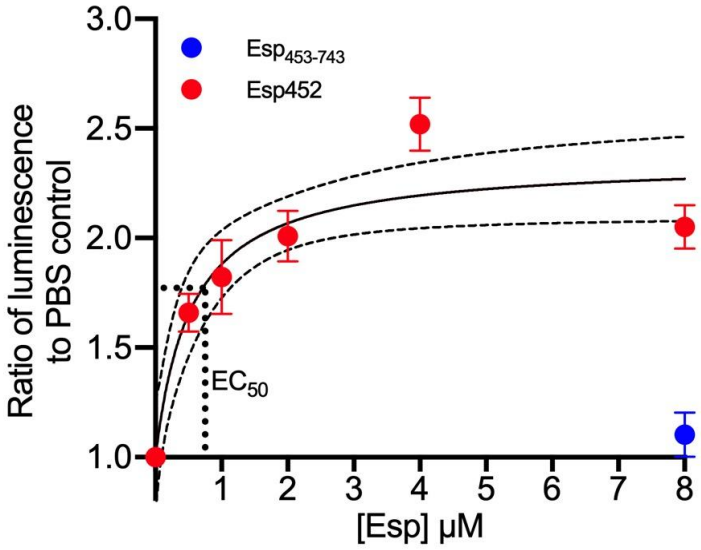

Figure 4.7. Dose-response curve of Esp452 on Enterococcal biofilms. Luminescence of biofilms to which Esp452 was added (red circles) at varying concentrations, divided by the average luminescence of biofilms to which PBS was added. The SEM is indicated with error bars. The 95% confidence interval (CI) of the dose-response curve is indicated in dashed lines. The EC_{50} is indicated with dotted lines.

Biofilm formation occurs in stages, beginning with attachment and initiation of biofilm matrix production [19]. We wondered if the stabilization provided by Esp452

was contingent upon its presence during the attachment and initiation phases. To test this, we first grew biofilms, then added PBS, $Esp_{453-743}$, or Esp452, and incubated the mixture for up to 3 hours (Fig. 4.8). Contrary to previous literature indicating that Esp is involved in initial attachment, we found that Esp452 did not need to be added at the attachment and initiation phases, and was capable of stabilizing pre-existing biofilms [60]. The stabilizing effect of Esp452 required more than 15 minutes and at most 60 minutes.

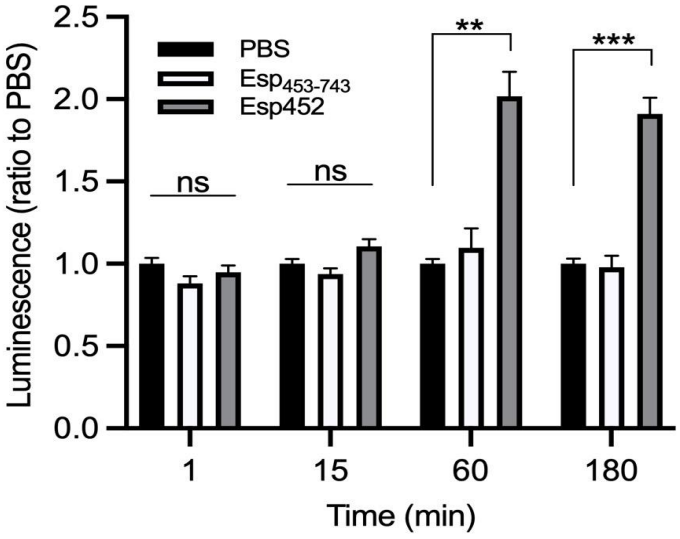

Figure. 4.8. Timecourse of Esp452 stabilization of enterococcal biofilms. Luminescence of biofilm extracts from biofilms to which PBS (black), $Esp_{453-743}$ (white), or Esp452 (gray) were added for the indicated time before washing and extraction. Values were normalized at each time point to the luminescence of the PBS sample. The SEM is shown with error bars. The samples were compared by Welch's ANOVA with Dunnett's T3 post hoc test. ** $p < 0.001$, *** $p < 0.0001$

We next asked if Esp452 possessed the capacity to strengthen biofilms against other types of perturbation besides mechanical stress (i.e., washing), such as enzymatic degradation by DNase. Enterococcal biofilms contain extracellular DNA and can be degraded by exposure to DNase [25, 69]. We found that enterococcal biofilms supplemented with Esp452 were significantly resistant to destruction by DNase, exhibiting only a 23.0% reduction in bacterial counts in biofilms after washing, compared to a 42.2% reduction when supplemented with PBS (Fig. 4.9). Biofilms supplemented with $Esp_{453\text{-}743}$ were not significantly different from biofilms supplemented with PBS. These data suggest that Esp452 is capable of protecting enterococcal biofilms from disruption caused by DNase.

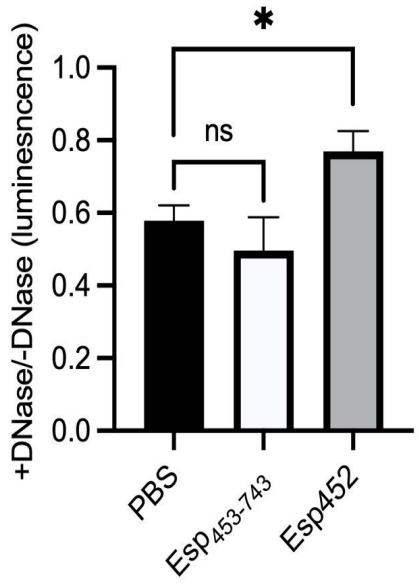

Figure 4.9. Resistance of Enterococcal biofilms supplemented with Esp452 to DNase treatment. Luminescence of biofilms grown overnight with PBS, $Esp_{453\text{-}743}$, or Esp452, and incubated with DNase II for 3 hours before washing and extraction, divided by luminescence of biofilms grown identically but with water added instead of DNase. The experiment was conducted with duplicates in at least three independent experiments. The SEM is indicated with error bars. Samples were compared by 1-Way ANOVA with Tukey's multiple comparison test. * $p < 0.05$

ESP452 FORMS AMYLOID-LIKE FIBRILS AT ACIDIC PH

I next decided to probe the mechanism by which Esp452 enhances biofilm stability. It has been previously reported that the effect of Esp on enterococcal biofilm production in strains OG1RF and FA2-2 is glucose-dependent [40]. I observed this to be true for MMH594b, finding a biofilm-stabilizing effect of Esp452 in media supplemented with 0.50% but not lower (0.18%) glucose concentration and of $Esp_{453-743}$ in neither condition (Fig. 4.10). *Enterococcus* acidifies its media when fermenting glucose, and we found the pH of the liquid overlaying the biofilm to be 4.5 for 0.50% glucose and 5.5 for 0.18% glucose (Fig. 4.11). The addition of Esp truncation fragments ($Esp_{453-743}$ or Esp452) had no effect on the pH of the cultures.

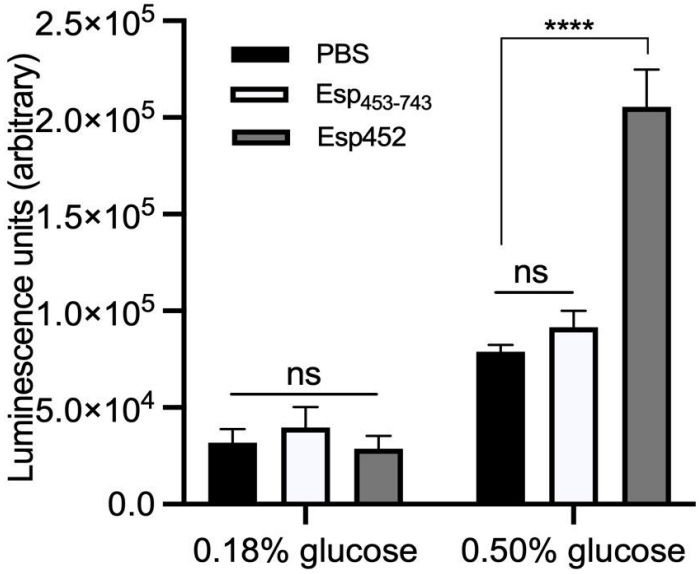

Figure 4.10. Effect of Esp452 at different glucose concentrations. The luminescence of biofilms supplemented with PBS, Esp453-743, or Esp452. Samples from three independent experiments were compared by 2-way ANOVA and Tukey's test.

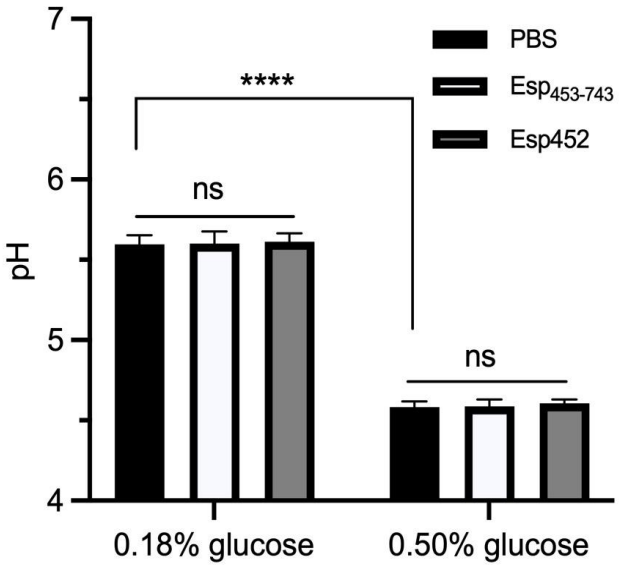

Figure 4.11. pH of Enterococcal cultures. The pH of biofilm cultures of *E. faecalis* grown in TSB with 0.18 or 0.50 % glucose, supplemented with Esp452, $Esp_{453-743}$, or PBS. Samples from three independent experiments were combined and compared by 2-way ANOVA and Tukey's test.

It was recently reported that a portion of the N-terminal region of Esp at low pH (4.2) binds Thioflavin T (ThT), a fluorescent dye that exhibits an emission shift when bound to β-rich protein aggregates such as amyloid fibrils [70]. Antigen I/II, a structural homologue of Esp452, has also been observed to form amyloid-like fibrils [71]. We found that ThT fluorescence of enteroccocal biofilms increased in a dose-dependent manner when supplemented with varying concentrations of Esp452, but not $Esp_{453-743}$ (Fig 4.12).

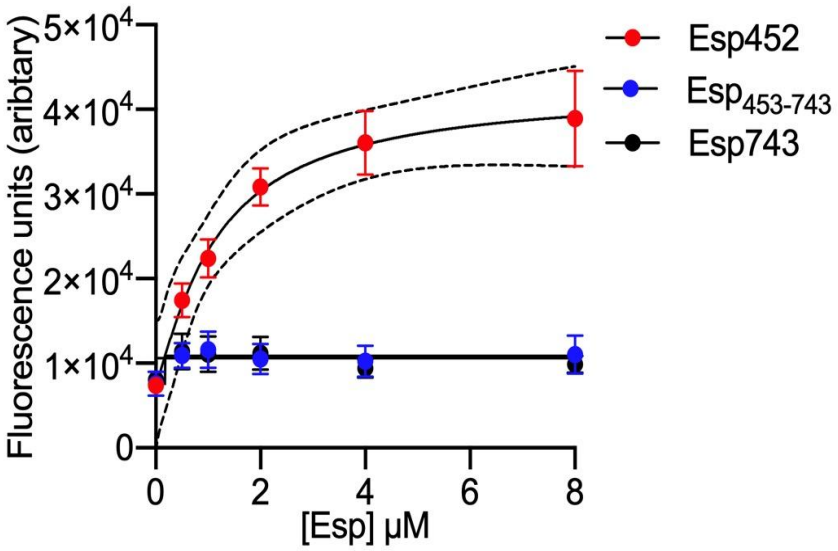

Figure 4.12. ThT signal of Enterococcal biofilms supplemented with Esp. Fluorescence of ThT added to biofilms that were supplemented with Esp452, $Esp_{453-743}$, or Esp743. Fluorescence measurements from three independent experiments were combined. The SEM is indicated with error bars. The 95% CI for the dose-response curve of Esp452 is shown as dashed lines.

As mentioned previously, I was unable to detect a difference between wild type *E. faecalis* strain MMH594 and the Δ*esp* strain, leading us to wonder if the entire N-terminal region is able to strengthen biofilms. I tested the full-length N-terminal region, Esp743, to compare its activity to Esp452. I found that Esp743 had no biofilm-enhancing effect compared to biofilms supplemented with PBS, in contrast to Esp452 (Fig 4.13). It also did not bind ThT on enterococcal biofilms (Fig 4.12).

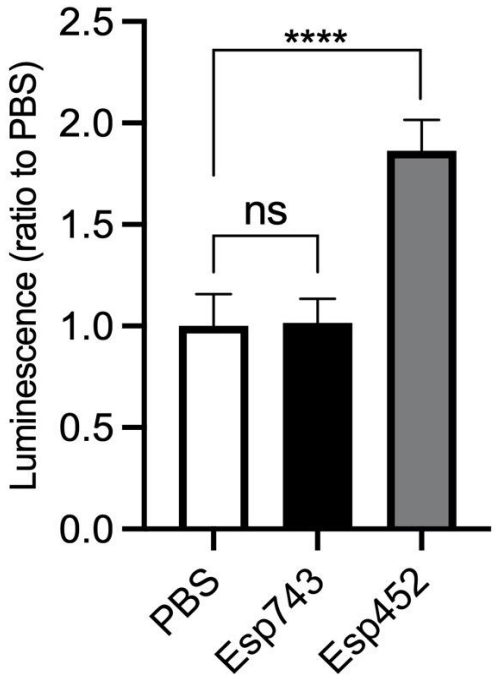

Figure 4.13. Esp743 has no effect on enterococcal biofilms. Luminescence of biofilms grown overnight with PBS, Esp743, or Esp452, divided by the average luminescence of the PBS samples. The experiment was conducted with triplicates in three independent experiments. The SEM is indicated with error bars. Samples were compared by Welch's ANOVA and D3 Dunnett's post hoc test. **** $p < 0.0001$

I next wondered if Esp452 colocalized with enterococcal biofilms, and if so, if Esp743 might be capable of binding the biofilms but simply have inhibited activity. To test this, I supplemented enterococcal biofilms with fluorescently-labeled Esp constructs and used confocal to examine them. These data revealed that Esp452, but not Esp743, colocalized with enterococcal biofilms, with Mander's overlap coefficients (MOC) of 0.42 and 0.03, respectively (Fig 4.14). I also found that the presence of Esp452 was higher at the surface of the biofilm facing the culture supernatant than at the center or the surface attached to the slide (Fig 4.15).

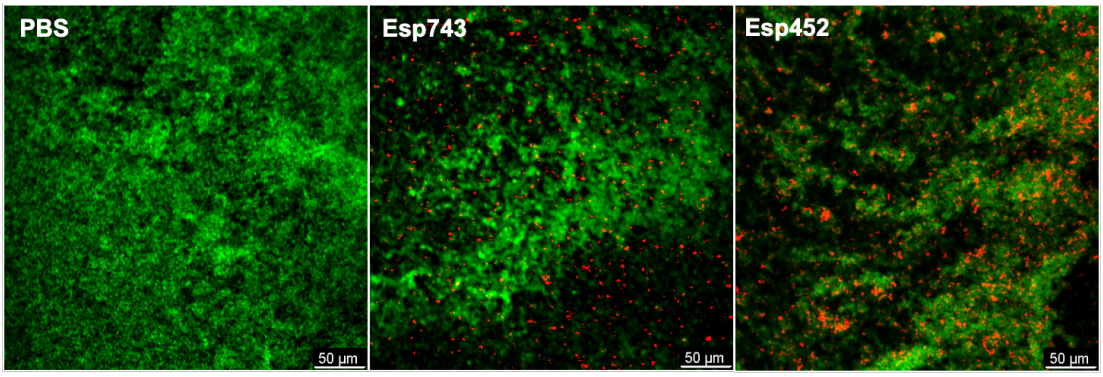

Figure 4.14. Fluorescent images of Enterococcal biofilms with supplemented Esp. Confocal microscopy images of *E. faecalis* biofilms supplemented with PBS, Esp743-AF647 or Esp452-AF647 (red). Biofilms were stained with Syto-13 (green). The images represent the Z-stacks with the highest number of red pixels.

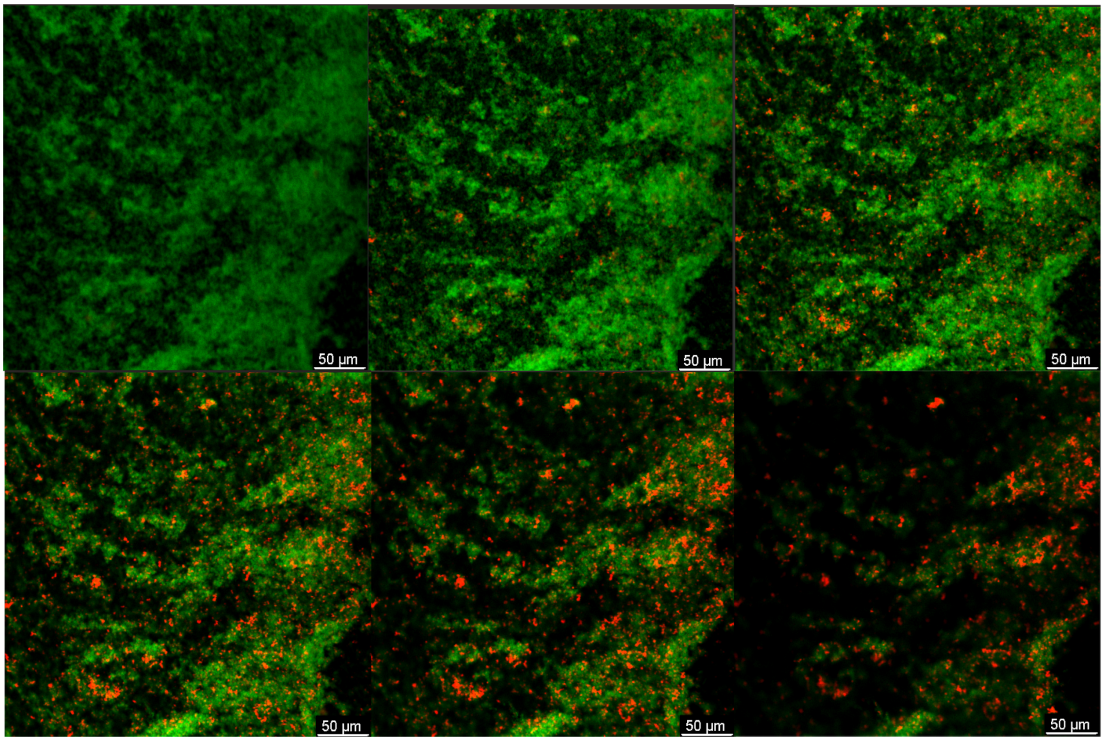

Figure 4.15 Esp452 is localized at the middle and surface of the biofilm. Z-stacks were numbered starting at the interface of the biofilm and the slide and increased in number towards the media-facing surface. Z-stack images 9, 18, 22, 25, 29 and 36 are shown from left to right, top to bottom.

We found that acidic buffer was sufficient to cause precipitation of Esp452 in a well plate, observing protein deposited on the plate at pH 4.6 and in increasing amounts down to pH 4.2 (Fig 4.16). No precipitation of Esp743 was observed within this range.

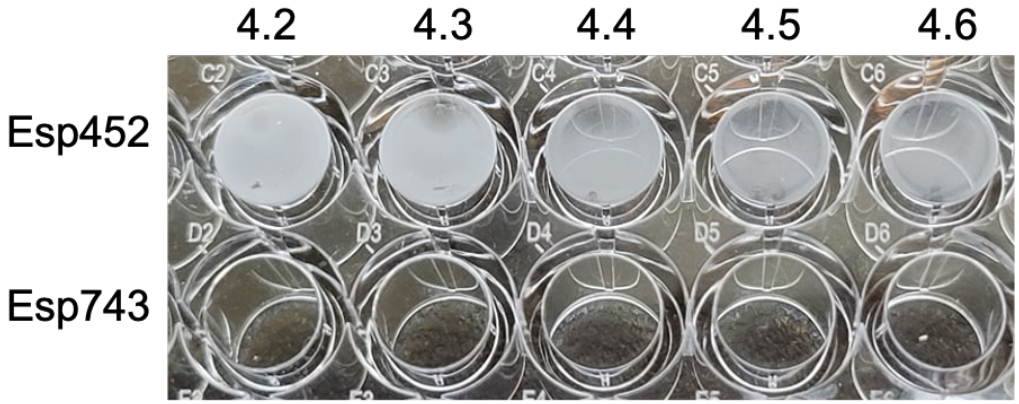

Figure 4.16. Esp452 and Esp743 precipitation at acidic pH. Fifty µg of Esp construct per well was incubated in each well for 1.5 h at 37˚ C in buffer at the indicated pH.

While acidic buffer was sufficient to cause precipitation of Esp452, it remained possible that glucose played a direct or indirect role besides acidic pH in the generation of fibril formation. To test whether acidic pH is sufficient to generate fibril formation, we incubated either Esp452 or Esp743 in solution at pH 4.5 or 7.4 (Fig. 4.17). At pH 7.4, neither protein construct bound ThT. At pH 4.5, Esp452 bound ThT in a dose-dependent manner, demonstrating that acidic pH is sufficient for fibril formation by Esp452. No ThT binding was observed at acidic pH for Esp743.

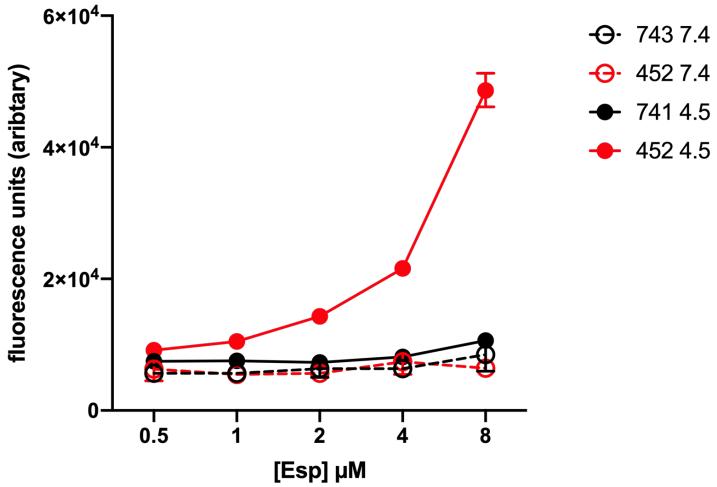

Figure 4.17 ThT-binding by Esp452 is pH-dependent. The fluorescence of varying concentrations of Esp452 (red) and Esp743 (black) incubated with ThT in neutral (open circles) or acidic (close circles) buffer. Data from three independent experiments were combined, and the SEM is shown with error bars.

ESP452 MAY BE STABILIZED FROM UNFOLDING BY STABILIZING CONTACTS WITH ANOTHER DOMAIN.

I wondered if there might be stabilizing interactions between Esp452 and the additional region contained in Esp743 which might inhibit the unfolding of the amyloid-forming region and would explain the stability of Esp743 at lower pH. Since I was unable to obtain structural information of Esp743 through X-ray crystallography, we elected to use size-exclusion chromatography small angle X-ray scattering (SEC-SAXS) to ask whether there were interactions between Esp452 and the C-terminal domains of Esp743 by comparing the structures of Esp452, $Esp_{453\text{-}743}$ and Esp743.

We first compared the SEC-SAXS data of Esp452 to its crystal structure. The extended SAXS data indicated an oblong shape rather than the rounded globular structure of the crystal structure, with a χ^2 fit of 110 (Fig. 4.18). A perfect fit would have a χ^2 of 1. As the SAXS data indicated a well-folded structure, we hypothesized that there was only a single conformation in solution and that the two domains in the crystal structure were shifted relative to their position in the crystal structure. Using the docking program FOXSDOCK, we identified several conformations that fit the SAXS data with a much better χ^2 fit of 3.5-4, as compared to the χ^2 fit of 110 to the crystal structure. No single conformation stood out, indicating that using SAXS alone was not sufficient to identify the conformation occurring in solution, or that the protein may adopt multiple conformations.

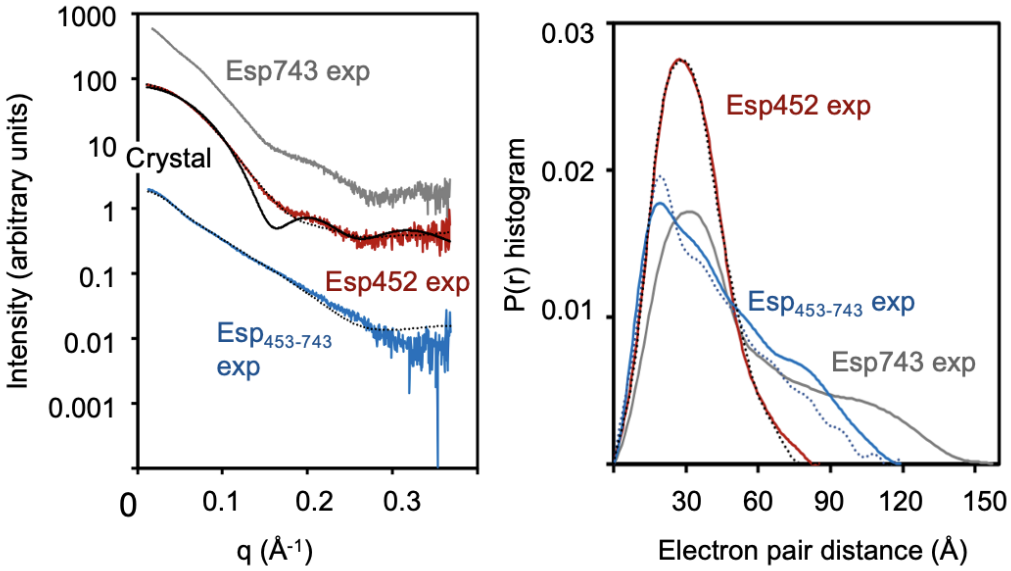

Figure 4.18. SEC-SAXS data for Esp constructs. (Left) In reciprocal space, Esp experimental SAXS data (exp, colored) is overlaid with SAXS curves calculated for Esp452 crystal structure (black solid) or models (black dash). (Right) Same as left, except in real space and only experimental data and SAXS curves predicted from models are shown. Curves normalized for area under the curve.

SAXS data of $Esp_{453\text{-}743}$ were consistent with an extended, multidomain structure, as can be seen in the SAXS-based *ab initio* shape prediction (Fig 4.19). *In silico* prediction using the Phyre server indicates that $Esp_{453\text{-}743}$ is composed of multiple Rib domains, similar to the Rib domains seen in Group B *Streptococcus*. With alterations in the domain interface of this *Streptococcus agalactiae* structure, a reasonable fit to the SAXS data was obtained (χ^2=4.4) and fit within the SAXS-based *ab initio* shape prediction. The structure is relatively flexible with a Porod's exponent of 2.5.

SEC-SAXS data for Esp 743 indicated that the protein is well folded (P_x=3.8) and shows a globular region with an extended tail. The extended tail is shorter than the

length of the SAXS model for Esp453-743 and the PHYRE prediction. Both SAXS models of Esp452 and $Esp_{453-743}$ can be accommodated if the N-terminal domain of Esp453-743 is placed as part of the globular region of Esp452. The Porod exponent and volume of Esp743 are consistent with a more condensed structure than Esp452 and Esp453-743 laid end to end, suggesting interactions between the N-terminal 452 portion of the protein and Esp453-743.

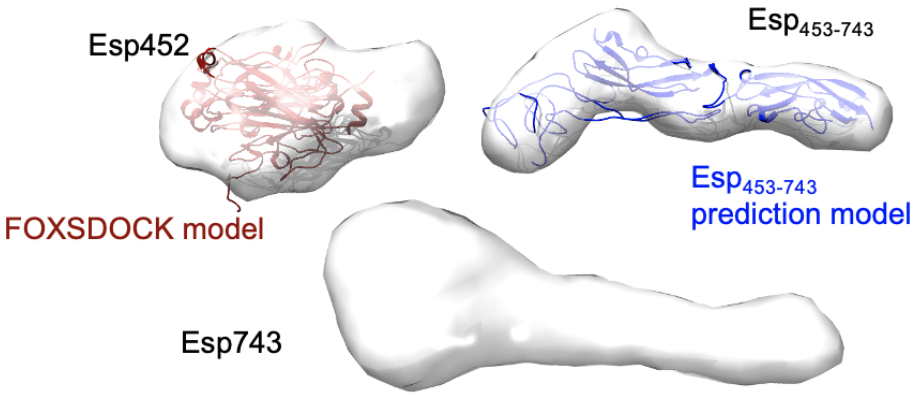

Figure 4.19. Shape reconstructions of Esp constructs from SAXS data. GASBOR shape reconstructions of Esp452, Esp743, and $Esp_{453-743}$ overlaid with Esp452 FOXSDOCK model or $Esp_{453-743}$ prediction model.

Taken together, these data indicate that there are contacts between the regions comprising Esp452 and Esp453-743, which may influence the ability of Esp452 to unfold and form amyloid-like fibrils.

Potential Mechanisms of Esp Activation

There was no difference in the effect of Esp452 between wild-type MMH594 and the *esp* deletion mutant MMH594b, suggesting that Esp expressed by MMH594 did not confer any additional biofilm strength compared to the knockout strain (Fig. 4.20).

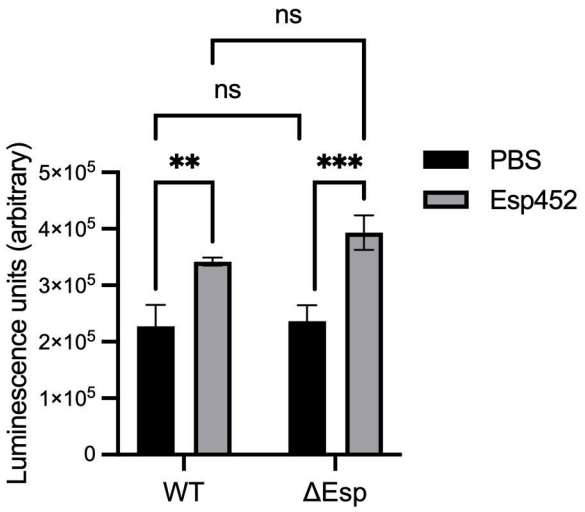

Figure 4.20. Effect of Esp452 on wild-type and Δ*esp* *E.* faecalis MMH594. Luminescence of biofilms grown from MMH594 or the isogenic *esp* deletion mutant with and without 2 μM Esp452. Samples were compared by 2-Way ANOVA with Tukey's multiple comparison test. **, $p < .01$; ***, $p < .001$

It was previously published that supplying *esp* on a vector to strain FA2-2 improves biofilm production. We wondered if the difference in activity could be due to a difference in pH reached by different strains of *Enterococcus*. We found that FA2-2 biofilm cultures reached a pH ranging from 3.9-4.2, compared to MMH594 which reached a pH range of 4.3-4.5. We also found that Esp743 strengthened the biofilms of FA2-2, compared to a PBS and Esp453-743 control, but did not have an effect on MMH594b biofilms (Fig. 4.21-4.22).

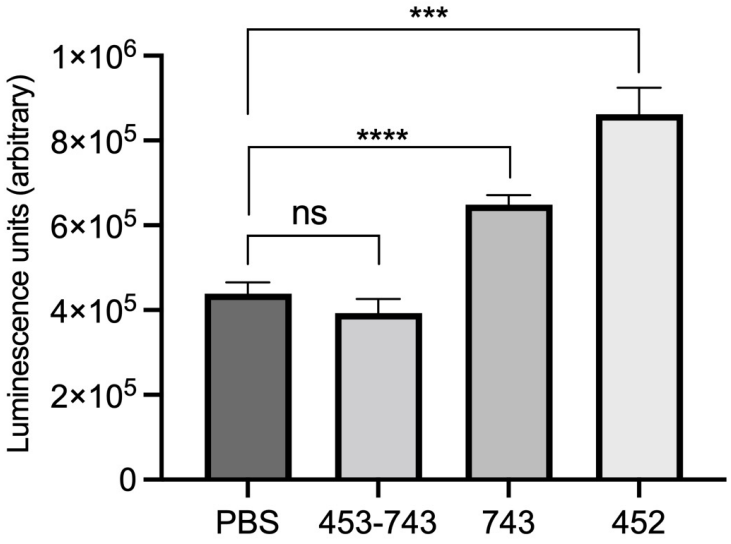

Figure 4.21. Effect of Esp constructs on FA2-2 biofilms. Luminescence of FA2-2 biofilms grown overnight with PBS, $Esp_{453-743}$, Esp743, or Esp452. The experiment was conducted with duplicates or triplicates in two or more independent experiments, with n ranging from 5 to 15. The SEM is indicated with error bars. Samples were compared by Welch's ANOVA and D3 Dunnet's post hoc test. $p < 0.001$, ***; $p < 0.0001$, ****

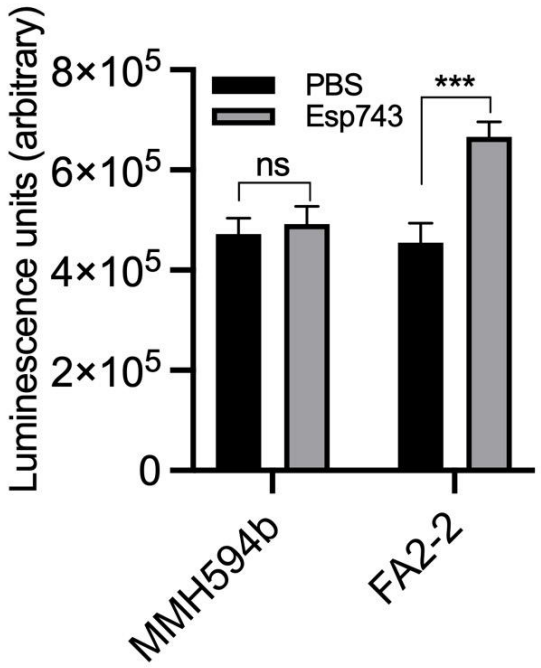

Figure 4.22. Effect of Esp743 on enterococcal biofilms produced by two different strains. Luminescence of biofilms grown overnight with PBS or Esp743. The experiment was conducted with triplicates in three independent experiments. The SEM is indicated with error bars. Samples were compared by 2-Way ANOVA and Tukey's test. *** $p < 0.001$

Another possible mechanism for activation of Esp's N-terminal region is cleavage of an active fragment from the rest of the protein on the cell surface. We sought to determine if proteolytic cleavage of Esp743 would generate an active fragment of the protein. Cleavage by trypsin and chymotrypsin generated a primary band pattern of three products, which were analyzed by MS/MS and determined to be equivalent to the first Ig domain, Esp1, the remaining amino acids generated by cleaving Esp1 from Esp743, and a fragment similar to $Esp_{453\text{-}743}$.

We tested both DEv-Ig domains, Esp1 and Esp2, for precipitation in acidic buffers, and found surprisingly that neither precipitated significantly, in contrast to Esp452 (Fig. 4.23-4.24). Biofilms supplemented with Esp1 and Esp2 did not exhibit any additional staining with crystal violet compared to biofilms supplemented with PBS or Esp743, or a BSA control. Additionally, I tested Esp1 for biofilm stabilization and found that it had no effect compared to $Esp_{453-743}$ (Figure 4.25). This indicates that different fragments require different levels of acidity to unfold.

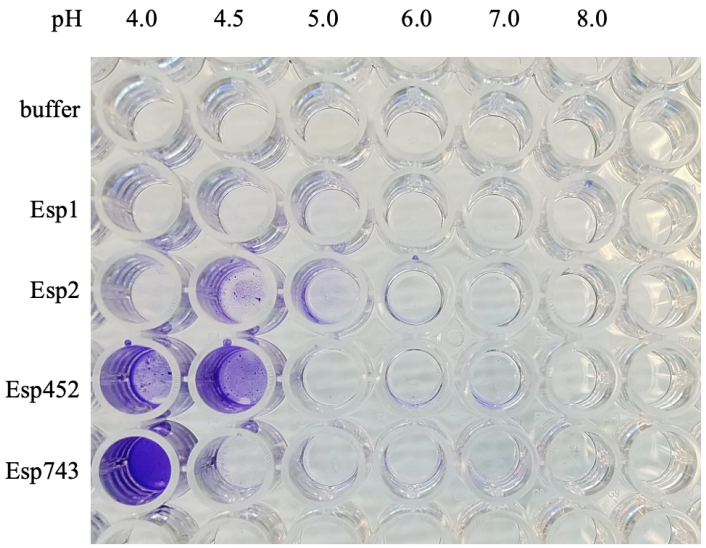

Figure 4.23. Differential precipitation of Esp fragments at acidic pH. Equivalent amounts of Esp were incubated in buffer at the indicated pH. Wells were washed and then stained with crystal violet.

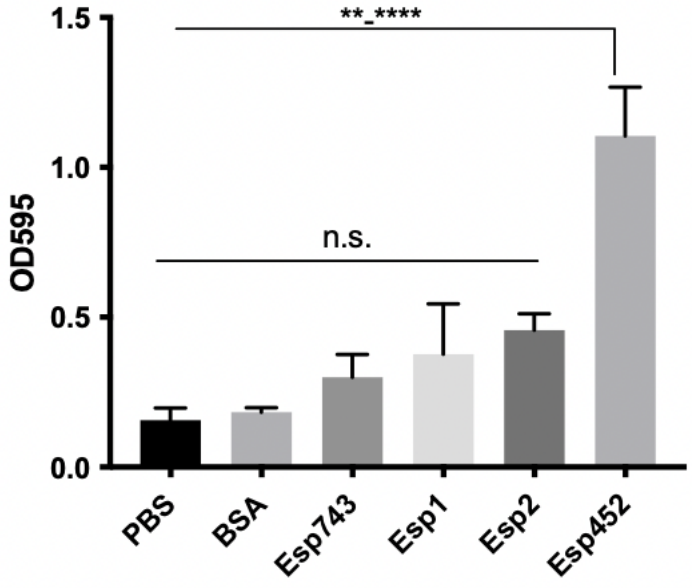

Figure 4.24. Effects of different Esp fragments on staining of *Enterococcal* biofilms. Enterococcal biofilms were supplemented with equivalent molar amounts of different Esp constructs and then stained with crystal violet. Samples were compared by 1-Way ANOVA and Tukey's post-hoc test. **, $p < .001$; ****, $p < .0001$

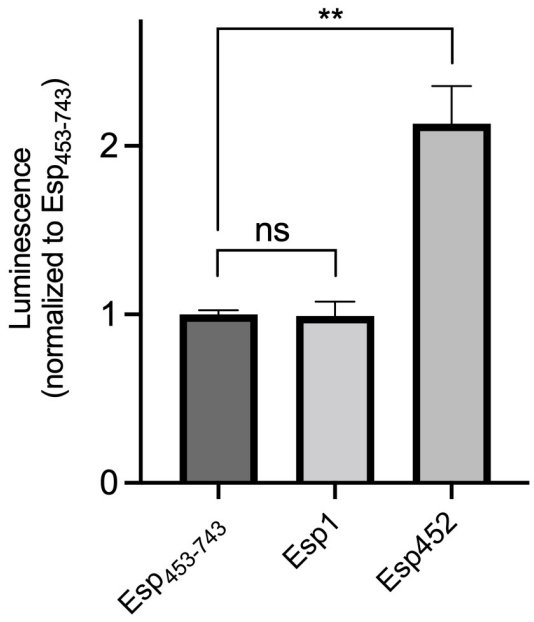

Figure 4.25. The effect of Esp1 on enterococcal biofilms. Luminescence of biofilms supplemented with Esp453-743, Esp452 or Esp1. All luminescence values were divided by the average luminescence of the $Esp_{453-743}$ biofilms. The experiment was performed in triplicate in two independent experiments. Samples were compared by Welch's ANOVA with D3 Dunnett's post-hoc test. **, $p < 0.01$.

We examined Esp743 for more specific protease cleavage sites using EXPASY and found that it possesses one full enteropeptidase cleavage site, DDDK, and one partial enteropeptidase cleavage site, DDK, located at amino acids 223-226 and 457-459, respectively (Fig 4.26). The full site is located on a surface-exposed loop between the final β-two strands of the Esp1 domain. We confirmed that human enteropeptidase is capable of cleaving Esp743 and generates fragments consistent in size with the hypothetical products generated by these two sites (Fig. 4.27).

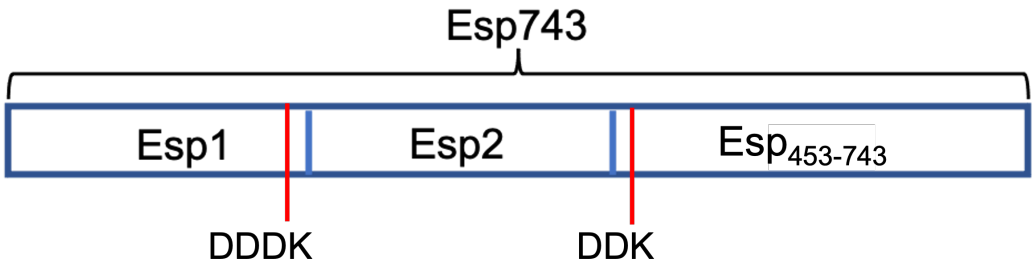

Figure 4.26. Hypothetical enteropeptidase cleavage sites in Esp743. A full cleavage site is located from amino acids 223-226 and a partial site at 457-459, located just before the end of Esp1 and just after the end of Esp2. Cleavage at the first site would produce two products of 20 and 57 kD in size. Cleavage at the second site would produce products of 46 and 31 kD, and cleavage at both sites would produce 3 products of 20, 26, and 31 kD.

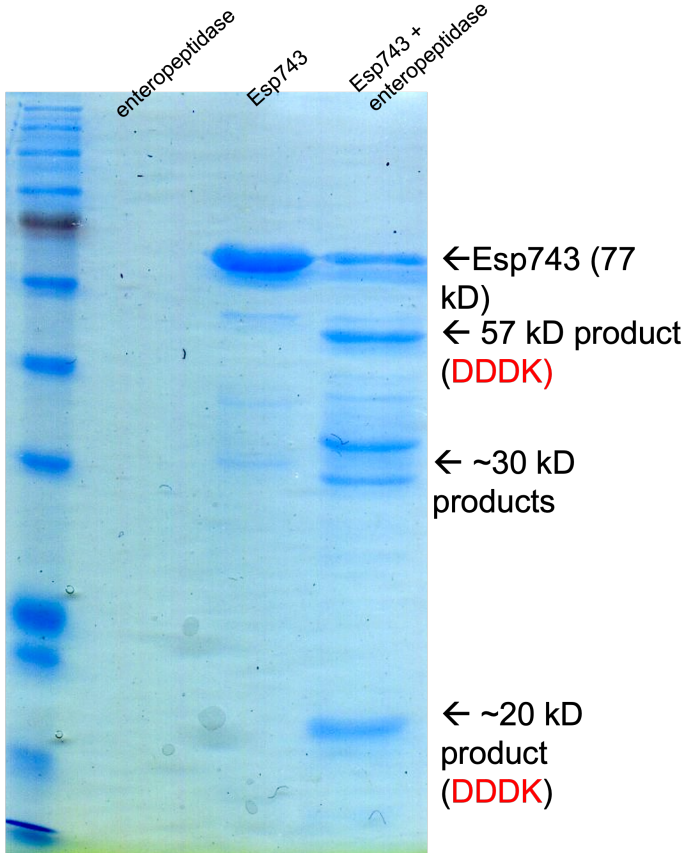

Figure 4.27. Digestion of Esp743 by human enteropeptidase. Fragments predicted to be generated by the full enteropeptidase cleavage site, DDDK, are indicated.

We used MS/MS to analyze the largest digestion product of the gel, and found that the majority of the population consists of aa 227-743, consistent with cleavage at the DDDK site. While we attempted to identify the fragment(s) in the smallest band, the results were suggestive of a mixed population and were inconclusive.

We cloned and purified the construct that would be generated by cleavage at the full cut site, Esp_{DDDK}, and found that it is capable of stabilizing enterococcal biofilms against washing at similar levels to Esp452 (Fig. 4.28). Interestingly, it also precipitated in buffer at higher levels than Esp452 at higher pH's, suggesting that precise construct identity determines stability at low pH (Fig. 4.29). Precipitation was observed as high as pH 5.3 (data not shown). It should be noted that the difference between Esp_{DDDK} and the Esp1 domain is only 15 amino acids, underscoring the potential importance of precise cleavage site.

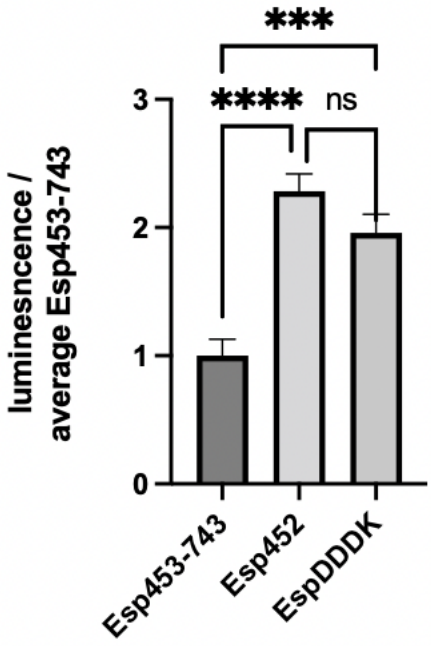

Figure 4.28. The effect of an enteropeptidase product on enterococcal biofilms. Luminescence of biofilms supplemented with Esp453-743, Esp452 or Esp_{DDDK}. All luminescence values were divided by the average luminescence of the $Esp_{453-743}$ biofilms. The experiment was performed in triplicate in two independent experiments. Samples were compared by 1-Way ANOVA with Tukey's post-hoc test. ***, $p < 0.001$; ****, $p < 0.0001$.

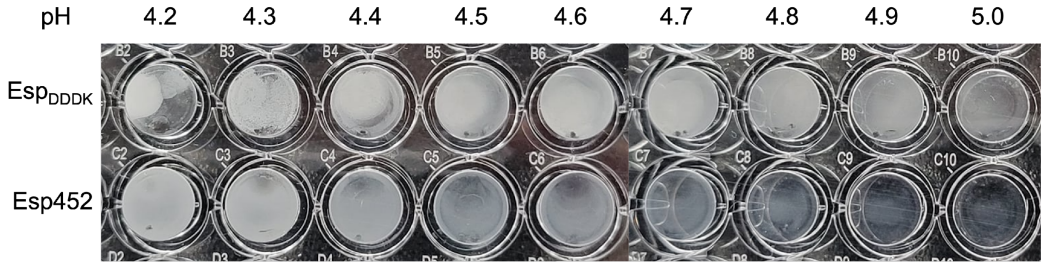

Figure 4.29. Esp452 and EspDDK precipitation at acidic pH. Fifty µg of Esp construct per well incubated for 1.5 h at 37˚ C in buffer at the indicated pH. A portion of this plate was shown in Figure 4.16.

DISCUSSION

The role of Esp in biofilms and its mechanism of action are unknown. One potential limitation of previous studies is the methods used; the vast majority of studies either knock out *esp* from an esp^+ strain or supply *esp* to an esp^- strain, and then look at biofilm production as measured by staining. From these experiments it was determined that the presence of *esp* corresponds to increased biofilm production in some strains, but is not required, and not all strains with *esp* form discernable biofilms. The contradictory results of these experiments necessitated a different avenue of study to elucidate the function of Esp, and we used a combination of biochemical and microbiological experiments to probe the function of the N-terminal region of the protein.

I found that the crystallizable fragment of Esp, Esp452, stabilized enterococcal biofilms against washing in a dose-dependent manner, an activity that had not yet been reported for Esp. In addition to stabilizing the biofilm against mechanical stress, it also shielded the biofilm from structural weakening by DNase. This effect could either be due to physical shielding of eDNA by the protein or that the additional strength afforded by Esp452 reduces the necessity of eDNA in maintaining the biofilm's structure.

While Esp has been reported to facilitate bacterial binding to abiotic surfaces and thus has been presumed to be involved in the initial attachment stage of biofilm development, I found that its presence during the initial phases of growth was not necessary, and that Esp452 required only an hour when added to biofilm cultures (grown overnight) to mechanically strengthen them against washing. It is possible that Esp provides a small advantage in initial binding due to weak interactions between the

protein and a contacted surface, explaining the reported advantage in binding to abiotic surfaces, but that this advantage is independent of the biofilm-strengthening that occurs at later stages of biofilm maturation.

A previous study on the role of *esp* in a rat model of endocarditis found that *esp*$^+$ bacteria had no effect on bacteria recovered from heart tissue compared to the isogenic *esp*$^-$ strain at 3 hours after inoculation, but that by 24 hours, more mice infected with the *esp*$^-$ strain had successfully cleared the infection than those that had received the *esp*$^+$ strain [39]. These data are consistent with observations in other mouse models of enterococcal urinary tract infection; in these experiments, mice were more likely to clear infections of *esp*$^-$ than *esp*$^+$ *Enterococcus*, but for mice that maintained significant populations of *Enterococcus*, the numbers of bacteria recovered were similar between *esp*$^+$ and *esp*$^-$ strains [37, 38]. This suggests that rather than playing a role in initial adherence, *esp* may play a role in persistence. The ability to form a biofilm is correlated with improved bacterial persistence and reduced ability of the host to clear the infection, consistent with our observations that Esp452 increases the resistance of enterococcal biofilms to mechanical and enzymatic degradation [72].

Our microscopy found that despite adding Esp452 at the time of inoculation, Esp452 was localized primarily to the surface of the biofilm facing the media, consistent with a physical barrier protecting the rest of the biofilm. Bacterial biofilms have been observed to exhibit a pH gradient in acidic conditions with the biofilm-media interface being the most acidic [73], so it is possible that the protein is only exposed to acidic enough conditions to precipitate at the biofilm-media interface. It should be noted, however, that this effect could be due to the addition of exogenous protein; the majority

of the media containing Esp452 is above the biofilm, so that when the bacteria sufficiently acidify their media to cause aggregation of Esp452, it then deposits on the media-facing surface of the biofilm and is unable to penetrate throughout the entire structure. Additional study is needed to confirm whether this surface localization is a natural phenomenon of Esp in biofilms.

We found that the amyloid-associated protective activity of Esp is pH-dependent, and acidification of the media is dependent on the amount of glucose supplied to the culture. In our assay, 0.5% glucose was sufficient to achieve a biofilm-stabilizing effect of Esp452, while 0.18% was not. This may explain some of the inconsistent results in the literature, as the amount of glucose used in biofilm assays is not standardized. Some studies examining *esp*$^{+}$ strains use 0.25% glucose, which may be insufficient to trigger a biofilm-stabilizing effect [43, 60]. Additionally, while *Enterococcus* has been reported to stabilize its environmental pH to 4.2 or higher, we found that strain FA2-2 acidified its media to a pH of 3.9, suggesting that different strains may have different tolerances for acidic conditions [43]. MMH594 reached on average pH of 4.4-4.5 and was not observed to reach a pH below 4.2. This variability in acidification of media between strains or glucose supplied may explain some of the reported differences in Esp activity in different publications.

Finally, I studied the difference in activity of various constructs of the Esp N-terminal region. The entire N-terminal region, Esp743, did not have fibril-forming or biofilm-strengthening activity in our MMH594 biofilm assay or in acidic buffer at the pH reached by MMH594. SAXS revealed that the structure of Esp743 is more compact than the sum of the lengths of the individual Esp452 and Esp$_{453\text{-}743}$ structures, and the

Esp743 structure has a Porod's value of 3.8, indicating that is significantly less flexible than that of $Esp_{453\text{-}743}$, which has a Porod's value of 2.5. These findings are consistent with the existence of stabilizing contacts between the two regions, which may explain why a more acidic pH was required to cause precipitation of Esp743.

Work recently published by Taglialegna et al. showed that a construct of Esp comprising approximately the first 500 amino acids was observed to precipitate at pH 4.2 and lower, suggesting that the additional 50 amino acids beyond Esp452 in that construct were sufficient to stabilize the protein at higher pH [70]. Additionally, I tested Esp_{DDDK}, a cleavage product predicted to be generated by human enteropeptidase, and found that the resulting truncation fragment of Esp, comprising the first 226 amino acids, strengthened enterococcal biofilms. In contrast, constructs comprising each of the two Ig domains in Esp452, Esp1 and Esp2, did not increase staining of enterococcal biofilms or precipitate at acidic pH, suggesting that the precise cleavage site determines at what pH the product is capable of exhibiting activity.

The work in this chapter specifically characterizes the ability of Esp452 to strengthen enterococcal biofilms. We found that it does so by forming amyloid-like fibrils, and that acidic pH (4.5) is sufficient to stimulate this activity. We observed no amyloid fibril formation or biofilm strengthening when the full-length N-terminal region was supplied to the bacteria, which I believe is due to stabilizing interactions between the domains in Esp452 and $Esp_{453\text{-}743}$ that prevent the protein from unfolding. I did observe biofilm strengthening by the full N-terminal region in another strain of *E. faecalis* that acidifies its media to pH 4.0. It is possible that a portion of Esp is proteolytically released from the bacterial surface, allowing it to strengthen biofilms at

less extreme pH; however, cleavage of Esp from the enterococcal surface has not been demonstrated to date, so it could be that the *in vivo* activity of this protein is limited to the full-length protein on the bacterial surface at very acidic pH's. We did determine that a specific fragment predicted to be generated by a host protease was capable of strengthening enterococcal biofilms. Additionally, we found that the precise cleave site of the N-terminal region determines at what pH the protein precipitates and stabilizes biofilms, suggesting that precise cleavage would be required to generate biofilm strengthening. Further study is needed to clarify the mechanism of activation of Esp in enterococcocal biofilms.

Adrian Bahn performed the experiments with ThT shown in 4.12 and 4.17 and assisted in data collection with the pH and glucose experiments in 4.10 and 4.11. Statistical analyses were performed by me. Elizabeth Montaño collected the confocal microscopy data shown in figures 4.14 and 4.15 from biofilms I prepared. SAXS data were collected and analyzed by Greg Hura and Susan Tsutakawa. All other work in this chapter was performed by me.

Work presented in Chapter 4 is being prepared for submission for publication. Spiegelman, Lindsey; Bahn, Adrian; Montaño, Elizabeth; Zhang, Ling; Hura, Greg; Patras, Katy; Tezcan, Akif; Nizet, Victor; Tsutakawa, Susan; and Partho Ghosh. "A portion of the N-terminal region of Enterococcal surface protein forms two Ig-like domains and stabilizes biofilms in a pH-dependent manner." Title subject to modification. I am the primary author of this work.

Chapter 5

Conclusions and Future Directions

I identified the structure and previously unreported activity of the majority of Esp's N-terminal domain. Esp452 has two domains each with a DE-variant Ig-fold and forms amyloid-like fibrils at low pH, which mechanically strengthen enterococcal biofilms and insulate them from DNase damage.

Esp452 possesses structural homology to many bacterial adhesins, but a conserved binding site between Esp452 and its homologues was not observed. Additionally, I did not detect binding of Esp452 to targets of its structural homologues. It should not be discounted that Esp452 may bind to an unidentified target, and I hope that our structure will help guide future biochemical studies of Esp.

We demonstrated the ability of Esp452 to form amyloid-like fibrils both in acidic buffer and in enterococcal biofilms. Amyloid-like fibrils have been identified in biofilms produced by many species of bacteria [74]. While the prototypical amyloid has a very specific conformation, the term "amyloid-like" is now used to apply to a wide variety of β-rich protein structures that functionally aggregate. These structures can be formed by either short peptides or larger proteins, and have been identified in biofilms generated by *Escherichia*, *Bacillus*, *Staphylococcus*, and many others [75-78]. Antigen I/II, a structural homologue of Esp452 expressed by the dental pathogen *Streptococcus mutans*, has recently been found to form amyloid-like fibrils in biofilms, and amyloid-inhibiting compounds were found to inhibit biofilm formation by *S. mutans* [71]. Additionally, Biofilm associated protein (Bap), a staphylococcal protein with 33% sequence identity to the N-terminal region of Esp, has also been found to form amyloid-like structures in a pH-dependent manner [78].

The pH requirement for amyloid fibril formation begs investigation into potential *in* vivo scenarios that this activity would be feasible. We observed activity of Esp743 in enterococcal biofilms at pH 4.2 and below. Acidic microenvironments exist throughout the body and are particularly associated with disease states. Dental lesions such as caries reach pH's under 5.0 [79]. The inflammatory response is acidic, and acidic pH is associated with healing wounds [80]. In healthy adults, the upper small intestine fluctuates in pH as gastric acid is periodically released by the stomach, temporarily reaching pH's as low as 4.0-5.0 during digestion [81, 82]. An acidic extracellular environment created by the host may not be necessary, as the ability of *Enterococci* to acidify their local environment through fermentation has been well established, and has even led to their use in cheese production. It is therefore feasible that the bacteria may sufficiently acidify their local environment for Esp to form amyloid-like fibrils, even in host tissues at neutral pH.

Further study is needed to explore the pH-dependent effect of amyloid fibril-formation by native Esp on live *Enterococcus*. Many strains of *Enterococcus* have been tested for Esp-dependent biofilm formation, with some positive and some negative results. These strains could be assayed for ThT binding on live biofilms and their pH's measured to confirm that the two correlate.

I demonstrated that, in the absence of extremely acidic pH, some shorter fragments of the N-terminal region of Esp precipitated and were capable of stabilizing enterococcal biofilms. Besides the Esp452 construct, a shorter construct predicted to be generated by human enteropeptidase, Esp_{DDDK}, was capable of precipitating as high as pH 5.3. Precise cleavage site appears to be crucial, as fragments comprising the

individual DEv-Ig domains of Esp452, Esp1 and Esp2, did not precipitate even at the most acidic pH tested. I expect that this is due to the stability of the constructs tested; Esp_{DDDK} terminates 15 amino acids earlier than Esp1, in between the penultimate and final beta strand of the first Ig domain, and thus is more prone to precipitation. While cleavage of Esp by *Enterococcus* has not yet been reported, in *Staphylococcus*, the N-terminal region of the Esp-homologue Bap is cleaved from the cell surface and is capable of forming amyloid-like aggregates [78]. Cleavage of bacterial surface proteins by host proteases is a well-established phenomenon [97-100].

Biofilms confer a wide range of advantages to bacteria, and there are several potential advantages of Esp-containing biofilms that have not yet been tested. One activity left to be assayed is whether Esp enhances horizontal transfer of genetic elements between enterococcal cells. Bacteria within biofilms more readily exchange genetic material than their planktonic counterparts, and the presence of *esp* is correlated with antibiotic resistance [83-85]. If Esp contributes to cell aggregation in biofilms, which would be consistent with other amyloid-like proteins, it is possible that it improves an individual bacterium's chance of initiating contact and genetic exchange with another bacterium [101-103].

Bacterial amyloids are currently under study as a potential therapeutic target [86]. A human antibody targeting amyloid-forming protein in *Salmonella* biofilms was found to disrupt the biofilm architecture and render the bacteria more susceptible to antibiotic treatment [87]. Another study found that amyloid-like fibrils confer an advantage to *E. coli* in UTI and that an amyloid-inhibiting drug reduced the ability of bacteria to colonize the urinary tract [88]. Its association with disease-causing and

antibiotic-resistant strains makes Esp an attractive potential target for therapeutics, and it would be interesting to test whether amyloid-inhibiting drugs are capable of disrupting Esp-dependent biofilm stability. I hope that this work will help the scientific community move one step closer to understanding its role in enterococcal disease.

BIBLIOGRAPHY

[1] Weiner-Lastinger LM, Abner S, Edwards JR, Kallen AJ, Karlsson M, Magill SS, Pollock D, See I, Soe MM, Walters MS, Dudeck MA. Antimicrobial-resistant pathogens associated with adult healthcare-associated infections: Summary of data reported to the National Healthcare Safety Network, 2015-2017. Infect Control Hosp Epidemiol. 2020;41:1-18.

[2] CDC. Antibiotic Resistance Threats in the United States. Atlanta, GA: US Department of Health and Human Services. 2019;CDC.

[3] M. M. Huycke DFS, and M. S. Gilmore. Multi-drug resistant enterococci- the nature of the problem and an agenda for the future. Emerg Infect Dis.4:239-49.

[4] Suppli M. Attributable Mortality Rate and Duration of Stay Associated with Enterococcal Bacteremia. Original Article Infectious Diseases. 2011;17:1078-83.

[5] <Vancomycin-Resistant Enterococcal Bacteremia- Natural History and Attributable Mortality.pdf>.

[6] Endo MS, Signoretti FGC, Kitayama VS, Marinho ACS, Martinho FC, Gomes BBPFdA. <b>Investigation in vivo of Enterococcus faecalis in endodontic retreatment by phenotypic and genotypic methods. Acta Scientiarum Health Sciences. 2015;37.

[7] Kayaoglu G, Orstavik D. Virulence factors of Enterococcus faecalis: relationship to endodontic disease. Crit Rev Oral Biol Med. 2004;15:308-20.

[8] Stuart CH, Schwartz SA, Beeson TJ, Owatz CB. Enterococcus faecalis: its role in root canal treatment failure and current concepts in retreatment. J Endod. 2006;32:93-8.

[9] Mayer Mpa PET. Enterococcus faecalis in Oral Infections. JBR Journal of Interdisciplinary Medicine and Dental Science. 2015;03.

[10] Ross KM, Mehr JS, Greeley RD, Montoya LA, Kulkarni PA, Frontin S, Weigle TJ, Giles H, Montana BE. Outbreak of bacterial endocarditis associated with an oral surgery practice: New Jersey public health surveillance, 2013 to 2014. J Am Dent Assoc. 2018;149:191-201.

[11] Lockhart PB, Brennan MT, Thornhill M, Michalowicz BS, Noll J, Bahrani-Mougeot FK, Sasser HC. Poor oral hygiene as a risk factor for infective endocarditis-related bacteremia. J Am Dent Assoc. 2009;140:1238-44.

[12] Alghamdi F, Shakir M. The Influence of Enterococcus faecalis as a Dental Root Canal Pathogen on Endodontic Treatment: A Systematic Review. Cureus. 2020;12:e7257.

[13] Stosor V, Peterson LR, Postelnick M, Noskin GA. Enterococcus faecium bacteremia: does vancomycin resistance make a difference? Arch Intern Med. 1998;158:522-7.

[14] Murray BE. Vancomycin-resistant enterococci. Am J Med. 1997;102:284-93.

[15] Lebreton F, Manson AL, Saavedra JT, Straub TJ, Earl AM, Gilmore MS. Tracing the Enterococci from Paleozoic Origins to the Hospital. Cell. 2017;169:849-61 e13.

[16] Gilmore MS, Salamzade R, Selleck E, Bryan N, Mello SS, Manson AL, Earl AM. Genes Contributing to the Unique Biology and Intrinsic Antibiotic Resistance of Enterococcus faecalis. mBio. 2020;11.

[17] de Niederhausern S, Bondi M, Messi P, Iseppi R, Sabia C, Manicardi G, Anacarso I. Vancomycin-resistance transferability from VanA enterococci to Staphylococcus aureus. Curr Microbiol. 2011;62:1363-7.

[18] Cong Y, Yang S, Rao X. Vancomycin resistant Staphylococcus aureus infections: A review of case updating and clinical features. J Adv Res. 2020;21:169-76.

[19] Ch'ng JH, Chong KKL, Lam LN, Wong JJ, Kline KA. Biofilm-associated infection by enterococci. Nat Rev Microbiol. 2019;17:82-94.

[20] Dale JL, Cagnazzo J, Phan CQ, Barnes AM, Dunny GM. Multiple roles for Enterococcus faecalis glycosyltransferases in biofilm-associated antibiotic resistance,

cell envelope integrity, and conjugative transfer. Antimicrob Agents Chemother. 2015;59:4094-105.

[21] Costerton JW, Stewart PS, Greenberg EP. Bacterial biofilms: a common cause of persistent infections. Science. 1999;284:1318-22.

[22] Hoyle BD, Costerton JW. Bacterial resistance to antibiotics: the role of biofilms. Prog Drug Res. 1991;37:91-105.

[23] Dale JL, Nilson JL, Barnes AMT, Dunny GM. Restructuring of Enterococcus faecalis biofilm architecture in response to antibiotic-induced stress. NPJ Biofilms Microbiomes. 2017;3:15.

[24] Jiang Y, Geng M, Bai L. Targeting Biofilms Therapy: Current Research Strategies and Development Hurdles. Microorganisms. 2020;8.

[25] Yu MK, Kim MA, Rosa V, Hwang YC, Del Fabbro M, Sohn WJ, Min KS. Role of extracellular DNA in Enterococcus faecalis biofilm formation and its susceptibility to sodium hypochlorite. J Appl Oral Sci. 2019;27:e20180699.

[26] Sharma D, Misba L, Khan AU. Antibiotics versus biofilm: an emerging battleground in microbial communities. Antimicrob Resist Infect Control. 2019;8:76.

[27] Nakayama J, Cao Y, Horii T, Sakuda S, Akkermans AD, de Vos WM, Nagasawa H. Gelatinase biosynthesis-activating pheromone: a peptide lactone that mediates a quorum sensing in Enterococcus faecalis. Mol Microbiol. 2001;41:145-54.

[28] Hancock LE, Perego M. The Enterococcus faecalis fsr two-component system controls biofilm development through production of gelatinase. J Bacteriol. 2004;186:5629-39.

[29] Shankar N, Baghdayan AS, Huycke M, G. L, Gilmore M. Infection-Derived Enterococcus faecalis Strains Are Enriched in esp, a Gene Encoding a Novel Surface Protein. INFECTION AND IMMUNITY. 1999;Jan. 1999:193-200.

[30] Shankar N, Baghdayan AS, Gilmore MS. Modulation of virulence within a pathogenicity island in vancomycin-resistant Enterococcus faecalis. Nature. 2002;417:746-50.

[31] Archimbaud C, Shankar N, Forestier C, Baghdayan A, Gilmore MS, Charbonne F, Joly B. In vitro adhesive properties and virulence factors of Enterococcus faecalis strains. Res Microbiol. 2002;153:75-80.

[32] Anderson AC, Jonas D, Huber I, Karygianni L, Wolber J, Hellwig E, Arweiler N, Vach K, Wittmer A, Al-Ahmad A. Enterococcus faecalis from Food, Clinical Specimens, and Oral Sites: Prevalence of Virulence Factors in Association with Biofilm Formation. Front Microbiol. 2015;6:1534.

[33] Tsikrikonis G, Maniatis AN, Labrou M, Ntokou E, Michail G, Daponte A, Stathopoulos C, Tsakris A, Pournaras S. Differences in biofilm formation and virulence factors between clinical and fecal enterococcal isolates of human and animal origin. Microb Pathog. 2012;52:336-43.

[34] Mohamed JA, Huang W, Nallapareddy SR, Teng F, Murray BE. Influence of origin of isolates, especially endocarditis isolates, and various genes on biofilm formation by Enterococcus faecalis. Infect Immun. 2004;72:3658-63.

[35] Eaton TJ, Gasson MJ. A variant enterococcal surface protein Esp(fm) in Enterococcus faecium; distribution among food, commensal, medical, and environmental isolates. FEMS Microbiol Lett. 2002;216:269-75.

[36] Mobarez HSKaAM. Spread of Esp in Antibiotic-Resistant E. facaelis and E. faecium isolates from UTI. The Open Microbiology Journal. 2015:14-7.

[37] Shankar N, Lockatell CV, Baghdayan AS, Drachenberg C, Gilmore MS, Johnson DE. Role of Enterococcus faecalis surface protein Esp in the pathogenesis of ascending urinary tract infection. Infect Immun. 2001;69:4366-72.

[38] Leendertse M, Heikens E, Wijnands LM, van Luit-Asbroek M, Teske GJ, Roelofs JJ, Bonten MJ, van der Poll T, Willems RJ. Enterococcal surface protein transiently aggravates Enterococcus faecium-induced urinary tract infection in mice. J Infect Dis. 2009;200:1162-5.

[39] Heikens E, Singh KV, Jacques-Palaz KD, van Luit-Asbroek M, Oostdijk EA, Bonten MJ, Murray BE, Willems RJ. Contribution of the enterococcal surface protein Esp to pathogenesis of Enterococcus faecium endocarditis. Microbes Infect. 2011;13:1185-90.

[40] Tendolkar PM, Baghdayan AS, Gilmore MS, Shankar N. Enterococcal surface protein, Esp, enhances biofilm formation by Enterococcus faecalis. Infect Immun. 2004;72:6032-9.

[41] Kristich CJ, Li YH, Cvitkovitch DG, Dunny GM. Esp-independent biofilm formation by Enterococcus faecalis. J Bacteriol. 2004;186:154-63.

[42] Heikens E, Bonten MJ, Willems RJ. Enterococcal surface protein Esp is important for biofilm formation of Enterococcus faecium E1162. J Bacteriol. 2007;189:8233-40.

[43] Elhadidy M, Elsayyad A. Uncommitted role of enterococcal surface protein, Esp, and origin of isolates on biofilm production by Enterococcus faecalis isolated from bovine mastitis. J Microbiol Immunol Infect. 2013;46:80-4.

[44] Kelley LA, Mezulis S, Yates CM, Wass MN, Sternberg MJ. The Phyre2 web portal for protein modeling, prediction and analysis. Nat Protoc. 2015;10:845-58.

[45] Almagro Armenteros JJ, Tsirigos KD, Sonderby CK, Petersen TN, Winther O, Brunak S, von Heijne G, Nielsen H. SignalP 5.0 improves signal peptide predictions using deep neural networks. Nat Biotechnol. 2019;37:420-3.

[46] Doublié S. Production of selenomethionyl proteins in prokaryotic and eukaryotic expression systems. Methods Mol Biol. 2007;363:91-108.

[47] Zhang L, Bailey JB, Subramanian RH, Groisman A, Tezcan FA. Hyperexpandable, self-healing macromolecular crystals with integrated polymer networks. Nature. 2018;557:86-91.

[48] Otwinowski Z, Minor W. Processing of X-ray diffraction data collected in oscillation mode. Methods Enzymol. 1997;276:307-26.

[49] Terwilliger TC, Adams PD, Read RJ, McCoy AJ, Moriarty NW, Grosse-Kunstleve RW, Afonine PV, Zwart PH, Hung LW. Decision-making in structure solution using Bayesian estimates of map quality: the PHENIX AutoSol wizard. Acta Crystallogr D Biol Crystallogr. 2009;65:582-601.

[50] Holm L. DALI and the persistence of protein shape. Protein Sci. 2020;29:128-40.

[51] Deivanayagam CCS, Wann ER, Chen W, Mike Carson, Rajashankar KR, Hook M, Narayana SVL. A novel variant of the immunoglobulin fold in surface adhesins of Staphylococcus aureus: crystal structure of the Fibrinogen-binding MSCRAMM, clumping factor A. The EMBO Journal. 2002;21:6660-72.

[52] Brady LJ, Maddocks SE, Larson MR, Forsgren N, Persson K, Deivanayagam CC, Jenkinson HF. The changing faces of Streptococcus antigen I/II polypeptide family adhesins. Mol Microbiol. 2010;77:276-86.

[53] Manzer HS, Nobbs AH, Doran KS. The Multifaceted Nature of Streptococcal Antigen I/II Proteins in Colonization and Disease Pathogenesis. Front Microbiol. 2020;11:602305.

[54] Hobley L, Ostrowski A, Rao FV, Bromley KM, Porter M, Prescott AR, MacPhee CE, van Aalten DM, Stanley-Wall NR. BslA is a self-assembling bacterial hydrophobin that coats the Bacillus subtilis biofilm. Proc Natl Acad Sci U S A. 2013;110:13600-5.

[55] Hura GL, Hodge CD, Rosenberg D, Guzenko D, Duarte JM, Monastyrskyy B, Grudinin S, Kryshtafovych A, Tainer JA, Fidelis K, Tsutakawa SE. Small angle X-ray scattering-assisted protein structure prediction in CASP13 and emergence of solution structure differences. Proteins. 2019;87:1298-314.

[56] Huycke MM, Spiegel CA, Gilmore MS. Bacteremia caused by hemolytic, high-level gentamicin-resistant Enterococcus faecalis. Antimicrob Agents Chemother. 1991;35:1626-34.

[57] McNamara C, Zinkernagel AS, Macheboeuf P, Cunningham MW, Nizet V, Ghosh P. Coiled-coil irregularities and instabilities in group A Streptococcus M1 are required for virulence. Science. 2008;319:1405-8.

[58] Cross BW, Ruhl S. Glycan recognition at the saliva - oral microbiome interface. Cell Immunol. 2018;333:19-33.

[59] Piroth L, Que YA, Widmer E, Panchaud A, Piu S, Entenza JM, Moreillon P. The fibrinogen- and fibronectin-binding domains of Staphylococcus aureus fibronectin-binding protein A synergistically promote endothelial invasion and experimental endocarditis. Infect Immun. 2008;76:3824-31.

[60] Toledo-Arana A, Valle J, Solano C, Arrizubieta MJ, Cucarella C, Lamata M, Amorena B, Leiva J, Penades JR, Lasa I. The Enterococcal Surface Protein, Esp, Is Involved in Enterococcus faecalis Biofilm Formation. Applied and Environmental Microbiology. 2001;67:4538-45.

[61] Tendolkar PM, Baghdayan AS, Shankar N. The N-terminal domain of enterococcal surface protein, Esp, is sufficient for Esp-mediated biofilm enhancement in Enterococcus faecalis. J Bacteriol. 2005;187:6213-22.

[62] Ran SJ, Jiang W, Zhu CL, Liang JP. Exploration of the mechanisms of biofilm formation by Enterococcus faecalis in glucose starvation environments. Aust Dent J. 2015;60:143-53.

[63] Di Rosa R, Creti R, Venditti M, D'Amelio R, Arciola CR, Montanaro L, Baldassarri L. Relationship between biofilm formation, the enterococcal surface protein (Esp) and gelatinase in clinical isolates of Enterococcus faecalis and Enterococcus faecium. FEMS Microbiol Lett. 2006;256:145-50.

[64] Dunny GM, Lee LN, LeBlanc DJ. Improved electroporation and cloning vector system for gram-positive bacteria. Appl Environ Microbiol. 1991;57:1194-201.

[65] Classen S, Hura GL, Holton JM, Rambo RP, Rodic I, McGuire PJ, Dyer K, Hammel M, Meigs G, Frankel KA, Tainer JA. Implementation and performance of SIBYLS: a dual endstation small-angle X-ray scattering and macromolecular crystallography beamline at the Advanced Light Source. J Appl Crystallogr. 2013;46:1-13.

[66] Manalastas-Cantos K, Konarev PV, Hajizadeh NR, Kikhney AG, Petoukhov MV, Molodenskiy DS, Panjkovich A, Mertens HDT, Gruzinov A, Borges C, Jeffries CM, Svergun DI, Franke D. ATSAS 3.0: expanded functionality and new tools for small-angle scattering data analysis. J Appl Crystallogr. 2021;54:343-55.

[67] Schneidman-Duhovny D, Hammel M, Tainer JA, Sali A. FoXS, FoXSDock and MultiFoXS: Single-state and multi-state structural modeling of proteins and their complexes based on SAXS profiles. Nucleic Acids Res. 2016;44:W424-9.

[68] Chiba A, Sugimoto S, Sato F, Hori S, Mizunoe Y. A refined technique for extraction of extracellular matrices from bacterial biofilms and its applicability. Microb Biotechnol. 2015;8:392-403.

[69] Schlafer S, Garcia J, Meyer RL, Vaeth M, Neuhaus KW. Effect of DNase Treatment on Adhesion and Early Biofilm Formation of Enterococcus Faecalis. Eur Endod J. 2018;3:82-6.

[70] Taglialegna A, Matilla-Cuenca L, Dorado-Morales P, Navarro S, Ventura S, Garnett JA, Lasa I, Valle J. The biofilm-associated surface protein Esp of Enterococcus faecalis forms amyloid-like fibers. NPJ Biofilms Microbiomes. 2020;6:15.

[71] Oli MW, Otoo HN, Crowley PJ, Heim KP, Nascimento MM, Ramsook CB, Lipke PN, Brady LJ. Functional amyloid formation by Streptococcus mutans. Microbiology (Reading). 2012;158:2903-16.

[72] Dostert M, Trimble MJ, Hancock REW. Antibiofilm peptides: overcoming biofilm-related treatment failure. RSC Advances. 2021;11:2718-28.

[73] Vroom JM, De Grauw KJ, Gerritsen HC, Bradshaw DJ, Marsh PD, Watson GK, Birmingham JJ, Allison C. Depth penetration and detection of pH gradients in biofilms by two-photon excitation microscopy. Appl Environ Microbiol. 1999;65:3502-11.

[74] Van Gerven N, Van der Verren SE, Reiter DM, Remaut H. The Role of Functional Amyloids in Bacterial Virulence. J Mol Biol. 2018;430:3657-84.

[75] Romero D, Aguilar C, Losick R, Kolter R. Amyloid fibers provide structural integrity to Bacillus subtilis biofilms. Proceedings of the National Academy of Sciences. 2010;107:2230-4.

[76] Kikuchi T, Mizunoe Y, Takade A, Naito S, Yoshida S. Curli fibers are required for development of biofilm architecture in Escherichia coli K-12 and enhance bacterial adherence to human uroepithelial cells. Microbiol Immunol. 2005;49:875-84.

[77] Hammer ND, Schmidt JC, Chapman MR. The curli nucleator protein, CsgB, contains an amyloidogenic domain that directs CsgA polymerization. Proc Natl Acad Sci U S A. 2007;104:12494-9.

[78] Taglialegna A, Navarro S, Ventura S, Garnett JA, Matthews S, Penades JR, Lasa I, Valle J. Staphylococcal Bap Proteins Build Amyloid Scaffold Biofilm Matrices in Response to Environmental Signals. PLoS Pathog. 2016;12:e1005711.

[79] Hojo S, Komatsu M, Okuda R, Takahashi N, Yamada T. Acid profiles and pH of carious dentin in active and arrested lesions. J Dent Res. 1994;73:1853-7.

[80] Lardner A. The effects of extracellular pH on immune function. J Leukoc Biol. 2001;69:522-30.

[81] Keller J. Gastrointestinal Digestion and Absorption. Encyclopedia of Biological Chemistry2013. p. 354-9.

[82] Dressman JB, Berardi RR, Dermentzoglou LC, Russell TL, Schmaltz SP, Barnett JL, Jarvenpaa KM. Upper gastrointestinal (GI) pH in young, healthy men and women. Pharm Res. 1990;7:756-61.

[83] Molin S, Tolker-Nielsen T. Gene transfer occurs with enhanced efficiency in biofilms and induces enhanced stabilisation of the biofilm structure. Curr Opin Biotechnol. 2003;14:255-61.

[84] Hausner M, Wuertz S. High rates of conjugation in bacterial biofilms as determined by quantitative in situ analysis. Appl Environ Microbiol. 1999;65:3710-3.

[85] Madsen JS, Burmolle M, Hansen LH, Sorensen SJ. The interconnection between biofilm formation and horizontal gene transfer. FEMS Immunol Med Microbiol. 2012;65:183-95.

[86] Matilla-Cuenca L, Toledo-Arana A, Valle J. Anti-Biofilm Molecules Targeting Functional Amyloids. Antibiotics (Basel). 2021;10.

[87] Tursi SA, Puligedda RD, Szabo P, Nicastro LK, Miller AL, Qiu C, Gallucci S, Relkin NR, Buttaro BA, Dessain SK, Tukel C. Salmonella Typhimurium biofilm disruption by a human antibody that binds a pan-amyloid epitope on curli. Nat Commun. 2020;11:1007.

[88] Cegelski L, Pinkner JS, Hammer ND, Cusumano CK, Hung CS, Chorell E, Aberg V, Walker JN, Seed PC, Almqvist F, Chapman MR, Hultgren SJ. Small-molecule inhibitors target Escherichia coli amyloid biogenesis and biofilm formation. Nat Chem Biol. 2009;5:913-9.

[89] Winn MD, Ballard CC, Cowtan KD, Dodson EJ, Emsley P, Evans PR, Keegan RM, Krissinel EB, Leslie AG, McCoy A, McNicholas SJ, Murshudov GN, Pannu NS, Potterton EA, Powell HR, Read RJ, Vagin A, Wilson KS. Overview of the CCP4 suite and current developments. Acta Crystallogr D Biol Crystallogr. 2011;67:235-42.

[90] Vagin A, Teplyakov A. Molecular replacement with MOLREP. Acta Crystallogr D Biol Crystallogr. 2010;66:22-5.

[91] Hall M, Nylander S, Jenkinson HF, Persson K. Structure of the C-terminal domain of AspA (antigen I/II-family) protein from Streptococcus pyogenes. FEBS Open Bio. 2014;4:283-9.

[92] Forsgren N, Lamont RJ, Persson K. Two intramolecular isopeptide bonds are identified in the crystal structure of the Streptococcus gordonii SspB C-terminal domain. J Mol Biol. 2010;397:740-51.

[93] Brady LJ, Maddocks SE, Larson MR, Forsgren N, Persson K, Deivanayagam CC, Jenkinson HF. The changing faces of Streptococcus antigen I/II polypeptide family adhesins. Mol Microbiol. 2010;77:276-86.

[94] Joh D, Speziale P, Gurusiddappa S, Manor J, Hook M. Multiple specificities of the staphylococcal and streptococcal fibronectin-binding microbial surface components recognizing adhesive matrix molecules. Eur J Biochem. 1998;258:897-905.

[95] Boucher LE, Bosch J. Development of a multifunctional tool for drug screening against plasmodial protein-protein interactions via surface plasmon resonance. J Mol Recognit. 2013;26:496-500.

[96] Beckett D, Kovaleva E, Schatz PJ. A minimal peptide substrate in biotin holoenzyme synthetase-catalyzed biotinylation. Protein Sci. 1999;8:921-9.

[97] Chen S, Zhang D, Roberts AJ, Lu HC, Cannon CL, Qin QM, de Figueiredo P. Host Protease Activity on Bacterial Pathogens Promotes Complement and Antibiotic-Directed Killing. Pathogens. 2021;10.

[98] Stapels DA, Geisbrecht BV, Rooijakkers SH. Neutrophil serine proteases in antibacterial defense. Curr Opin Microbiol. 2015;23:42-8.

[99] Pham CT. Neutrophil serine proteases fine-tune the inflammatory response. Int J Biochem Cell Biol. 2008;40:1317-33.

[100] Thomas EL, van der Hoorn RAL. Ten Prominent Host Proteases in Plant-Pathogen Interactions. Int J Mol Sci. 2018;19.

[101] Manzer HS, Nobbs AH, Doran KS. The Multifaceted Nature of Streptococcal Antigen I/II Proteins in Colonization and Disease Pathogenesis. Front Microbiol. 2020;11:602305.

[102] Garcia MC, Lee JT, Ramsook CB, Alsteens D, Dufrene YF, Lipke PN. A role for amyloid in cell aggregation and biofilm formation. PLoS One. 2011;6:e17632.

[103] Cucarella C, Solano C, Valle J, Amorena B, Lasa I, Penades JR. Bap, a Staphylococcus aureus surface protein involved in biofilm formation. J Bacteriol. 2001;183:2888-96.

APPENDIX

Chart ID	Streptavidin-488 (5ug/ml) Barcode #10127154 Slide #427 Request #3496	Average RFU	StDev	%CV
1	Gala-Sp8	28	15	55
2	Glca-Sp8	16	10	67
3	Mana-Sp8	6	5	87
4	GalNAca-Sp8	15	15	101
5	GalNAca-Sp15	7	11	169
6	Fuca-Sp8	42	52	123
7	Fuca-Sp9	24	13	54
8	Rhaa-Sp8	19	19	98
9	Neu5Aca-Sp8	27	13	51
10	Neu5Aca-Sp11	14	7	52
11	Neu5Acb-Sp8	8	5	61
12	Galb-Sp8	20	18	93
13	Glcb-Sp8	23	23	100
14	Manb-Sp8	53	22	42
15	GalNAcb-Sp8	21	14	69
16	GlcNAcb-Sp0	18	16	90
17	GlcNAcb-Sp8	14	9	65
18	GlcN(Gc)b-Sp8	20	14	69
19	Galb1-4GlcNAcb1-6(Galb1-4GlcNAcb1-3)GalNAca-Sp8	12	6	49
20	Galb1-4GlcNAcb1-6(Galb1-4GlcNAcb1-3)GalNAc-Sp14	39	17	42
21	GlcNAcb1-6(GlcNAcb1-4)(GlcNAcb1-3)GlcNAc-Sp8	24	25	105
22	6S(3S)Galb1-4(6S)GlcNAcb-Sp0	14	10	73
23	6S(3S)Galb1-4GlcNAcb-Sp0	11	6	61
24	(3S)Galb1-4(Fuca1-3)(6S)Glc-Sp0	-4	80	-2002
25	(3S)Galb1-4Glcb-Sp8	23	12	51
26	(3S)Galb1-4(6S)Glcb-Sp0	8	3	34
27	(3S)Galb1-4(6S)Glcb-Sp8	0	2	600
28	(3S)Galb1-3(Fuca1-4)GlcNAcb-Sp8	4	6	151
29	(3S)Galb1-3GalNAca-Sp8	6	7	122
30	(3S)Galb1-3GlcNAcb-Sp0	7	7	104
31	(3S)Galb1-3GlcNAcb-Sp8	-3	8	-304
32	(3S)Galb1-4(Fuca1-3)GlcNAc-Sp0	44	6	15
33	(3S)Galb1-4(Fuca1-3)GlcNAc-Sp8	7	4	63
34	(3S)Galb1-4(6S)GlcNAcb-Sp0	9	12	129

35	(3S)Galb1-4(6S)GlcNAcb-Sp8	10	6	68
36	(3S)Galb1-4GlcNAcb-Sp0	7	3	49
37	(3S)Galb1-4GlcNAcb-Sp8	13	9	73
38	(3S)Galb-Sp8	6	5	82
39	(6S)(4S)Galb1-4GlcNAcb-Sp0	3	3	113
40	(4S)Galb1-4GlcNAcb-Sp8	5	4	78
41	(6P)Mana-Sp8	17	6	35
42	(6S)Galb1-4Glcb-Sp0	5	1	22
43	(6S)Galb1-4Glcb-Sp8	5	8	167
44	(6S)Galb1-4GlcNAcb-Sp8	8	1	8
45	(6S)Galb1-4(6S)Glcb-Sp8	2	6	328
46	Neu5Aca2-3(6S)Galb1-4GlcNAcb-Sp8	6	2	43
47	(6S)GlcNAcb-Sp8	6	3	48
48	Neu5,9Ac_2a-Sp8	0	8	-3000
49	Neu5,9Ac2a2-6Galb1-4GlcNAcb-Sp8	6	3	48
50	Mana1-6(Mana1-3)Manb1-4GlcNAcb1-4GlcNAcb-Sp12	9	2	20
51	Mana1-6(Mana1-3)Manb1-4GlcNAcb1-4GlcNAcb-Sp13	15	6	39
52	GlcNAcb1-2Mana1-6(GlcNAcb1-2Mana1-3)Manb1-4GlcNAcb1-4GlcNAcb-Sp12	15	3	19
53	GlcNAcb1-2Mana1-6(GlcNAcb1-2Mana1-3)Manb1-4GlcNAcb1-4GlcNAcb-Sp13	2	4	212
54	Galb1-4GlcNAcb1-2Mana1-6(Galb1-4GlcNAcb1-2Mana1-3)Manb1-4GlcNAcb1-4GlcNAcb-Sp12	4	4	101
55	Neu5Aca2-6Galb1-4GlcNAcb1-2Mana1-6(Neu5Aca2-6Galb1-4GlcNAcb1-2Mana1-3)Manb1-4GlcNAcb1-4GlcNAcb-Sp12	4	4	106
56	Neu5Aca2-6Galb1-4GlcNAcb1-2Mana1-6(Neu5Aca2-6Galb1-4GlcNAcb1-2Man-a1-3)Manb1-4GlcNAcb1-4GlcNAcb-Sp21	9	4	43
57	Neu5Aca2-6Galb1-4GlcNAcb1-2Mana1-6(Neu5Aca2-6Galb1-4GlcNAcb1-2Mana1-3)Manb1-4GlcNAcb1-4GlcNAcb-Sp24	81	7	9
58	Fuca1-2Galb1-3GalNAcb1-3Gala-Sp9	6	4	68
59	Fuca1-2Galb1-3GalNAcb1-3Gala1-4Galb1-4Glcb-Sp9	10	5	47

60	Fuca1-2Galb1-3(Fuca1-4)GlcNAcb-Sp8	9	10	108
61	Fuca1-2Galb1-3GalNAca-Sp8	16	6	39
62	Fuca1-2Galb1-3GalNAca-Sp14	4	2	49
63	Fuca1-2Galb1-3GalNAcb1-4(Neu5Aca2-3)Galb1-4Glcb-Sp0	9	6	65
64	Fuca1-2Galb1-3GalNAcb1-4(Neu5Aca2-3)Galb1-4Glcb-Sp9	5	6	122
65	Fuca1-2Galb1-3GlcNAcb1-3Galb1-4Glcb-Sp8	8	5	61
66	Fuca1-2Galb1-3GlcNAcb1-3Galb1-4Glcb-Sp10	8	3	40
67	Fuca1-2Galb1-3GlcNAcb-Sp0	7	2	31
68	Fuca1-2Galb1-3GlcNAcb-Sp8	9	7	80
69	Fuca1-2Galb1-4(Fuca1-3)GlcNAcb1-3Galb1-4(Fuca1-3)GlcNAcb-Sp0	11	2	20
70	Fuca1-2Galb1-4(Fuca1-3)GlcNAcb1-3Galb1-4(Fuca1-3)GlcNAcb1-3Galb1-4(Fuca1-3)GlcNAcb-Sp0	32	5	15
71	Fuca1-2Galb1-4(Fuca1-3)GlcNAcb-Sp0	5	3	55
72	Fuca1-2Galb1-4(Fuca1-3)GlcNAcb-Sp8	8	3	32
73	Fuca1-2Galb1-4GlcNAcb1-3Galb1-4GlcNAcb-Sp0	2	2	99
74	Fuca1-2Galb1-4GlcNAcb1-3Galb1-4GlcNAcb1-3Galb1-4GlcNAcb-Sp0	1	3	503
75	Fuca1-2Galb1-4GlcNAcb-Sp0	26	3	12
76	Fuca1-2Galb1-4GlcNAcb-Sp8	8	6	81
77	Fuca1-2Galb1-4Glcb-Sp0	10	3	27
78	Fuca1-2Galb-Sp8	7	5	67
79	Fuca1-3GlcNAcb-Sp8	6	5	88
80	Fuca1-4GlcNAcb-Sp8	2	2	91
81	Fucb1-3GlcNAcb-Sp8	9	2	24
82	GalNAca1-3(Fuca1-2)Galb1-3GlcNAcb-Sp0	23	4	17
83	GalNAca1-3(Fuca1-2)Galb1-4(Fuca1-3)GlcNAcb-Sp0	72	26	36
84	(3S)Galb1-4(Fuca1-3)Glcb-Sp0	8	4	44
85	GalNAca1-3(Fuca1-2)Galb1-4GlcNAcb-Sp0	5	2	47
86	GalNAca1-3(Fuca1-2)Galb1-4GlcNAcb-Sp8	0	2	887

87	GalNAca1-3(Fuca1-2)Galb1-4Glcb-Sp0	5	2	43
88	GlcNAcb1-3Galb1-3GalNAca-Sp8	6	6	112
89	GalNAca1-3(Fuca1-2)Galb-Sp8	6	1	23
90	GalNAca1-3(Fuca1-2)Galb-Sp18	12	10	80
91	GalNAca1-3GalNAcb-Sp8	8	2	23
92	GalNAca1-3Galb-Sp8	10	4	42
93	GalNAca1-4(Fuca1-2)Galb1-4GlcNAcb-Sp8	9	5	52
94	GalNAcb1-3GalNAca-Sp8	4	4	101
95	GalNAcb1-3(Fuca1-2)Galb-Sp8	1	4	808
96	GalNAcb1-3Gala1-4Galb1-4GlcNAcb-Sp0	9	23	258
97	GalNAcb1-4(Fuca1-3)GlcNAcb-Sp0	15	17	115
98	GalNAcb1-4GlcNAcb-Sp0	-3	4	-147
99	GalNAcb1-4GlcNAcb-Sp8	27	11	40
100	Gala1-2Galb-Sp8	14	14	102
101	Gala1-3(Fuca1-2)Galb1-3GlcNAcb-Sp0	13	6	52
102	Gala1-3(Fuca1-2)Galb1-3GlcNAcb-Sp8	81	28	34
103	Gala1-3(Fuca1-2)Galb1-4(Fuca1-3)GlcNAcb-Sp0	5	4	93
104	Gala1-3(Fuca1-2)Galb1-4(Fuca1-3)GlcNAcb-Sp8	41	9	21
105	Gala1-3(Fuca1-2)Galb1-4GlcNAc-Sp0	11	6	53
106	Gala1-3(Fuca1-2)Galb1-4Glcb-Sp0	9	4	47
107	Gala1-3(Fuca1-2)Galb-Sp8	2	7	457
108	Gala1-3(Fuca1-2)Galb-Sp18	15	4	30
109	Gala1-4(Gala1-3)Galb1-4GlcNAcb-Sp8	-9	24	-269
110	Gala1-3GalNAca-Sp8	14	8	58
111	Gala1-3GalNAca-Sp16	43	10	23
112	Gala1-3GalNAcb-Sp8	4	2	59
113	Gala1-3Galb1-4(Fuca1-3)GlcNAcb-Sp8	9	2	18
114	Gala1-3Galb1-3GlcNAcb-Sp0	8	2	31
115	Gala1-3Galb1-4GlcNAcb-Sp8	2	5	235
116	Gala1-3Galb1-4Glcb-Sp0	16	21	129
117	Gala1-3Galb1-4Glc-Sp10	14	6	42
118	Gala1-3Galb-Sp8	8	7	84
119	Gala1-4(Fuca1-2)Galb1-4GlcNAcb-Sp8	6	6	114

120	Gala1-4Galb1-4GlcNAcb-Sp0	6	10	175
121	Gala1-4Galb1-4GlcNAcb-Sp8	1	2	228
122	Gala1-4Galb1-4Glcb-Sp0	24	2	10
123	Gala1-4GlcNAcb-Sp8	28	11	39
124	Gala1-6Glcb-Sp8	15	3	20
125	Galb1-2Galb-Sp8	0	7	#####
126	Galb1-3(Fuca1-4)GlcNAcb1-3Galb1-4(Fuca1-3)GlcNAcb-Sp0	7	4	62
127	Galb1-3GlcNAcb1-3Galb1-4(Fuca1-3)GlcNAcb-Sp0	1	4	309
128	Galb1-3(Fuca1-4)GlcNAc-Sp0	13	11	85
129	Galb1-3(Fuca1-4)GlcNAc-Sp8	7	11	154
130	Fuca1-4(Galb1-3)GlcNAcb-Sp8	0	7	2681
131	Galb1-4GlcNAcb1-6GalNAca-Sp8	14	8	60
132	Galb1-4GlcNAcb1-6GalNAc-Sp14	13	8	64
133	GlcNAcb1-6(Galb1-3)GalNAca-Sp8	9	6	73
134	GlcNAcb1-6(Galb1-3)GalNAca-Sp14	-1	1	-258
135	Neu5Aca2-6(Galb1-3)GalNAca-Sp8	4	1	34
136	Neu5Aca2-6(Galb1-3)GalNAca-Sp14	15	11	75
137	Neu5Acb2-6(Galb1-3)GalNAca-Sp8	4	1	37
138	Neu5Aca2-6(Galb1-3)GlcNAcb1-4Galb1-4Glcb-Sp10	0	7	2946
139	Galb1-3GalNAca-Sp8	7	2	21
140	Galb1-3GalNAca-Sp14	8	5	73
141	Galb1-3GalNAca-Sp16	9	6	64
142	Galb1-3GalNAcb-Sp8	10	3	29
143	Galb1-3GalNAcb1-3Gala1-4Galb1-4Glcb-Sp0	9	4	47
144	Galb1-3GalNAcb1-4(Neu5Aca2-3)Galb1-4Glcb-Sp0	2	1	86
145	Galb1-3GalNAcb1-4Galb1-4Glcb-Sp8	16	6	34
146	Galb1-3Galb-Sp8	20	6	29
147	Galb1-3GlcNAcb1-3Galb1-4GlcNAcb-Sp0	10	5	54
148	Galb1-3GlcNAcb1-3Galb1-4Glcb-Sp10	0	4	-1709
149	Galb1-3GlcNAcb-Sp0	10	8	87
150	Galb1-3GlcNAcb-Sp8	14	9	69
151	Galb1-4(Fuca1-3)GlcNAcb-Sp0	6	7	120
152	Galb1-4(Fuca1-3)GlcNAcb-Sp8	2	4	240
153	Galb1-4(Fuca1-3)GlcNAcb1-3Galb1-4(Fuca1-3)GlcNAcb-Sp0	9	4	46

154	Galb1-4(Fuca1-3)GlcNAcb1-3Galb1-4(Fuca1-3)GlcNAcb1-3Galb1-4(Fuca1-3)GlcNAcb-Sp0	6	2	35
155	Galb1-4(6S)Glcb-Sp0	7	5	69
156	Galb1-4(6S)Glcb-Sp8	8	5	63
157	Galb1-4GalNAca1-3(Fuca1-2)Galb1-4GlcNAcb-Sp8	4	4	120
158	Galb1-4GalNAcb1-3(Fuca1-2)Galb1-4GlcNAcb-Sp8	0	3	#####
159	Galb1-4GlcNAcb1-3GalNAca-Sp8	-1	8	-804
160	Galb1-4GlcNAcb1-3GalNAc-Sp14	5	4	84
161	Galb1-4GlcNAcb1-3Galb1-4(Fuca1-3)GlcNAcb1-3Galb1-4(Fuca1-3)GlcNAcb-Sp0	6	7	113
162	Galb1-4GlcNAcb1-3Galb1-4GlcNAcb1-3Galb1-4GlcNAcb-Sp0	0	3	1000
163	Galb1-4GlcNAcb1-3Galb1-4GlcNAcb-Sp0	38	17	45
164	Galb1-4GlcNAcb1-3Galb1-4Glcb-Sp0	-3	12	-476
165	Galb1-4GlcNAcb1-3Galb1-4Glcb-Sp8	4	1	12
166	Galb1-4GlcNAcb1-6(Galb1-3)GalNAca-Sp8	4	2	49
167	Galb1-4GlcNAcb1-6(Galb1-3)GalNAc-Sp14	2	4	178
168	Galb1-4GlcNAcb-Sp0	15	10	69
169	Galb1-4GlcNAcb-Sp8	16	6	40
170	Galb1-4GlcNAcb-Sp23	-5	3	-54
171	Galb1-4Glcb-Sp0	12	9	81
172	Galb1-4Glcb-Sp8	9	4	41
173	GlcNAca1-3Galb1-4GlcNAcb-Sp8	4	4	85
174	GlcNAca1-6Galb1-4GlcNAcb-Sp8	3	7	295
175	GlcNAcb1-2Galb1-3GalNAca-Sp8	1	6	1238
176	GlcNAcb1-6(GlcNAcb1-3)GalNAca-Sp8	2	10	521
177	GlcNAcb1-6(GlcNAcb1-3)GalNAca-Sp14	6	4	61
178	GlcNAcb1-6(GlcNAcb1-3)Galb1-4GlcNAcb-Sp8	4	3	91
179	GlcNAcb1-3GalNAca-Sp8	2	7	296
180	GlcNAcb1-3GalNAca-Sp14	-1	7	-536
181	GlcNAcb1-3Galb-Sp8	6	3	42
182	GlcNAcb1-3Galb1-4GlcNAcb-Sp0	5	4	75
183	GlcNAcb1-3Galb1-4GlcNAcb-Sp8	-1	2	-151

184	GlcNAcb1-3Galb1-4GlcNAcb1-3Galb1-4GlcNAcb-Sp0	4	4	102
185	GlcNAcb1-3Galb1-4Glcb-Sp0	25	41	168
186	GlcNAcb1-4-MDPLys	3	3	115
187	GlcNAcb1-6(GlcNAcb1-4)GalNAca-Sp8	2	6	303
188	GlcNAcb1-4Galb1-4GlcNAcb-Sp8	-3	6	-191
189	GlcNAcb1-4GlcNAcb1-4GlcNAcb1-4GlcNAcb1-4GlcNAcb1-4GlcNAcb1-Sp8	7	1	12
190	GlcNAcb1-4GlcNAcb1-4GlcNAcb1-4GlcNAcb1-4GlcNAcb1-Sp8	2	2	118
191	GlcNAcb1-4GlcNAcb1-4GlcNAcb-Sp8	3	9	304
192	GlcNAcb1-6GalNAca-Sp8	1	2	245
193	GlcNAcb1-6GalNAca-Sp14	6	2	36
194	GlcNAcb1-6Galb1-4GlcNAcb-Sp8	-2	1	-43
195	Glca1-4Glcb-Sp8	20	5	25
196	Glca1-4Glca-Sp8	14	7	48
197	Glca1-6Glca1-6Glcb-Sp8	9	5	56
198	Glcb1-4Glcb-Sp8	7	2	37
199	Glcb1-6Glcb-Sp8	10	4	34
200	G-ol-Sp8	15	7	50
201	GlcAa-Sp8	4	3	59
202	GlcAb-Sp8	93	5	5
203	GlcAb1-3Galb-Sp8	5	6	108
204	GlcAb1-6Galb-Sp8	10	7	71
205	KDNa2-3Galb1-3GlcNAcb-Sp0	6	2	38
206	KDNa2-3Galb1-4GlcNAcb-Sp0	4	3	71
207	Mana1-2Mana1-2Mana1-3Mana-Sp9	5	4	72
208	Mana1-2Mana1-6(Mana1-2Mana1-3)Mana-Sp9	0	5	-2151
209	Mana1-2Mana1-3Mana-Sp9	7	2	26
210	Mana1-6(Mana1-2Mana1-3)Mana1-6(Mana1-2Mana1-3)Manb1-4GlcNAcb1-4GlcNAcb-Sp12	2	4	164
211	Mana1-2Mana1-6(Mana1-3)Mana1-6(Mana1-2Mana1-2Mana1-3)Manb1-4GlcNAcb1-4GlcNAcb-Sp12	7	4	57
212	Mana1-2Mana1-6(Mana1-2Mana1-3)Mana1-6(Mana1-2Mana1-2Mana1-3)Manb1-4GlcNAcb1-4GlcNAcb-Sp12	27	11	40
213	Mana1-6(Mana1-3)Mana-Sp9	2	2	82

214	Mana1-2Mana1-2Mana1-6(Mana1-3)Mana-Sp9	10	5	46
215	Mana1-6(Mana1-3)Mana1-6(Mana1-2Mana1-3)Manb1-4GlcNAcb1-4GlcNAcb-Sp12	77	40	52
216	Mana1-6(Mana1-3)Mana1-6(Mana1-3)Manb1-4GlcNAcb1-4GlcNAcb-Sp12	9	4	43
217	Manb1-4GlcNAcb-Sp0	0	2	683
218	Neu5Aca2-3Galb1-4GlcNAcb1-3Galb1-4(Fuca1-3)GlcNAcb-Sp0	-3	4	-127
219	(3S)Galb1-4(Fuca1-3)(6S)GlcNAcb-Sp8	22	5	21
220	Fuca1-2(6S)Galb1-4GlcNAcb-Sp0	9	2	20
221	Fuca1-2Galb1-4(6S)GlcNAcb-Sp8	2	2	82
222	Fuca1-2(6S)Galb1-4(6S)Glcb-Sp0	6	4	65
223	Neu5Aca2-3Galb1-3GalNAca-Sp8	2	4	220
224	Neu5Aca2-3Galb1-3GalNAca-Sp14	1	5	666
225	GalNAcb1-4(Neu5Aca2-8Neu5Aca2-8Neu5Aca2-8Neu5Aca2-3)Galb1-4Glcb-Sp0	21	11	54
226	GalNAcb1-4(Neu5Aca2-8Neu5Aca2-8Neu5Aca2-3)Galb1-4Glcb-Sp0	50	33	66
227	Neu5Aca2-8Neu5Aca2-8Neu5Aca2-3Galb1-4Glcb-Sp0	3	1	40
228	GalNAcb1-4(Neu5Aca2-8Neu5Aca2-3)Galb1-4Glcb-Sp0	2	1	71
229	Neu5Aca2-8Neu5Aca2-8Neu5Aca-Sp8	-1	1	-141
230	GalNAcb1-4(Neu5Aca2-3)Galb1-4GlcNAcb-Sp0	22	3	12
231	GalNAcb1-4(Neu5Aca2-3)Galb1-4GlcNAcb-Sp8	5	4	74
232	GalNAcb1-4(Neu5Aca2-3)Galb1-4Glcb-Sp0	1	2	228
233	Neu5Aca2-3Galb1-3GalNAcb1-4(Neu5Aca2-3)Galb1-4Glcb-Sp0	1	3	529
234	Neu5Aca2-6(Neu5Aca2-3)GalNAca-Sp8	2	5	203
235	Neu5Aca2-3GalNAca-Sp8	2	5	311
236	Neu5Aca2-3GalNAcb1-4GlcNAcb-Sp0	-2	4	-221
237	Neu5Aca2-3Galb1-3(6S)GlcNAc-Sp8	95	10	10

238	Neu5Aca2-3Galb1-3(Fuca1-4)GlcNAcb-Sp8	-8	12	-145
239	Neu5Aca2-3Galb1-3(Fuca1-4)GlcNAcb1-3Galb1-4(Fuca1-3)GlcNAcb-Sp0	0	1	#####
240	Neu5Aca2-3Galb1-4(Neu5Aca2-3Galb1-3)GlcNAcb-Sp8	0	3	-1194
241	Neu5Aca2-3Galb1-3(6S)GalNAca-Sp8	3	4	111
242	Neu5Aca2-6(Neu5Aca2-3Galb1-3)GalNAca-Sp8	3	1	23
243	Neu5Aca2-6(Neu5Aca2-3Galb1-3)GalNAca-Sp14	12	9	79
244	Neu5Aca2-3Galb-Sp8	9	3	30
245	Neu5Aca2-3Galb1-3GalNAcb1-3Gala1-4Galb1-4Glcb-Sp0	11	11	106
246	Neu5Aca2-3Galb1-3GlcNAcb1-3Galb1-4GlcNAcb-Sp0	-1	5	-535
247	Fuca1-2(6S)Galb1-4Glcb-Sp0	22	8	37
248	Neu5Aca2-3Galb1-3GlcNAcb-Sp0	76	56	74
249	Neu5Aca2-3Galb1-4(6S)GlcNAcb-Sp8	9	9	96
250	Neu5Aca2-3Galb1-4(Fuca1-3)(6S)GlcNAcb-Sp8	1	3	503
251	Neu5Aca2-3Galb1-4(Fuca1-3)GlcNAcb1-3Galb1-4(Fuca1-3)GlcNAcb1-3Galb1-4(Fuca1-3)GlcNAcb-Sp0	77	22	28
252	Neu5Aca2-3Galb1-4(Fuca1-3)GlcNAcb-Sp0	3	1	38
253	Neu5Aca2-3Galb1-4(Fuca1-3)GlcNAcb-Sp8	-4	5	-122
254	Neu5Aca2-3Galb1-4(Fuca1-3)GlcNAcb1-3Galb-Sp8	7	4	60
255	Neu5Aca2-3Galb1-4(Fuca1-3)GlcNAcb1-3Galb1-4GlcNAcb-Sp8	36	12	33
256	Neu5Aca2-3Galb1-4GlcNAcb1-3Galb1-4GlcNAcb1-3Galb1-4GlcNAcb-Sp0	3	3	105
257	Neu5Aca2-3Galb1-4GlcNAcb-Sp0	33	5	15
258	Neu5Aca2-3Galb1-4GlcNAcb-Sp8	3	6	198
259	Neu5Aca2-3Galb1-4GlcNAcb1-3Galb1-4GlcNAcb-Sp0	-9	2	-24
260	Fuca1-2Galb1-4(6S)Glcb-Sp0	2	4	280

261	Neu5Aca2-3Galb1-4Glcb-Sp0	42	39	93
262	Neu5Aca2-3Galb1-4Glcb-Sp8	0	6	-2474
263	Neu5Aca2-6GalNAca-Sp8	5	2	43
264	Neu5Aca2-6GalNAcb1-4GlcNAcb-Sp0	-1	2	-216
265	Neu5Aca2-6Galb1-4(6S)GlcNAcb-Sp8	1	1	67
266	Neu5Aca2-6Galb1-4GlcNAcb-Sp0	3	2	75
267	Neu5Aca2-6Galb1-4GlcNAcb-Sp8	8	8	106
268	Neu5Aca2-6Galb1-4GlcNAcb1-3Galb1-4(Fuca1-3)GlcNAcb1-3Galb1-4(Fuca1-3)GlcNAcb-Sp0	6	9	148
269	Neu5Aca2-6Galb1-4GlcNAcb1-3Galb1-4GlcNAcb-Sp0	2	5	231
270	Neu5Aca2-6Galb1-4Glcb-Sp0	1	9	1243
271	Neu5Aca2-6Galb1-4Glcb-Sp8	3	2	81
272	Neu5Aca2-6Galb-Sp8	6	3	53
273	Neu5Aca2-8Neu5Aca-Sp8	0	4	#####
274	Neu5Aca2-8Neu5Aca2-3Galb1-4Glcb-Sp0	0	4	#####
275	Galb1-3(Fuca1-4)GlcNAcb1-3Galb1-3(Fuca1-4)GlcNAcb-Sp0	11	5	45
276	Neu5Acb2-6GalNAca-Sp8	-1	2	-476
277	Neu5Acb2-6Galb1-4GlcNAcb-Sp8	2	4	204
278	Neu5Gca2-3Galb1-3(Fuca1-4)GlcNAcb-Sp0	3	5	179
279	Neu5Gca2-3Galb1-3GlcNAcb-Sp0	3	6	225
280	Neu5Gca2-3Galb1-4(Fuca1-3)GlcNAcb-Sp0	6	4	67
281	Neu5Gca2-3Galb1-4GlcNAcb-Sp0	3	7	293
282	Neu5Gca2-3Galb1-4Glcb-Sp0	43	13	30
283	Neu5Gca2-6GalNAca-Sp0	10	8	80
284	Neu5Gca2-6Galb1-4GlcNAcb-Sp0	3	3	104
285	Neu5Gca-Sp8	10	3	27
286	Neu5Aca2-3Galb1-4GlcNAcb1-6(Galb1-3)GalNAca-Sp14	10	4	47
287	Galb1-3GlcNAcb1-3Galb1-3GlcNAcb-Sp0	6	8	130
288	Galb1-4(Fuca1-3)(6S)GlcNAcb-Sp0	6	3	52
289	Galb1-4(Fuca1-3)(6S)Glcb-Sp0	18	1	8
290	Galb1-4(Fuca1-3)GlcNAcb1-3Galb1-3(Fuca1-4)GlcNAcb-Sp0	21	4	17
291	Galb1-4GlcNAcb1-3Galb1-3GlcNAcb-Sp0	20	7	38

292	Neu5Aca2-3Galb1-3GlcNAcb1-3Galb1-3GlcNAcb-Sp0	5	3	55
293	Neu5Aca2-3Galb1-4GlcNAcb1-3Galb1-3GlcNAcb-Sp0	0	5	2101
294	4S(3S)Galb1-4GlcNAcb-Sp0	27	17	62
295	(6S)Galb1-4(6S)GlcNAcb-Sp0	4	4	89
296	(6P)Glcb-Sp10	7	2	31
297	Neu5Aca2-3Galb1-4(Fuca1-3)GlcNAcb1-6(Galb1-3)GalNAca-Sp14	76	36	48
298	Galb1-3Galb1-4GlcNAcb-Sp8	9	4	48
299	Neu5Aca2-6Galb1-4GlcNAcb1-2Mana1-6(Galb1-4GlcNAcb1-2Mana1-3)Manb1-4GlcNAcb1-4GlcNAcb-Sp12	9	2	27
300	Galb1-4GlcNAcb1-6(Galb1-4GlcNAcb1-3)Galb1-4GlcNAc-Sp0	5	3	60
301	GlcNAcb1-6(Galb1-4GlcNAcb1-3)Galb1-4GlcNAc-Sp0	-1	4	-775
302	Galb1-4GlcNAca1-6Galb1-4GlcNAcb-Sp0	4	3	68
303	Galb1-4GlcNAcb1-6Galb1-4GlcNAcb-Sp0	24	17	69
304	GalNAcb1-3Galb-Sp8	26	8	31
305	GlcAb1-3GlcNAcb-Sp8	7	6	83
306	Neu5Aca2-6Galb1-4GlcNAcb1-2Mana1-6(GlcNAcb1-2Mana1-3)Manb1-4GlcNAcb1-4GlcNAcb-Sp12	5	2	29
307	GlcNAcb1-3Man-Sp10	10	3	36
308	GlcNAcb1-4GlcNAcb-Sp10	-1	2	-228
309	GlcNAcb1-4GlcNAcb-Sp12	6	2	39
310	MurNAcb1-4GlcNAcb-Sp10	6	8	128
311	Mana1-6Manb-Sp10	1	3	333
312	Mana1-6(Mana1-3)Mana1-6(Mana1-3)Manb-Sp10	6	6	105
313	Mana1-2Mana1-6(Mana1-3)Mana1-6(Mana1-2Mana1-2Mana1-3)Mana-Sp9	3	3	109
314	Mana1-2Mana1-6(Mana1-2Mana1-3)Mana1-6(Mana1-2Mana1-2Mana1-3)Mana-Sp9	3	2	95

315	Neu5Aca2-3Galb1-4GlcNAcb1-6(Neu5Aca2-3Galb1-3)GalNAca-Sp14	3	7	254
316	Neu5Aca2-6Galb1-4GlcNAcb1-2Mana1-6(Neu5Aca2-3Galb1-4GlcNAcb1-2Mana1-3)Manb1-4GlcNAcb1-4GlcNAcb-Sp12	3	2	61
317	Galb1-4GlcNAcb1-2Mana1-6(Neu5Aca2-6Galb1-4GlcNAcb1-2Mana1-3)Manb1-4GlcNAcb1-4GlcNAcb-Sp12	3	3	115
318	Neu5Aca2-8Neu5Acb-Sp17	5	4	88
319	Neu5Aca2-8Neu5Aca2-8Neu5Acb-Sp8	0	3	#####
320	Neu5Gcb2-6Galb1-4GlcNAc-Sp8	4	2	54
321	Galb1-3GlcNAcb1-2Mana1-6(Galb1-3GlcNAcb1-2Mana1-3)Manb1-4GlcNAcb1-4GlcNAcb-Sp19	28	7	26
322	Neu5Aca2-3Galb1-4GlcNAcb1-2Mana1-6(Neu5Aca2-3Galb1-4GlcNAcb1-2Mana1-3)Manb1-4GlcNAcb1-4GlcNAcb-Sp12	1	2	137
323	Neu5Aca2-3Galb1-4GlcNAcb1-2Mana1-6(Neu5Aca2-6Galb1-4GlcNAcb1-2Mana1-3)Manb1-4GlcNAcb1-4GlcNAcb-Sp12	0	4	1612
324	Galb1-4(Fuca1-3)GlcNAcb1-2Mana1-6(Galb1-4(Fuca1-3)GlcNAcb1-2Mana1-3)Manb1-4GlcNAcb1-4GlcNAcb-Sp20	10	1	13
325	Neu5,9Ac2a2-3Galb1-4GlcNAcb-Sp0	44	26	59
326	Neu5,9Ac2a2-3Galb1-3GlcNAcb-Sp0	0	5	#####
327	Neu5Aca2-6Galb1-4GlcNAcb1-3Galb1-3GlcNAcb-Sp0	-10	10	-110
328	Neu5Aca2-3Galb1-3(Fuca1-4)GlcNAcb1-3Galb1-3(Fuca1-4)GlcNAcb-Sp0	9	4	48
329	Neu5Aca2-6Galb1-4GlcNAcb1-3Galb1-4GlcNAcb1-3Galb1-4GlcNAcb-Sp0	-3	3	-112
330	Gala1-4Galb1-4GlcNAcb1-3Galb1-4Glcb-Sp0	4	3	68
331	GalNAcb1-3Gala1-4Galb1-4GlcNAcb1-3Galb1-4Glcb-Sp0	8	2	29

332	GalNAca1-3(Fuca1-2)Galb1-4GlcNAcb1-3Galb1-4GlcNAcb-Sp0	4	1	34
333	GalNAca1-3(Fuca1-2)Galb1-4GlcNAcb1-3Galb1-4GlcNAcb1-3Galb1-4GlcNAcb-Sp0	63	48	77
334	Neu5Aca2-3Galb1-4(Fuca1-3)GlcNAcb1-6(Neu5Aca2-3Galb1-3)GalNAc-Sp14	46	14	30
335	GlcNAca1-4Galb1-4GlcNAcb1-3Galb1-4GlcNAcb1-3Galb1-4GlcNAcb-Sp0	-6	6	-108
336	GlcNAca1-4Galb1-4GlcNAcb-Sp0	5	4	82
337	GlcNAca1-4Galb1-3GlcNAcb-Sp0	4	1	20
338	GlcNAca1-4Galb1-4GlcNAcb1-3Galb1-4Glcb-Sp0	3	1	40
339	GlcNAca1-4Galb1-4GlcNAcb1-3Galb1-4(Fuca1-3)GlcNAcb1-3Galb1-4(Fuca1-3)GlcNAcb-Sp0	33	10	30
340	GlcNAca1-4Galb1-4GlcNAcb1-3Galb1-4GlcNAcb-Sp0	6	2	31
341	GlcNAca1-4Galb1-3GalNAc-Sp14	4	3	78
342	Neu5Aca2-6Galb1-4GlcNAcb1-2Mana1-6(Mana1-3)Manb1-4GlcNAcb1-4GlcNAc-Sp12	5	3	53
343	Mana1-6(Neu5Aca2-6Galb1-4GlcNAcb1-2Mana1-3)Manb1-4GlcNAcb1-4GlcNAc-Sp12	9	4	43
344	Neu5Aca2-6Galb1-4GlcNAcb1-2Mana1-6Manb1-4GlcNAcb1-4GlcNAc-Sp12	4	2	63
345	Neu5Aca2-6Galb1-4GlcNAcb1-2Mana1-3Manb1-4GlcNAcb1-4GlcNAc-Sp12	17	19	117
346	Galb1-4GlcNAcb1-2Mana1-3Manb1-4GlcNAcb1-4GlcNAc-Sp12	-4	2	-54
347	Galb1-4GlcNAcb1-2Mana1-6Manb1-4GlcNAcb1-4GlcNAc-Sp12	8	2	29
348	Mana1-6(Galb1-4GlcNAcb1-2Mana1-3)Manb1-4GlcNAcb1-4GlcNAcb-Sp12	4	5	134
349	GlcNAcb1-2Mana1-6(GlcNAcb1-2Mana1-3)Manb1-4GlcNAcb1-4(Fuca1-6)GlcNAcb-Sp22	34	8	23

350	Galb1-4GlcNAcb1-2Mana1-6(Galb1-4GlcNAcb1-2Mana1-3)Manb1-4GlcNAcb1-4(Fuca1-6)GlcNAcb-Sp22	83	32	38
351	Galb1-3GlcNAcb1-2Mana1-6(Galb1-3GlcNAcb1-2Mana1-3)Manb1-4GlcNAcb1-4(Fuca1-6)GlcNAcb-Sp22	22	7	30
352	(6S)GlcNAcb1-3Galb1-4GlcNAcb-Sp0	35	1	4
353	KDNa2-3Galb1-4(Fuca1-3)GlcNAc-Sp0	18	5	29
354	KDNa2-6Galb1-4GlcNAc-Sp0	5	7	140
355	KDNa2-3Galb1-4Glc-Sp0	5	6	141
356	KDNa2-3Galb1-3GalNAca-Sp14	9	3	34
357	Fuca1-2Galb1-3GlcNAcb1-2Mana1-6(Fuca1-2Galb1-3GlcNAcb1-2Mana1-3)Manb1-4GlcNAcb1-4GlcNAcb-Sp20	123	13	11
358	Fuca1-2Galb1-4GlcNAcb1-2Mana1-6(Fuca1-2Galb1-4GlcNAcb1-2Mana1-3)Manb1-4GlcNAcb1-4GlcNAcb-Sp20	52	43	82
359	Fuca1-2Galb1-4(Fuca1-3)GlcNAcb1-2Mana1-6(Fuca1-2Galb1-4(Fuca1-3)GlcNAcb1-2Mana1-3)Manb1-4GlcNAcb1-4GlcNAb-Sp20	71	13	18
360	Gala1-3Galb1-4GlcNAcb1-2Mana1-6(Gala1-3Galb1-4GlcNAcb1-2Mana1-3)Manb1-4GlcNAcb1-4GlcNAcb-Sp20	15	6	39
361	Galb1-4GlcNAcb1-2Mana1-6(Mana1-3)Manb1-4GlcNAcb1-4GlcNAcb-Sp12	8	4	46
362	Fuca1-4(Galb1-3)GlcNAcb1-2Mana1-6(Fuca1-4(Galb1-3)GlcNAcb1-2Mana1-3)Manb1-4GlcNAcb1-4(Fuca1-6)GlcNAcb-Sp22	111	4	4
363	Neu5Aca2-6GlcNAcb1-4GlcNAc-Sp21	12	3	28
364	Neu5Aca2-6GlcNAcb1-4GlcNAcb1-4GlcNAc-Sp21	10	2	23
365	Galb1-4(Fuca1-3)GlcNAcb1-6(Fuca1-2Galb1-4GlcNAcb1-3)Galb1-4Glc-Sp21	15	4	30

366	Galb1-4GlcNAcb1-2Mana1-6(Galb1-4GlcNAcb1-4(Galb1-4GlcNAcb1-2)Mana1-3)Manb1-4GlcNAcb1-4GlcNAc-Sp21	22	8	35
367	GalNAca1-3(Fuca1-2)Galb1-4GlcNAcb1-2Mana1-6(GalNAca1-3(Fuca1-2)Galb1-4GlcNAcb1-2Mana1-3)Manb1-4GlcNAcb1-4GlcNAcb-Sp20	13	2	13
368	Gala1-3(Fuca1-2)Galb1-4GlcNAcb1-2Mana1-6(Gala1-3(Fuca1-2)Galb1-4GlcNAcb1-2Mana1-3)Manb1-4GlcNAcb1-4GlcNAcb-Sp20	16	6	37
369	Gala1-3Galb1-4(Fuca1-3)GlcNAcb1-2Mana1-6(Gala1-3Galb1-4(Fuca1-3)GlcNAcb1-2Mana1-3)Manb1-4GlcNAcb1-4GlcNAcb-Sp20	59	17	28
370	GalNAca1-3(Fuca1-2)Galb1-3GlcNAcb1-2Mana1-6(GalNAca1-3(Fuca1-2)Galb1-3GlcNAcb1-2Mana1-3)Manb1-4GlcNAcb1-4GlcNAcb-Sp20	69	17	25
371	Fuca1-4(Fuca1-2Galb1-3)GlcNAcb1-2Mana1-3(Fuca1-4(Fuca1-2Galb1-3)GlcNAcb1-2Mana1-3)Manb1-4GlcNAcb1-4GlcNAcb-Sp19	43	28	65
372	Neu5Aca2-3Galb1-4GlcNAcb1-3GalNAc-Sp14	5	5	102
373	Neu5Aca2-6Galb1-4GlcNAcb1-3GalNAc-Sp14	10	3	30
374	Neu5Aca2-3Galb1-4(Fuca1-3)GlcNAcb1-3GalNAca-Sp14	94	24	25
375	GalNAcb1-4GlcNAcb1-2Mana1-6(GalNAcb1-4GlcNAcb1-2Mana1-3)Manb1-4GlcNAcb1-4GlcNAc-Sp12	28	5	16
376	Galb1-3GalNAca1-3(Fuca1-2)Galb1-4Glc-Sp0	3	3	86
377	Galb1-3GalNAca1-3(Fuca1-2)Galb1-4GlcNAc-Sp0	3	3	120
378	Galb1-3GlcNAcb1-3Galb1-4GlcNAcb1-6(Galb1-3GlcNAcb1-3)Galb1-4Glcb-Sp0	10	4	42
379	Galb1-4(Fuca1-3)GlcNAcb1-6(Galb1-3GlcNAcb1-3)Galb1-4Glc-Sp21	25	3	13

380	Galb1-4GlcNAcb1-6(Fuca1-4(Fuca1-2Galb1-3)GlcNAcb1-3)Galb1-4Glc-Sp21	47	10	21
381	Galb1-4(Fuca1-3)GlcNAcb1-6(Fuca1-4(Fuca1-2Galb1-3)GlcNAcb1-3)Galb1-4Glc-Sp21	15	4	24
382	Galb1-3GlcNAcb1-3Galb1-4(Fuca1-3)GlcNAcb1-6(Galb1-3GlcNAcb1-3)Galb1-4Glc-Sp21	15	2	14
383	Galb1-4GlcNAcb1-6(Galb1-4GlcNAcb1-2)Mana1-6(Galb1-4GlcNAcb1-4(Galb1-4GlcNAcb1-2)Mana1-3)Manb1-4GlcNAcb1-4GlcNAcb-Sp21	15	2	12
384	GlcNAcb1-2Mana1-6(GlcNAcb1-4(GlcNAcb1-2)Mana1-3)Manb1-4GlcNAcb1-4GlcNAc-Sp21	24	3	11
385	Fuca1-2Galb1-3GalNAca1-3(Fuca1-2)Galb1-4Glcb-Sp0	11	5	47
386	Fuca1-2Galb1-3GalNAca1-3(Fuca1-2)Galb1-4GlcNAcb-Sp0	11	6	50
387	Galb1-3GlcNAcb1-3GalNAca-Sp14	11	3	24
388	GalNAcb1-4(Neu5Aca2-3)Galb1-4GlcNAcb1-3GalNAca-Sp14	66	12	19
389	GalNAca1-3(Fuca1-2)Galb1-3GalNAca1-3(Fuca1-2)Galb1-4GlcNAcb-Sp0	1	5	476
390	Gala1-3Galb1-3GlcNAcb1-2Mana1-6(Gala1-3Galb1-3GlcNAcb1-2Mana1-3)Manb1-4GlcNAcb1-4GlcNAc-Sp19	63	3	5
391	Gala1-3Galb1-3(Fuca1-4)GlcNAcb1-2Mana1-6(Gala1-3Galb1-3(Fuca1-4)GlcNAcb1-2Mana1-3)Manb1-4GlcNAcb1-4GlcNAc-Sp19	88	15	17
392	Neu5Aca2-3Galb1-3GlcNAcb1-2Mana1-6(Neu5Aca2-3Galb1-3GlcNAcb1-2Mana1-3)Manb1-4GlcNAcb1-4GlcNAc-Sp19	6	3	45
393	GlcNAcb1-2Mana1-6(Galb1-4GlcNAcb1-2Mana1-3)Manb1-4GlcNAcb1-4GlcNAc-Sp12	5	4	79
394	Galb1-4GlcNAcb1-2Mana1-6(GlcNAcb1-2Mana1-3)Manb1-4GlcNAcb1-4GlcNAc-Sp12	3	2	62

395	Neu5Aca2-3Galb1-3GlcNAcb1-3GalNAca-Sp14	21	3	12
396	Fuca1-2Galb1-4GlcNAcb1-3GalNAca-Sp14	32	3	10
397	Galb1-4(Fuca1-3)GlcNAcb1-3GalNAca-Sp14	37	8	22
398	GalNAca1-3GalNAcb1-3Gala1-4Galb1-4GlcNAcb-Sp0	0	2	-887
399	Gala1-4Galb1-3GlcNAcb1-2Mana1-6(Gala1-4Galb1-3GlcNAcb1-2Mana1-3)Manb1-4GlcNAcb1-4GlcNAcb-Sp19	56	4	6
400	Gala1-4Galb1-4GlcNAcb1-2Mana1-6(Gala1-4Galb1-4GlcNAcb1-2Mana1-3)Manb1-4GlcNAcb1-4GlcNAcb-Sp24	119	7	6
401	Gala1-3Galb1-4GlcNAcb1-3GalNAca-Sp14	0	2	#####
402	Galb1-3GlcNAcb1-6Galb1-4GlcNAcb-Sp0	2	3	158
403	Galb1-3GlcNAca1-6Galb1-4GlcNAcb-Sp0	-2	2	-67
404	GalNAcb1-3Gala1-6Galb1-4Glcb-Sp8	5	3	50
405	Gala1-3(Fuca1-2)Galb1-4(Fuca1-3)Glcb-Sp21	13	2	17
406	Galb1-4GlcNAcb1-6(Neu5Aca2-6Galb1-3GlcNAcb1-3)Galb1-4Glc-Sp21	16	4	24
407	Galb1-3GalNAcb1-4(Neu5Aca2-8Neu5Aca2-3)Galb1-4Glcb-Sp0	12	3	22
408	Neu5Aca2-3Galb1-3GalNAcb1-4(Neu5Aca2-8Neu5Aca2-3)Galb1-4Glcb-Sp0	20	6	31
409	Gala1-3(Fuca1-2)Galb1-4GlcNAcb1-3GalNAca-Sp14	2	5	257
410	GalNAca1-3(Fuca1-2)Galb1-4GlcNAcb1-3GalNAca-Sp14	14	5	39
411	GalNAca1-3GalNAcb1-3Gala1-4Galb1-4Glcb-Sp0	10	2	18
412	Fuca1-2Galb1-4(Fuca1-3)GlcNAcb1-3GalNAca-Sp14	168	16	10
413	Gala1-3(Fuca1-2)Galb1-4(Fuca1-3)GlcNAcb1-3GalNAc-Sp14	51	12	23

414	GalNAca1-3(Fuca1-2)Galb1-4(Fuca1-3)GlcNAcb1-3GalNAc-Sp14	106	20	19
415	Galb1-4(Fuca1-3)GlcNAcb1-2Mana1-6(Galb1-4(Fuca1-3)GlcNAcb1-2Mana1-3)Manb1-4GlcNAcb1-4(Fuca1-6)GlcNAcb-Sp22	26	27	101
416	Fuca1-2Galb1-4GlcNAcb1-2Mana1-6(Fuca1-2Galb1-4GlcNAcb1-2Mana1-3)Manb1-4GlcNAcb1-4(Fuca1-6)GlcNAcb-Sp22	123	20	17
417	GlcNAcb1-2(GlcNAcb1-6)Mana1-6(GlcNAcb1-2Mana1-3)Manb1-4GlcNAcb1-4GlcNAcb-Sp19	9	6	66
418	Fuca1-2Galb1-3GlcNAcb1-3GalNAc-Sp14	9	6	64
419	Gala1-3(Fuca1-2)Galb1-3GlcNAcb1-3GalNAc-Sp14	8	7	82
420	GalNAca1-3(Fuca1-2)Galb1-3GlcNAcb1-3GalNAc-Sp14	58	31	54
421	Gala1-3Galb1-3GlcNAcb1-3GalNAc-Sp14	8	3	41
422	Fuca1-2Galb1-3GlcNAcb1-2Mana1-6(Fuca1-2Galb1-3GlcNAcb1-2Mana1-3)Manb1-4GlcNAcb1-4(Fuca1-6)GlcNAcb-Sp22	94	13	13
423	Gala1-3(Fuca1-2)Galb1-4GlcNAcb1-2Mana1-6(Gala1-3(Fuca1-2)Galb1-4GlcNAcb1-2Mana1-3)Manb1-4GlcNAcb1-4(Fuca1-6)GlcNAcb-Sp22	175	49	28
424	Galb1-3GlcNAcb1-6(Galb1-3GlcNAcb1-2)Mana1-6(Galb1-3GlcNAcb1-2Mana1-3)Manb1-4GlcNAcb1-4GlcNAcb-Sp19	28	6	23
425	Galb1-4GlcNAcb1-6(Fuca1-2Galb1-3GlcNAcb1-3)Galb1-4Glc-Sp21	18	6	34
426	Fuca1-3GlcNAcb1-6(Galb1-4GlcNAcb1-3)Galb1-4Glc-Sp21	19	11	56
427	GlcNAcb1-2Mana1-6(GlcNAcb1-4)(GlcNAcb1-2Mana1-3)Manb1-4GlcNAcb1-4GlcNAc-Sp21	18	9	49
428	GlcNAcb1-2Mana1-6(GlcNAcb1-4)(GlcNAcb1-4(GlcNAcb1-2)Mana1-3)Manb1-4GlcNAcb1-4GlcNAc-Sp21	10	3	30

429	GlcNAcb1-6(GlcNAcb1-2)Mana1-6(GlcNAcb1-4)(GlcNAcb1-2Mana1-3)Manb1-4GlcNAcb1-4GlcNAc-Sp21	12	1	11
430	GlcNAcb1-6(GlcNAcb1-2)Mana1-6(GlcNAcb1-4)(GlcNAcb1-4(GlcNAcb1-2)Mana1-3)Manb1-4GlcNAcb1-4GlcNAc-Sp21	25	4	17
431	Galb1-4GlcNAcb1-2Mana1-6(GlcNAcb1-4)(Galb1-4GlcNAcb1-2Mana1-3)Manb1-4GlcNAcb1-4GlcNAc-Sp21	20	10	49
432	Galb1-4GlcNAcb1-2Mana1-6(GlcNAcb1-4)(Galb1-4GlcNAcb1-4(Galb1-4GlcNAcb1-2)Mana1-3)Manb1-4GlcNAcb1-4GlcNAc-Sp21	22	6	29
433	Galb1-4GlcNAcb1-6(Galb1-4GlcNAcb1-2)Mana1-6(GlcNAcb1-4)(Galb1-4GlcNAcb1-2Mana1-3)Manb1-4GlcNAcb1-4GlcNAc-Sp21	22	9	40
434	Galb1-4GlcNAcb1-6(Galb1-4GlcNAcb1-2)Mana1-6(GlcNAcb1-4)(Galb1-4GlcNAcb1-4(Galb1-4GlcNAcb1-2)Mana1-3)Manb1-4GlcNAcb1-4GlcNAc-Sp21	15	11	73
435	Galb1-4Galb-Sp10	12	7	55
436	Galb1-6Galb-Sp10	10	6	58
437	Neu5Aca2-3Galb1-4GlcNAcb1-3Galb-Sp8	4	3	67
438	GalNAcb1-6GalNAcb-Sp8	4	2	40
439	(6S)Galb1-3GlcNAcb-Sp0	5	3	67
440	(6S)Galb1-3(6S)GlcNAc-Sp0	13	7	52
441	Fuca1-2Galb1-4 GlcNAcb1-2Mana1-6(Fuca1-2Galb1-4GlcNAcb1-2(Fuca1-2Galb1-4GlcNAcb1-4)Mana1-3)Manb1-4GlcNAcb1-4GlcNAcb-Sp12	73	9	12
442	Fuca1-2Galb1-4(Fuca1-3)GlcNAcb1-2Mana1-6(Fuca1-2Galb1-4(Fuca1-3)GlcNAcb1-4(Fuca1-2Galb1-4(Fuca1-3)GlcNAcb1-2)Mana1-3)Manb1-4GlcNAcb1-4GlcNAcb-Sp12	92	4	4
443	Galb1-4(Fuca1-3)GlcNAcb1-6GalNAc-Sp14	68	14	21
444	Galb1-4GlcNAcb1-2Mana-Sp0	28	2	7

445	Fuca1-2Galb1-4GlcNAcb1-6(Fuca1-2Galb1-4GlcNAcb1-3)GalNAc-Sp14	16	3	20
446	Gala1-3(Fuca1-2)Galb1-4GlcNAcb1-6(Gala1-3(Fuca1-2)Galb1-4GlcNAcb1-3)GalNAc-Sp14	8	2	27
447	GalNAca1-3(Fuca1-2)Galb1-4GlcNAcb1-6(GalNAca1-3(Fuca1-2)Galb1-4GlcNAcb1-3)GalNAc-Sp14	2	4	216
448	Neu5Aca2-8Neu5Aca2-3Galb1-3GalNAcb1-4(Neu5Aca2-8Neu5Aca2-3)Galb1-4Glcb-Sp0	9	4	40
449	GalNAcb1-4Galb1-4Glcb-Sp0	15	8	53
450	GalNAca1-3(Fuca1-2)Galb1-4GlcNAcb1-2Mana1-6(GalNAca1-3(Fuca1-2)Galb1-4GlcNAcb1-2Mana1-3)Manb1-4GlcNAcb1-4(Fuca1-6)GlcNAcb-Sp22	24	4	17
451	Gala1-3(Fuca1-2)Galb1-3GlcNAcb1-2Mana1-6(Gala1-3(Fuca1-2)Galb1-3GlcNAcb1-2Mana1-3)Manb1-4GlcNAcb1-4(Fuca1-6)GlcNAcb-Sp22	179	12	6
452	Neu5Aca2-6Galb1-4GlcNAcb1-6(Fuca1-2Galb1-3GlcNAcb1-3)Galb1-4Glc-Sp21	24	3	14
453	GalNAca1-3(Fuca1-2)Galb1-3GlcNAcb1-2Mana1-6(GalNAca1-3(Fuca1-2)Galb1-3GlcNAcb1-2Mana1-3)Manb1-4GlcNAcb1-4(Fuca1-6)GlcNAcb-Sp22	260	51	20
454	Galb1-4GlcNAcb1-6(Galb1-4GlcNAcb1-2)Mana1-6(Galb1-4GlcNAcb1-2Mana1-3)Manb1-4GlcNAcb1-4GlcNAcb-Sp19	35	3	10
455	Neu5Aca2-3Galb1-4GlcNAcb1-2Mana1-6(GlcNAcb1-4)(Neu5Aca2-3Galb1-4GlcNAcb1-2Mana1-3)Manb1-4GlcNAcb1-4GlcNAcb-Sp21	11	5	48
456	Neu5Aca2-3Galb1-4GlcNAcb1-4Mana1-6(GlcNAcb1-4)(Neu5Aca2-3Galb1-4GlcNAcb1-4(Neu5Aca2-3Galb1-4GlcNAcb1-2)Mana1-3)Manb1-4GlcNAcb1-4GlcNAcb-Sp21	10	1	12

457	Neu5Aca2-3Galb1-4GlcNAcb1-6(Neu5Aca2-3Galb1-4GlcNAcb1-2)Mana1-6(GlcNAcb1-4)(Neu5Aca2-3Galb1-4GlcNAcb1-2Mana1-3)Manb1-4GlcNAcb1-4GlcNAcb-Sp21	7	4	65
458	Neu5Aca2-3Galb1-4GlcNAcb1-6(Neu5Aca2-3Galb1-4GlcNAcb1-2)Mana1-6(GlcNAcb1-4)(Neu5Aca2-3Galb1-4GlcNAcb1-4(Neu5Aca2-3Galb1-4GlcNAcb1-2)Mana1-3)Manb1-4GlcNAcb1-4GlcNAcb-Sp21	7	2	21
459	Neu5Aca2-6Galb1-4GlcNAcb1-2Mana1-6(GlcNAcb1-4)(Neu5Aca2-6Galb1-4GlcNAcb1-2Mana1-3)Manb1-4GlcNAcb1-4GlcNAcb-Sp21	25	11	42
460	Neu5Aca2-6Galb1-4GlcNAcb1-4Mana1-6(GlcNAcb1-4)(Neu5Aca2-6Galb1-4GlcNAcb1-4(Neu5Aca2-6Galb1-4GlcNAcb1-2)Mana1-3)Manb1-4GlcNAcb1-4GlcNAcb-Sp21	12	6	47
461	Neu5Aca2-6Galb1-4GlcNAcb1-6(Neu5Aca2-6Galb1-4GlcNAcb1-2)Mana1-6(GlcNAcb1-4)(Neu5Aca2-6Galb1-4GlcNAcb1-2Mana1-3)Manb1-4GlcNAcb1-4GlcNAcb-Sp21	17	4	23
462	Neu5Aca2-6Galb1-4GlcNAcb1-6(Neu5Aca2-6Galb1-4GlcNAcb1-2)Mana1-6(GlcNAcb1-4)(Neu5Aca2-6Galb1-4GlcNAcb1-4(Neu5Aca2-6Galb1-4GlcNAcb1-2)Mana1-3)Manb1-4GlcNAcb1-4GlcNAcb-Sp21	9	3	31
463	Gala1-3(Fuca1-2)Galb1-3GalNAca-Sp8	9	4	39
464	Gala1-3(Fuca1-2)Galb1-3GalNAcb-Sp8	2	11	564
465	Glca1-6Glca1-6Glca1-6Glcb-Sp10	14	10	72
466	Glca1-4Glca1-4Glca1-4Glcb-Sp10	19	13	71

467	Neu5Aca2-3Galb1-4GlcNAcb1-6(Neu5Aca2-3Galb1-4GlcNAcb1-3)GalNAca-Sp14	-4	6	-181
468	Fuca1-2Galb1-4(Fuca1-3)GlcNAcb1-2Mana1-6(Fuca1-2Galb1-4(Fuca1-3)GlcNAcb1-2Mana1-3)Manb1-4GlcNAcb1-4(Fuca1-6)GlcNAcb-Sp24	24	44	186
469	Fuca1-2Galb1-3(Fuca1-4)GlcNAcb1-2Mana1-6(Fuca1-2Galb1-3(Fuca1-4)GlcNAcb1-2Mana1-3)Manb1-4GlcNAcb1-4(Fuca1-6)GlcNAcb1-4(Fuca1-6)GlcNAcb-Sp19	85	20	24
470	GlcNAcb1-6(GlcNAcb1-2)Mana1-6(GlcNAcb1-2Mana1-3)Manb1-4GlcNAcb1-4(Fuca1-6)GlcNAcb-Sp24	128	24	18
471	Galb1-3GlcNAcb1-2Mana1-6(GlcNAcb1-4)(Galb1-3GlcNAcb1-2Mana1-3)Manb1-4GlcNAcb1-4GlcNAcb-Sp21	69	14	21
472	Neu5Aca2-6Galb1-4GlcNAcb1-6(Galb1-3GlcNAcb1-3)Galb1-4Glcb-Sp21	22	5	25
473	Neu5Aca2-3Galb1-4GlcNAcb1-2Mana-Sp0	49	7	14
474	Neu5Aca2-3Galb1-4GlcNAcb1-6GalNAca-Sp14	3	5	186
475	Neu5Aca2-6Galb1-4GlcNAcb1-6GalNAca-Sp14	10	6	65
476	Neu5Aca2-6Galb1-4 GlcNAcb1-6(Neu5Aca2-6Galb1-4GlcNAcb1-3)GalNAca-Sp14	4	1	23
477	Neu5Aca2-6Galb1-4GlcNAcb1-2Mana1-6(Neu5Aca2-6Galb1-4GlcNAcb1-2Mana1-3)Manb1-4GlcNAcb1-4(Fuca1-6)GlcNAcb-Sp24	60	14	24
478	Neu5Aca2-3Galb1-4GlcNAcb1-2Mana1-6(Neu5Aca2-3Galb1-4GlcNAcb1-2Mana1-3)Manb1-4GlcNAcb1-4(Fuca1-6)GlcNAcb-Sp24	45	22	49

479	Mana1-6(Mana1-3)Manb1-4GlcNAcb1-4(Fuca1-6)GlcNAcb-Sp19	12	6	53
480	Galb1-4GlcNAcb1-6(Galb1-4GlcNAcb1-2)Mana1-6(Galb1-4GlcNAcb1-2Mana1-3)Manb1-4GlcNAcb1-4(Fuca1-6)GlcNAcb-Sp24	94	10	11
481	Neu5Aca2-3Galb1-3GlcNAcb1-2Mana1-6(GlcNAcb1-4)(Neu5Aca2-3Galb1-3GlcNAcb1-2Mana1-3)Manb1-4GlcNAcb1-4GlcNAc-Sp21	10	15	156
482	Neu5Aca2-6Galb1-4GlcNAcb1-6(Fuca1-2Galb1-4(Fuca1-3)GlcNAcb1-3)Galb1-4Glc-Sp21	46	22	47
483	Galb1-3GlcNAcb1-6GalNAca-Sp14	2	2	86
484	Gala1-3Galb1-3GlcNAcb1-6GalNAca-Sp14	3	5	200
485	Galb1-3(Fuca1-4)GlcNAcb1-6GalNAca-Sp14	37	11	30
486	Neu5Aca2-3Galb1-3GlcNAcb1-6GalNAca-Sp14	6	4	69
487	(3S)Galb1-3(Fuca1-4)GlcNAcb-Sp0	15	5	31
488	Galb1-4(Fuca1-3)GlcNAcb1-6(Neu5Aca2-6(Neu5Aca2-3Galb1-3)GlcNAcb1-3)Galb1-4Glc-Sp21	30	18	62
489	Fuca1-2Galb1-4GlcNAcb1-6GalNAca-Sp14	-1	5	-959
490	Gala1-3Galb1-4GlcNAcb1-6GalNAca-Sp14	3	5	191
491	Galb1-4(Fuca1-3)GlcNAcb1-2Mana-Sp0	12	5	38
492	Fuca1-2(6S)Galb1-3GlcNAcb-Sp0	0	2	#####
493	Gala1-3(Fuca1-2)Galb1-4GlcNAcb1-6GalNAca-Sp14	12	8	64
494	Fuca1-2Galb1-4GlcNAcb1-2Mana-Sp0	12	8	69
495	Fuca1-2Galb1-3(6S)GlcNAcb-Sp0	22	9	41
496	Fuca1-2(6S)Galb1-3(6S)GlcNAcb-Sp0	51	6	11
497	Neu5Aca2-6GalNAcb1-4(6S)GlcNAcb-Sp8	3	3	102
498	GalNAcb1-4(Fuca1-3)(6S)GlcNAcb-Sp8	7	3	53

499	(3S)GalNAcb1-4(Fuca1-3)GlcNAcb-Sp8	8	1	14
500	Fuca1-2Galb1-3GlcNAcb1-6(Fuca1-2Galb1-3GlcNAcb1-3)GalNAca-Sp14	10	2	24
501	GalNAca1-3(Fuca1-2)Galb1-3GlcNAcb1-6GalNAca-Sp14	-1	7	-1428
502	GlcNAcb1-6(GlcNAcb1-2)Mana1-6(GlcNAcb1-4)(GlcNAcb1-4(GlcNAcb1-2)Mana1-3)Manb1-4GlcNAcb1-4(Fuca1-6)GlcNAc-Sp21	10	3	27
503	Galb1-4GlcNAcb1-6(Galb1-4GlcNAcb1-2)Mana1-6(GlcNAcb1-4)Galb1-4GlcNAcb1-4(Gal b1-4GlcNAcb1-2)Mana1-3)Manb1-4GlcNAcb1-4(Fuca1-6)GlcNAc-Sp21	14	2	13
504	Galb1-3GlcNAca1-3Galb1-4GlcNAcb-Sp8	4	2	46
505	Galb1-3(6S)GlcNAcb-Sp8	-4	7	-188
506	(6S)(4S)GalNAcb1-4GlcNAc-Sp8	5	8	161
507	(6S)GalNAcb1-4GlcNAc-Sp8	-2	5	-346
508	(3S)GalNAcb1-4(3S)GlcNAc-Sp8	4	3	59
509	GalNAcb1-4(6S)GlcNAc-Sp8	5	4	78
510	(3S)GalNAcb1-4GlcNAc-Sp8	4	2	41
511	(4S)GalNAcb-Sp10	-1	2	-383
512	Galb1-4(6P)GlcNAcb-Sp0	6	5	94
513	(6P)Galb1-4GlcNAcb-SP0	10	4	42
514	GalNAca1-3(Fuca1-2)Galb1-4GlcNAcb1-6GalNAc-Sp14	0	3	#####
515	Neu5Aca2-6Galb1-4GlcNAcb1-2Man-Sp0	9	3	32
516	Gala1-3Galb1-4GlcNAcb1-2Mana-Sp0	1	8	845
517	Gala1-3(Fuca1-2)Galb1-4GlcNAcb1-2Mana-Sp0	6	3	53
518	GalNAca1-3(Fuca1-2)Galb1-4 GlcNAcb1-2Mana-Sp0	5	2	36
519	Galb1-3GlcNAcb1-2Mana-Sp0	10	4	41
520	Gala1-3(Fuca1-2)Galb1-3GlcNAcb1-6GalNAc-Sp14	1	8	829
521	Neu5Aca2-3Galb1-3GlcNAcb1-2Mana-Sp0	6	2	26
522	Gala1-3Galb1-3GlcNAcb1-2Mana-Sp0	3	2	83
523	GalNAcb1-4GlcNAcb1-2Mana-Sp0	5	2	43

524	Neu5Aca2-3Galb1-3GalNAcb1-4Galb1-4Glcb-Sp0	12	8	66
525	GlcNAcb1-2 Mana1-6(GlcNAcb1-4)(GlcNAcb1-2Mana1-3)Manb1-4GlcNAcb1-4(Fuca1-6)GlcNAc-Sp21	8	5	61
526	Galb1-4GlcNAcb1-2 Mana1-6(GlcNAcb1-4)(Galb1-4GlcNAcb1-2Mana1-3)Manb1-4GlcNAcb1-4(Fuca1-6)GlcNAc-Sp21	12	8	71
527	Galb1-4GlcNAcb1-2 Mana1-6(Galb1-4GlcNAcb1-4)(Galb1-4GlcNAcb1-2Mana1-3)Manb1-4GlcNAcb1-4(Fuca1-6)GlcNAc-Sp21	22	3	14
528	Fuca1-4(Galb1-3)GlcNAcb1-2 Mana-Sp0	79	2	2
529	Neu5Aca2-3Galb1-4(Fuca1-3)GlcNAcb1-2Mana-Sp0	5	4	99
530	GlcNAcb1-3Galb1-4GlcNAcb1-6(GlcNAcb1-3)Galb1-4GlcNAc-Sp0	6	7	127
531	GalNAca1-3(Fuca1-2)Galb1-3GalNAcb1-3Gala1-4Galb1-4Glc-Sp21	7	7	105
532	Gala1-3(Fuca1-2)Galb1-3GalNAcb1-3Gala1-4Galb1-4Glc-Sp21	24	10	44
533	Galb1-3GalNAcb1-3Gal-Sp21	13	10	78
534	GlcNAcb1-3Galb1-4GlcNAcb1-2Mana1-6(GlcNAcb1-3Galb1-4GlcNAcb1-2Mana1-3)Manb1-4GlcNAcb1-4GlcNAcb-Sp12	7	6	90
535	GlcNAcb1-3Galb1-4GlcNAcb1-2Mana1-6(GlcNAcb1-3Galb1-4GlcNAcb1-2Mana1-3)Manb1-4GlcNAcb1-4GlcNAcb-Sp25	98	10	11
536	Fuca1-2Galb1-4GlcNAcb1-3Galb1-4GlcNAcb1-2Mana1-6(Fuca1-2Galb1-4GlcNAcb1-3Galb1-4GlcNAcb1-2Mana1-3)Manb1-4GlcNAcb1-4GlcNAcb-Sp24	93	13	14
537	GlcNAcb1-3Galb1-4GlcNAcb1-3Galb1-4GlcNAcb1-2Mana1-6(GlcNAcb1-3Galb1-4GlcNAcb1-3Galb1-4GlcNAcb1-2Mana1-3)Manb1-4GlcNAcb1-4GlcNAcb-Sp12	382	151	39

538	GlcNAcb1-3Galb1-4GlcNAcb1-3Galb1-4GlcNAcb1-2Mana1-6(GlcNAcb1-3Galb1-4GlcNAcb1-3Galb1-4GlcNAcb1-2Mana1-3)Manb1-4GlcNAcb1-4GlcNAcb-Sp25	124	29	24
539	Galb1-4GlcNAcb1-3Galb1-4GlcNAcb1-3Galb1-4GlcNAcb1-2Mana1-6(Galb1-4GlcNAcb1-3Galb1-4GlcNAcb1-3Galb1-4GlcNAcb1-2Mana1-3)Manb1-4GlcNAcb1-4GlcNAcb-Sp12	968	168	17
540	Galb1-4GlcNAcb1-3Galb1-4GlcNAcb1-3Galb1-4GlcNAcb1-2Mana1-6(Galb1-4GlcNAcb1-3Galb1-4GlcNAcb1-3Galb1-4GlcNAcb1-2Mana1-3)Manb1-4GlcNAcb1-4GlcNAcb-Sp24	102	12	12
541	Galb1-3GlcNAcb1-3Galb1-4GlcNAcb1-2Mana1-6(Galb1-3GlcNAcb1-3Galb1-4GlcNAcb1-2Mana1-3)Manb1-4GlcNAcb1-4GlcNAc-Sp25	60	11	18
542	Neu5Gca2-8Neu5Gca2-3Galb1-4GlcNAc-Sp0	4	2	55
543	Neu5Aca2-8Neu5Gca2-3Galb1-4GlcNAc-Sp0	-5	7	-146
544	Neu5Gca2-8Neu5Aca2-3Galb1-4GlcNAc-Sp0	-2	4	-178
545	Neu5Gca2-8Neu5Gca2-3Galb1-4GlcNAcb1-3Galb1-4GlcNAc-Sp0	1	6	648
546	Neu5Gca2-8Neu5Gca2-6Galb1-4GlcNAc-Sp0	0	4	#####
547	Neu5Aca2-8Neu5Aca2-3Galb1-4GlcNAc-Sp0	0	7	2641
548	GlcNAcb1-3Galb1-4GlcNAcb1-6(GlcNAcb1-3Galb1-4GlcNAcb1-2)Mana1-6(GlcNAcb1-3Galb1-4GlcNAcb1-2Man a1-3)Manb1-4GlcNAcb1-4GlcNAc-Sp24	149	18	12
549	Galb1-4GlcNAcb1-3Galb1-4GlcNAcb1-6(Galb1-4GlcNAcb1-3Galb1-4GlcNAcb1-2)Mana1-6(Galb1-4GlcNAcb1-3Galb1-	69	20	29

	4GlcNAcb1-2Mana1-3)Mana1-4GlcNAcb1-4GlcNAc-Sp24			
550	Gala1-3Galb1-4GlcNAcb1-2Mana1-6(Gala1-3Galb1-4GlcNAcb1-2Mana1-3)Manb1-4GlcNAcb1-4GlcNAc-Sp24	175	49	28
551	GlcNAcb1-3Galb1-4GlcNAcb1-6(GlcNAcb1-3Galb1-3)GalNAca-Sp14	-2	3	-192
552	GalNAcb1-3GlcNAcb-Sp0	3	4	125
553	GalNAcb1-4GlcNAcb1-3GalNAcb1-4GlcNAcb-Sp0	-6	5	-91
554	GlcNAcb1-3Galb1-4GlcNAcb1-3Galb1-4GlcNAcb1-3Galb1-4GlcNAcb1-3Galb1-4GlcNAcb1-2Mana1-6(GlcNAcb1-3Galb1-4GlcNAcb1-3Galb1-4GlcNAcb1-3Galb1-4GlcNAcb1-3Galb1-4GlcNAcb1-2Mana1-3)Manb1-4GlcNAcb1-4GlcNAcb-Sp25	68	22	33
555	Galb1-4GlcNAcb1-3Galb1-4GlcNAcb1-3Galb1-4GlcNAcb1-3Galb1-4GlcNAcb1-2Mana1-6(Galb1-4GlcNAcb1-3Galb1-4GlcNAcb1-3Galb1-4GlcNAcb1-3Galb1-4GlcNAcb1-3Galb1-4GlcNAcb1-2Mana1-3)Manb1-4GlcNAcb1-4GlcNAcb-Sp25	57	32	56
556	GlcNAb1-3Galb1-3GalNAc-Sp14	-3	4	-127
557	Galb1-3GlcNAcb1-6(Galb1-3)GalNAc-Sp14	1	3	427
558	Galb1-4GlcNAcb1-3Galb1-4GlcNAcb1-3Galb1-4GlcNAcb1-3Galb1-4GlcNAcb1-3Galb1-4GlcNAcb1-2Mana1-6(Galb1-4GlcNAcb1-3Galb1-4GlcNAcb1-3Galb1-4GlcNAcb1-3Galb1-4GlcNAcb1-3Galb1-4GlcNAcb1-2Mana1-3)Manb1-4GlcNAcb1-4GlcNAcb-Sp25	-1	3	-337
559	(3S)GlcAb1-3Galb1-4GlcNAcb1-3Galb1-4Glc-Sp0	-1	3	-316

560	(3S)GlcAb1-3Galb1-4GlcNAcb1-2Mana-Sp0	-2	1	-41
561	Galb1-3GlcNAcb1-3Galb1-4GlcNAcb1-3Galb1-4GlcNAcb1-6(Galb1-3GlcNAcb1-3Galb1-4GlcNAcb1-3Galb1-4GlcNAb1-2)Mana1-6(Galb1-3GlcNAcb1-3Galb1-4GlcNAcb1-3Galb1-4GlcNAcb1-2Mana1-3)Manb1-4GlcNAcb1-4(Fuca1-6)GlcNAcb-Sp24	52	34	67
562	Galb1-3GlcNAcb1-3Galb1-4GlcNAcb1-6(Galb1-3GlcNAcb1-3Galb1-4GlcNAb1-2)Mana1-6(Galb1-3GlcNAcb1-3Galb1-4GlcNAcb1-2Mana1-3)Manb1-4GlcNAcb1-4(Fuca1-6)GlcNAcb-Sp24	90	36	40
563	Neu5Aca2-8Neu5Aca2-3Galb1-3GalNAcb1-4(Neu5Aca2-3)Galb1-4Glc-Sp21	19	12	64
564	GlcNAcb1-3Galb1-4GlcNAcb1-2Mana1-6(GlcNAcb1-3Galb1-4GlcNAcb1-2Mana1-3)Manb1-4GlcNAcb1-4(Fuca1-6)GlcNAcb-Sp24	87	25	29
565	Galb1-4GlcNAcb1-3Galb1-4GlcNAcb1-2Mana1-6(Galb1-4GlcNAcb1-3Galb1-4GlcNAcb1-2Mana1-3)Manb1-4GlcNAcb1-4(Fuca1-6)GlcNAcb-Sp24	113	28	25
566	GlcNAcb1-3Galb1-4GlcNAcb1-3Galb1-4GlcNAcb1-2Mana1-6(GlcNAcb1-3Galb1-4GlcNAcb1-3Galb1-4GlcNAcb1-2Mana1-3)Manb1-4GlcNAcb1-4(Fuca1-6)GlcNAcb-Sp24	7	5	67
567	Galb1-4GlcNAcb1-3Galb1-4GlcNAcb1-3Galb1-4GlcNAcb1-2Mana1-6(Galb1-4GlcNAcb1-3Galb1-4GlcNAcb1-3Galb1-4GlcNAcb1-2Mana1-3)Manb1-4GlcNAcb1-4(Fuca1-6)GlcNAcb-Sp24	42	16	39
568	GlcNAcb1-3Galb1-4GlcNAcb1-3Galb1-4GlcNAcb1-3Galb1-	68	9	13

	4GlcNAcb1-2Mana1-6(GlcNAcb1-3Galb1-4GlcNAcb1-3Galb1-4GlcNAcb1-3Galb1-4GlcNAcb1-2Mana1-3)Manb1-4GlcNAcb1-4(Fuca1-6)GlcNAcb-Sp24			
569	Galb1-4GlcNAcb1-3Galb1-4GlcNAcb1-3Galb1-4GlcNAcb1-3Galb1-4GlcNAcb1-2Mana1-6(Galb1-4GlcNAcb1-3Galb1-4GlcNAcb1-3Galb1-4GlcNAcb1-3Galb1-4GlcNAcb1-2Mana1-3)Manb1-4GlcNAcb1-4(Fuca1-6)GlcNAcb-Sp24	94	69	74
570	GlcNAcb1-3Galb1-4GlcNAcb1-3Galb1-4GlcNAcb1-3Galb1-4GlcNAcb1-3Galb1-4GlcNAcb1-2Mana1-6(GlcNAcb1-3Galb1-4GlcNAcb1-3Galb1-4GlcNAcb1-3Galb1-4GlcNAcb1-3Galb1-4GlcNAcb1-2Mana1-3)Manb1-4GlcNAcb1-4(Fuca1-6)GlcNAcb-Sp19	18	14	79
571	Galb1-4GlcNAcb1-3Galb1-4GlcNAcb1-3Galb1-4GlcNAcb1-3Galb1-4GlcNAcb1-3Galb1-4GlcNAcb1-2Mana1-6(Galb1-4GlcNAcb1-3Galb1-4GlcNAcb1-3Galb1-4GlcNAcb1-3Galb1-4GlcNAcb1-3Galb1-4GlcNAcb1-2Mana1-3)Manb1-4GlcNAcb1-4(Fuca1-6)GlcNAcb-Sp19	70	9	14
572	Galb1-4GlcNAcb1-3Galb1-4GlcNAcb1-6(Galb1-4GlcNAcb1-3Galb1-4GlcNAb1-2)Mana1-6(Galb1-4GlcNAcb1-3Galb1-4GlcNAcb1-2Mana1-3)Manb1-4GlcNAcb1-4(Fuca1-6)GlcNAcb-Sp24	82	56	68
573	GlcNAcb1-3Galb1-4GlcNAcb1-3Galb1-4GlcNAcb1-6(GlcNAcb1-3Galb1-4GlcNAcb1-3Galb1-4GlcNAb1-2)Mana1-6(GlcNAcb1-3Galb1-4GlcNAcb1-3Galb1-4GlcNAcb1-2Mana1-3)Manb1-4GlcNAcb1-4(Fuca1-6)GlcNAcb-Sp24	42	18	44

574	Galb1-4GlcNAcb1-3Galb1-4GlcNAcb1-3Galb1-4GlcNAcb1-6(Galb1-4GlcNAcb1-3Galb1-4GlcNAcb1-3Galb1-4GlcNAb1-2)Mana1-6(Galb1-4GlcNAcb1-3Galb1-4GlcNAcb1-3Galb1-4GlcNAcb1-2Mana1-3)Manb1-4GlcNAcb1-4(Fuca1-6)GlcNAcb-Sp24	70	67	96
575	GlcNAcb1-3Galb1-4GlcNAcb1-3Galb1-4GlcNAcb1-3Galb1-4GlcNAcb1-6(GlcNAcb1-3Galb1-4GlcNAcb1-3Galb1-4GlcNAcb1-3Galb1-4GlcNAb1-2)Mana1-6(GlcNAcb1-3Galb1-4GlcNAcb1-3Galb1-4GlcNAcb1-3Galb1-4GlcNAcb1-2Mana1-3)Manb1-4GlcNAcb1-4(Fuca1-6)GlcNAcb-Sp24	42	25	59
576	Galb1-4GlcNAcb1-3Galb1-4GlcNAcb1-3Galb1-4GlcNAcb1-3Galb1-4GlcNAcb1-6(Galb1-4GlcNAcb1-3Galb1-4GlcNAcb1-3Galb1-4GlcNAcb1-3Galb1-4GlcNAb1-2)Mana1-6(Galb1-4GlcNAcb1-3Galb1-4GlcNAcb1-3Galb1-4GlcNAcb1-3Galb1-4GlcNAcb1-2Mana1-3)Manb1-4GlcNAcb1-4(Fuca1-6)GlcNAcb-Sp24	62	52	84
577	GlcNAcb1-3Galb1-4GlcNAcb1-3Galb1-4GlcNAcb1-3Galb1-4GlcNAcb1-6(GlcNAcb1-3Galb1-4GlcNAcb1-3Galb1-4GlcNAcb1-3Galb1-4GlcNAcb1-3Galb1-4GlcNAb1-2)Mana1-6(GlcNAcb1-3Galb1-4GlcNAcb1-3Galb1-4GlcNAcb1-3Galb1-4GlcNAcb1-3Galb1-4GlcNAcb1-2Mana1-3)Manb1-4GlcNAcb1-4(Fuca1-6)GlcNAcb-Sp24	190	56	29
578	Galb1-4GlcNAcb1-3Galb1-4GlcNAcb1-3Galb1-4GlcNAcb1-3Galb1-4GlcNAcb1-3Galb1-	123	40	32

	4GlcNAcb1-6(Galb1-4GlcNAcb1-3Galb1-4GlcNAcb1-3Galb1-4GlcNAcb1-3Galb1-4GlcNAcb1-3Galb1-4GlcNAb1-2)Mana1-6(Galb1-4GlcNAcb1-3Galb1-4GlcNAcb1-3Galb1-4GlcNAcb1-3Galb1-4GlcNAcb1-3Galb1-4GlcNAcb1-2Mana1-3)Manb1-4GlcNAcb1-4(Fuca1-6)GlcNAcb-Sp24			
579	Galb1-4GlcNAcb1-3Galb1-4GlcNAcb1-3GalNAca-Sp14	138	23	16
580	Galb1-4GlcNAcb1-3Galb1-4GlcNAcb1-6(Galb1-3)GalNAca-Sp14	180	78	43
581	Galb1-4GlcNAcb1-3Galb1-4GlcNAcb1-6(Galb1-4GlcNAcb1-3Galb1-4GlcNAcb1-3)GalNAca-Sp14	239	177	74
582	Neu5Aca2-3Galb1-4GlcNAcb1-3Galb1-4GlcNAcb1-3GalNAca-Sp14	-8	2	-29
583	GlcNAcb1-3Galb1-4GlcNAcb1-3GalNAca-Sp14	-7	4	-61
584	GlcNAcb1-3Galb1-4GlcNAcb1-6(Galb1-3)GalNAca-Sp14	0	2	#####
585	GlcNAcb1-3Galb1-4GlcNAcb1-6(GlcNAcb1-3Galb1-4GlcNAcb1-3)GalNAca-Sp14	1	1	40
586	Neu5Aca2-3Galb1-4GlcNAcb1-3Galb1-4GlcNAcb1-6(Neu5Aca2-3Galb1-4GlcNAcb1-3Galb1-4GlcNAcb1-3)GalNAca-Sp14	23	13	58
587	Neu5Aca2-6Galb1-4GlcNAcb1-3Galb1-4GlcNAcb1-3GalNAca-Sp14	7	4	52
588	GlcNAcb1-3Galb1-4GlcNAcb1-3Galb1-4GlcNAcb1-3GalNAca-Sp14	1	4	383
589	Galb1-4GlcNAcb1-3Galb1-3GalNAca-Sp14	2	1	72
590	Neu5Aca2-3Galb1-4GlcNAcb1-3Galb1-4GlcNAcb1-6(Galb1-3)GalNAca-Sp14	59	11	19
591	Neu5Aca2-6Galb1-4GlcNAcb1-3Galb1-4GlcNAcb1-6(Galb1-3)GalNAca-Sp14	189	20	11
592	Neu5Aca2-6Galb1-4GlcNAcb1-6(Galb1-3)GalNAca-Sp14	8	2	18

593	Neu5Aca2-3Galb1-4GlcNAcb1-3Galb1-4GlcNAcb1-2Mana1-6(Neu5Aca2-3Galb1-4GlcNAcb1-3Galb1-4GlcNAcb1-2Mana1-3)Manb1-4GlcNAcb1-4GlcNAcb-Sp12	128	49	38
594	GlcNAcb1-6(Neu5Aca2-3Galb1-3)GalNAca-Sp14	1	4	288
595	Neu5Aca2-6Galb1-4GlcNAcb1-3Galb1-4GlcNAcb1-6(Neu5Aca2-6Galb1-4GlcNAcb1-3Galb1-4GlcNAcb1-3)GalNAca-Sp14	73	21	29
596	Neu5Aca2-6Galb1-4GlcNAcb1-3Galb1-4GlcNAcb1-3Galb1-4GlcNAcb1-2Mana1-6(Neu5Aca2-6Galb1-4GlcNAcb1-3Galb1-4GlcNAcb1-3Galb1-4GlcNAcb1-2Mana1-3)Manb1-4GlcNAcb1-4GlcNAcb-Sp12	296	53	18
597	Neu5Aca2-3Galb1-4GlcNAcb1-3Galb1-4GlcNAcb1-3Galb1-4GlcNAcb1-2Mana1-6(Neu5Aca2-3Galb1-4GlcNAcb1-3Galb1-4GlcNAcb1-3Galb1-4GlcNAcb1-2Mana1-3)Manb1-4GlcNAcb1-4GlcNAcb-Sp12	490	110	22
598	Neu5Aca2-6Galb1-4GlcNAcb1-3Galb1-4GlcNAcb1-2Mana1-6(Neu5Aca2-6Galb1-4GlcNAcb1-3Galb1-4GlcNAcb1-2Mana1-3)Manb1-4GlcNAcb1-4GlcNAcb-Sp12	67	13	19
599	GlcNAcb1-3Fuca-Sp21	6	3	59
600	Galb1-3GalNAcb1-4(Neu5Aca2-8Neu5Aca2-8Neu5Aca2-3)Galb1-4Glcb-Sp21	16	15	93